**UiT** The Arctic University of Norway

Faculty of Science and Technology
Department of Computer Science

# Predictive Modeling for Fair and Efficient Transaction Inclusion in Proof-of-Work Blockchain Systems

Enrico Tedeschi

A dissertation for the degree of Philosophiae Doctor

June, 2023

# Abstract

This dissertation investigates the strategic integration of Proof-of-Work (PoW)-based blockchains and ML models to improve transaction inclusion, and consequently molding transaction fees, for clients using cryptocurrencies such as Bitcoin. The research begins with an in-depth exploration of the Bitcoin fee market, focusing on the interdependence between users and miners, and the emergence of a fee market in POW-based blockchains. Our observations are used to formalize a transaction inclusion pattern. To support our research, we developed the Blockchain Analytics System (BAS) to acquire, store, and pre-process a local dataset of the Bitcoin blockchain. BAS employs various methods for data acquisition, including web scraping, web browser APIs, and direct access to the blockchain using Bitcoin Core software. We utilize time-series data analysis as a tool for predicting future trends, and transactions are sampled on a monthly basis with a fixed interval, incorporating a notion of relative time represented by block-creation epochs.

We create a comprehensive model for transaction inclusion in a POW-based blockchain system, with a focus on factors of revenue and fairness. Revenue serves as an incentive for miners to participate in the network and validate transactions, while fairness ensures equal opportunity for all users to have their transactions included upon paying an adequate fee value. The ML architecture used for prediction consists of three critical stages: the ingestion engine, the pre-processing stage, and the ML model. The ingestion engine processes and transforms raw data obtained from the blockchain, while the pre-processing phase transforms the data further into a suitable form for analysis, including feature extraction and additional data processing to generate a complete dataset. Our ML model showcases its effectiveness in predicting transaction inclusion, with an accuracy of more than 90%. Such a model enables users to save at least 10% on transaction fees while maintaining a likelihood of inclusion above 80%. Furthermore, adopting such model based on fairness and revenue, demonstrates that miners' average loss is never higher than 1.3%.

Our research proves the efficacy of a formal transaction inclusion model and

ML prototype in predicting transaction inclusion. The insights gained from our study shed light on the underlying mechanisms governing miners' decisions, improving the overall user experience, and enhancing the trust and reliability of cryptocurrencies. Consequently, this enables Bitcoin users to better select suitable fees and predict transaction inclusion with notable precision, contributing to the continued growth and adoption of cryptocurrencies.

# Acknowledgements

To all those who courageously stood by my side and provided unwavering support throughout these years and along this journey, I extend my heartfelt gratitude.

I would like to express my deepest appreciation to my thesis advisor Håvard Dagenborg, and co-advisor Dag Johansen, for their support, invaluable guidance, and insightful suggestions throughout the course of this research. Your expertise and encouragement have been instrumental in the successful completion of this thesis. Thanks to your availability and willingness to assist, I had the privilege of attending several international technical schools, where I received valuable insights and advice to inform my dissertation research. As a foreign student, your guidance provided me with not only technical and academic support, but also personal and cultural insights that proved invaluable throughout my studies. For all these reasons, I consider you to have been my primary point of reference during my academic journey.

I am grateful for the support and camaraderie of the Cyber Security Group (CSG) colleagues at the Arctic University of Norway (UiT) who shared my journey, from the lighthearted moments in the office to the trying times of failed tests and the anxiety of submitting papers for review. I extend a special thanks to my main co-author Tor-Arne Nordmo, whose invaluable knowledge, constant support, and willingness to assist have been instrumental to my success. I would also like to express my gratitude towards my other colleagues for their valuable contributions and for making my time at CSG a memorable experience. Thomas Bye Nilsen, deserves a special mention for the enjoyable table tennis matches we had during our coffee breaks and for his insightful discussions about Norwegian culture and society. Aakash Sharma has been an excellent office mate and a source of laughter with his unique sense of humor, including his joke about his "spiced" Indian heritage and his perspective on being a foreigner in our department, like myself. Aril Bernhard Ovesen, with whom I shared an office and taught a course, has been an excellent collaborator and a supportive colleague. Lars Brenna, with whom I traveled to Los Angeles

to present my first publication. His invaluable help and advice were always welcome and precious to me, and our interactions over the course of the trip and beyond have made him a valuable friend. Finally, Bjørn Aslak Juliussen's legal expertise has been an invaluable asset to the CSG, and in the face of the tragedy of the commons, he quickly became my go-to legal consultant. I thank all of my other colleagues, and especially Magnus, Anders, and Andreas, for making my time at CSG a memorable and enriching experience, and I look forward to continuing our collaboration and friendship in the future.

I would like to express my deep appreciation to the Cryptology and Data Security team at the University of Bern for their invaluable contribution to my Ph.D. journey. Specifically, I am grateful for the expert guidance of Dr. Prof. Christian Cachin, whose mentorship helped me expand my knowledge in the fields of blockchain technology, algorithm for distributed consensus, and cyber security. In addition to his exceptional research skills, Dr. Cachin's grounded personality and willingness to be available for his students make him an extraordinary person. His guidance and support have been instrumental to my success, and I am honored to have had the opportunity to work with him. I am grateful for the support and friendship of all my colleagues in this fabulous group, but I would like to give special thanks to Ignacio Amores Sesar. His expertise was fundamental to achieving a valuable publication, and our collaboration has led to a wonderful friendship. Despite his aversion to skiing, we have discovered many shared interests and experiences, such as hikes, board game nights, and trips together, which have made our friendship even more rewarding. I would also like to extend my appreciation to Orestis Alpos for being an excellent skiing buddy in the beautiful Bernese Oberland, and to Jovana Micic and Luca Zanolini for their guidance and tips on exploring Bern. Their support and kindness have made my time here even more enjoyable and memorable.

Thanks to the strong bonds formed within the well-established community of international students and the amiable locals in Tromsø, I have remained in this city far beyond what I initially anticipated. I want to express my heartfelt gratitude to my adventure buddies who have been instrumental in my experiences here. Gigi, you have been an exceptional friend and a constant companion for hiking, skiing, tennis, and partying from the very beginning. Paolo, our delightful conversations, tea sessions, and memorable photography excursions together have meant the world to me. Pietro, your unique personality has brought endless joy and laughter to our adventures. Helge, your friendship has been invaluable, even though you relocated to Milan now, I forgive you for that. Lorenzo, you have always been there as a supportive friend. Mara and Jenny, your joy, kindness, and friendship throughout these years have been

essential in keeping me focused and motivated. William, you truly are my favorite drama queen, bringing excitement to every situation. Behrooz, you are are a wonderful person and an incredible flatmate. I must express a hint of sympathy towards you for enduring my challenging presence for such an extended period of time. Ranieri, Greta, and Ilaria, you have been irreplaceable travel companions who have become cherished friends over time.

I would like to take a moment to express my deep appreciation for the exceptional friendships I have cultivated over the years. I firmly believe that friendships between individuals of different genders are not only possible but also incredibly meaningful and invaluable in our lives. First and foremost, I want to extend my heartfelt thanks to Benedetta. Our friendship has encompassed some of the most remarkable years of my life, and it continues to grow stronger every day. You are an incredible person and a dear friend, and I cannot adequately express my gratitude for the positive impact you have had on me. To Elena, our friendship has been invaluable from the very beginning. Your knowledge, unwavering support, and constant presence have played a significant role in shaping the person I am today. I truly consider you one of the most intelligent individuals I have ever had the pleasure of knowing. Your friendship has always been a cherished gift, and I will forever be grateful to you. Please know that you can always count on my unshakable devotion and friendship. I would also like to extend my heartfelt appreciation to my dear friend Julia, whom I had the pleasure of meeting during my first year in Tromsø. Despite the passage of time, our bond remains strong, and your support has always meant the world to me. Francesca, you hold a special place in my heart. The semester we spent together was truly remarkable, and every time we reunite, it feels as though time has not passed at all. Your kindness, honesty, and captivating smile make you someone truly delightful to be around. Being in your presence brings immense joy, and I feel incredibly fortunate to have you as a friend. Michela, your joy and enthusiasm for Tromsø greatly contributed to my enjoyment during those initial months. Our friendship has endured, and you hold a special place among my most treasured friends. Lastly, I want to express my deepest gratitude to my dear friend Sofia. Your invaluable advice, contagious joy, and enthusiasm provided immense support during the final stages of my PhD journey. Your presence in my life has been truly transformative, and I am genuinely grateful for everything you have contributed. To Benedetta, Elena, Julia, Francesca, Michela, and Sofia – each of you has made an immeasurable impact on my journey. I want to express my heartfelt appreciation for being part of my life and for the profound influence you have had on me. Thank you for your friendship and the incredible memories we have shared.

During my time in northern Norway, I had the incredible opportunity to indulge

in my passion for photography as a northern lights enthusiast. Embracing the cold nights and venturing into the icy wilderness provided an occasional escape from my studies and work. I am deeply grateful to my initial colleagues, Alessandro and Truls, who not only shared their expertise but also became cherished friends. Gratitude also extends to the entire guiding community and the great individuals I had the pleasure of meeting, including Nicola, Cecilia, Hannah, Jeff, Per, and Raquel. Their warm presence and unwavering support enriched my experience beyond measure.

My journey would have been impossible without the support of my friends in Milan. Despite the distance, their enduring presence was indispensable. I am grateful to those I grew up with and my university friends: Susan, Debora, Francesca, Veronica, Matteo, and Stefano. Their constant support fueled my strength and determination. I also would like to express my heartfelt gratitude to the individuals in the "non belligeranti" group, my dear friends and closest allies, who have been by my side since our days in primary school. Tommaso, your unwavering friendship and frankness have always been a constant source of support, and I truly appreciate your presence. Francesco, you embody the essence of being "non belligerante" within our group, and your friendship has been invaluable throughout the years, and being a physiotherapist, I know I can always count on you if I ever need a massage. Andrea, as our professional flaker, your rational nature and friendship have undeniably shaped my journey. I must express my gratitude for your consistently unpredictable presence and the valuable advice you've provided, which has surprisingly contributed to my success. Simone, my dear friend and cousin, thank you for beating us in every video game we've played together, this has humbled us all and it has been a valuable learning experience that has kept us on our toes and pushed us to improve. Your presence throughout my entire life has been of utmost importance, providing unwavering support and companionship. Lastly, I want to express my deepest gratitude to Bonny, my best friend since we were three years old. Your kind-hearted nature and caring attitude make you the epitome of an ideal friend. Although you may have recently stepped back from the gaming realm due to Andrea's dominance, your friendship remains unmatched. Thank you for being the best friend one could ever imagine.

Last but certainly not least, I want to convey my deepest and warmest appreciation to my family, my father Franco and my mother Antonella. Their constant support, both emotionally and financially, during my studies has been invaluable. They have not only provided for me but also instilled in me a strong set of values including respect, kindness, fairness, integrity, open-mindedness, generosity, and love. Their kindness and love have touched my heart profoundly, they have never opposed my decisions but instead wholeheartedly supported

me in realizing my dreams, and for this, I am eternally grateful. I also want to extend my heartfelt thanks to my brother, whose soundtracks have accompanied me on this incredible journey. Your music has brought joy and motivation to every step of the way.

Finally, I want to express my gratitude to myself for persevering, staying resilient, and never giving up on my dreams. Throughout this journey, I have faced numerous challenges and obstacles, but I have remained steadfast in my belief in my abilities and the path I have chosen. I am grateful to myself for the courage to take risks, the determination to overcome setbacks, and the belief in my own potential. Through moments of self-doubt and uncertainty, I have found the strength within me to keep pushing forward and striving for excellence.

# Contents

# List of Figures

# List of Tables

# List of definitions

# List of Abbreviations

**aBFT** asynchronous Byzantine Fault-Tolerant
**ACL** Access Control List
**ACM** Association for Computing Machinery
**AI** Artificial Intelligence
**ANN** Artificial Neural Network
**API** Application Programming Interface
**ASIC** Application Specific Integrated Circuits
**AUC** Area Under Curve
**AUC-ROC** Area Under Curve of Receiver Operator Characteristic
**BA** Byzantine Agreement
**BAS** Blockchain Analytics System
**BBChain** Efficient Trustworthy Computing with Blockchains and Biometrics
**bct** block creation time
**BFT** Byzantine Fault Tolerant
**BNE** Bayesian Nash equilibrium
**BTC** Bitcoin Currency
**CA** Certificate Authority
**CBDC** Central Bank Digital Currency
**CDF** Cumulative Distribution Function
**CSG** Cyber Security Group
**CSV** Comma-Separated Values
**DAG** Directed Acyclic Graph
**DDoS** Distributed Denial of Service
**DLT** Distributed Ledger Technology
**DNN** Deep Neural Network
**DoS** Denial of Service
**EBI** Epoch Before Inclusion
**EM** Expectation–Maximization
**ETH** Ether
**EU** European Union
**EULA** End-User License Agreement
**EVM** Ethereum virtual machine
**FBFT** Federated Byzantine Fault Tolerance

**FNR** False Negative Rate
**FPGA** Field Programmable Gate Array
**FPR** False Positive Rate
**FPSBA** First-Price Sealed-Bid Auction
**GCS** Group Communication System
**GRASP** General Responsibility Assignment Software Patterns
**GSP** Generalized Second Price
**HMAC** Hash-based Message Authentication Code
**HTML** HyperText Markup Language
**HTTP** Hypertext Transfer Protocol
**IFC** Information Flow Control
**JSON** JavaScript Object Notation
**kNN** k-Nearest-Neighbors
**LF** Latency Function
**ls** linearly solvable
**LSM** Least Squares Methods
**MAE** Mean Absolute Error
**ML** Machine Learning
**MPE** Miner Power Efficiency
**MPF** Miner Profit Function
**MTS** Multivariate Time Series
**nls** non linearly solvable
**NN** Neural Network
**NP** nondeterministic polynomial time
**OPT** Ordered Pending Transaction
**P2P** Peer-to-Peer
**PBFT** Practical Byzantine Fault Tolerance
**PKI** Public Key Infrastructure
**PoA** Proof-of-Activity
**PoAu** Proof-of-Authority
**PoB** Proof-of-Burn
**PoET** Proof-of-Elapsed-Time
**PoR** Proof-of-Replication
**PoS** Proof-of-Stake
**PoSp** Proof-of-Space
**PoSt** Proof-of-Storage
**PoSTi** Proof-of-Storage-Time
**PoW** Proof-of-Work
**ReLU** Rectified Linear Unit
**ResNet** Residual Neural Network
**RF** Random Forest

**RLP** Recursive Length Prefix
**ROC** Receiver Operator Characteristic
**RPOW** Reusable Proof-of-Work
**RPT** Relapsed Pending Transaction
**SPA** Second-Price Auction
**SPV** Simplified Payment Verification
**SSL** Secure Socet Layer
**SVM** Support Vector Machines
**TAT** Temporarily Approved Transaction
**TCB** Trusted Computing Base
**TNR** True Negative Rate
**TPR** True Positive Rate
**UiS** University of Stavanger
**UiT** the Arctic University of Norway
**UPA** Uniform-Price Auction
**URI** Universal Resource Identifier
**UTC** Universal Time Coordinate
**UTM** Universal Transverse Mercator
**UTXO** Unspent Transaction Outputs
**VDF** Verifiable Delay Functions
**VM** Virtual Machine

*"The relative success of the Bitcoin proves that money first and foremost depends on trust. Neither gold nor bonds are needed to back up a currency."*

Arnon Grunberg, Writer

# 1

# Introduction

Digital money and cryptocurrencies have revolutionized payment systems, making monetary transactions cheaper and faster. These digital currencies, rooted in public-key cryptography and digital signatures, offer robust authentication and secure algorithms for confidential and non-repudiable digital communication. They can be *centralized*, where institutions or banks control the supply as Central Bank Digital Currencys (CBDCs), or *decentralized*, regulated by a network of users through consensus. Decentralized digital currencies encompass cryptocurrencies and online tokens issued by anyone, operating independently of specific financial security mechanisms.

The underlying data structure of most cryptocurrencies is called a *blockchain*. Blockchains are distributed databases that do not require a central trusted party to operate. They are append only, immutable, and experts believe that they will disrupt many industries, from finance [1, 2] and law [3] to healthcare [4] and education [5, 6].

Cryptocurrencies, such as Bitcoin and Ethereum, have emerged as the main assets in the digital currency landscape. Bitcoin and Ethereum secure around 80% of the total cryptocurrency market cap, as of mid-2020 [7]. Bitcoin, in particular, was designed to provide users with a low-cost payment scheme, with transaction fees initially close to zero [8]. However, the increasing popularity of cryptocurrencies like Bitcoin has revealed scalability challenges, with the

underlying POW scheme posing limitations on transaction throughput [9, 10].

These challenges highlight the importance of exploring transaction fees, fee markets, and scalability issues within cryptocurrencies like Bitcoin. By addressing these issues, we aim to enhance the efficiency and cost-effectiveness of transactions within the Bitcoin network, improving the overall user experience and facilitating wider adoption of digital currencies.

In this thesis, we address three main aspects related to blockchain technology: (1) fee mechanisms and overpaying; (2) the incorporation of ML models into POW-based blockchains at scale; (3) optimization of user experiences and trust of such systems. Our contributions stem from the analysis of the largest POW-based blockchain implementation, Bitcoin,[1] by examining fee trends, mining-related monetary costs, and the subsequent fee markets. We introduce a novel formal model, implemented using ML, to investigate patterns and comprehend fee complexity in the context of large-scale blockchain systems. The practical application of this scheme holds the potential to render blockchain technology more cost-effective and enhance user trust in the system by making it cheaper to use.

## 1.1 Blockchain Consensus Types

The pioneering electronic payment system developed in the 1990s by David Chaum, Digicash [11], provided payments without the need for a trusted third party. While such invention was innovative and ahead of its time, Digicash faced challenges in gaining widespread adoption and ultimately filed for bankruptcy in 1998. The onset of decentralized digital currencies began when the still anonymous character of Satoshi Nakamoto released in 2008 the Bitcoin paper [8]. Bitcoin's underlying technology challenged the efficiency of traditional financial systems. Digital signatures enable trust among participants, while to prevent double spending Bitcoin uses a Peer-to-Peer (P2P) network that timestamps transactions into an ever-growing chain of hash-based blocks. Each block must carry an evidence, or *proof*, of the *work* that has been carried out while creating it, such that the consensus is reached by the largest pool of CPU power. Each block is immutable and similarly to hashcash [12], the cost-function used in the Bitcoin consensus computes a token which can be used as a proof of work. This function is efficiently verifiable, but expensive to compute alongside

1. Throughout this study, when we talk about Bitcoin blockchain we refer specifically to BTC

customizable parameters, in order to prevent double spending and Distributed Denial of Service (DDOS) attacks. The Bitcoin blockchain is then secured with a consensus mechanism called Proof-of-Work (PoW).

POW is a decentralized consensus mechanism that requires members of a network to solve mathematical puzzles before agreeing on any decision, so to deter malicious use of computing power, e.g., sending spam emails or launching DDOS attacks. This idea was firstly conceived in 2004 by the developer Han Finney, when he implemented Reusable Proof-of-Work (RPOW), using hashcash and RSA-signed tokens [8, 13]. In 2009 Bitcoin became the first widely adopted implementation of a POW scheme, and Finney was proven to be the recipient of the very first Bitcoin transaction [14]. Systems based on POW proved to be secure, and decentralized in terms of consensus and governance. However, they also demonstrated to be inefficient in terms of throughput (tps), and they struggle to provide cheap fees. Furthermore, the equipment needed to secure the network, used by the so called *miners*, is powerful and expensive. This increase system's overall energy consumption, miners want to maximize their revenue, and this impacts *how* transactions are included in the next mined block, and eventually, in the blockchain.

In response to ameliorate POW drawbacks, different classes of consensus mechanism for blockchain have been designed, and the deep-seated monetary value for each information exchange, made the cryptocurrency domain well suited for the advance of new blockchain systems. Ouroboros [15], Casper [16], Tendermint [17, 18] and Ppcoin [19], want to reduce POW computational costs, and implement a Proof-of-Stake (POS) consensus mechanism, which selects validators in proportion to their quantity of holdings. Algorand [20], Ripple [21, 22], and Stellar [23] implement a Byzantine Agreement (BA)-based blockchain which aim is to improve POW low latency, by using a consensus mechanism that varies from the traditional Practical Byzantine Fault Tolerance (PBFT). Avalanche [24] does not provide total order of transactions, and it builds instead a Directed Acyclic Graph (DAG)-chain which keeps strong probabilistic safety guarantee in the presence of Byzantine adversaries, while its Byzantine Fault Tolerant (BFT) nature enables it to achieve high throughput and scalability. Filecoin [25, 26] implements a Proof-of-Storage (POSt) consensus mechanism. The system turns cloud storage into an algorithmic market, and the network is secured by miners. They make profits by providing storage to clients.

More blockchain protocols have been proposed and studied, such as Proof-of-Elapsed-Time (POET) [27], Proof-of-Burn (POB) [28, 29], Proof-of-Activity (POA) [30], Proof-of-Space (POSp) [31] using Verifiable Delay Functions (VDF) [32, 33], Proof-of-Authority (POAu) [34, 35], Proof-of-Storage-Time (POSTi) [36],

Proof-of-Replication (POR) [37] whose sets the origin to Filecoin's POSt, and many more. Analysis on such systems is made easier by the public and accessible nature of blockchains, and the amount of data available is directly proportioned to their popularity.

## 1.2 Pattern Recognition and Big Data

The inherent append-only property of blockchains leads to accumulation of data. Information stored in blockchains is publicly accessible and easy to retrieve. This sets up a disposition towards big data analysis, and it opens up for technological progress derived by the study of *patterns* and ML modeling [38]. ML is a branch of Artificial Intelligence (AI) that enables programs and algorithms to *self-learn* and *detect certain patterns in large datasets*. Pattern recognition is the discipline whose goal is to classify data or objects into certain classes or categories [39], it has applications in statistical data analysis [40, 41], signal processing [42], image analysis [43, 44], information retrieval [45], and due to the increased availability of large datasets, ML. We will use this automated mechanism of decision making during our research and throughout the whole thesis.

The opportunities and challenges of ML and big data are subject of study [46, 47, 48], and prediction models are used to foresee future events when enough data are available [49, 50]. Furthermore, ML applications span from healthcare [51, 52] and solar energy [53], to financial market predictions [54, 55], and yet not much attention has been given to the blockchain and cryptocurrency domain. This thesis analyzes different blockchain technologies, such as POW-based like Bitcoin, or POS and DAG-based like Avalanche. We conduct an extensive and longitudinal study on Bitcoin, where a consistent amount of data and information is retrieved, in order to detect main POW drawbacks. Furthermore, we evaluate separately, a security analysis on Avalanche. Our main contribution is the study and formalization of the patterns that govern miners' decisions in POW-based blockchains, particularly Bitcoin. Finally, we use this pattern formalization to build a ML model that can predict transaction inclusion in Bitcoin, while optimizing fees and overpaying.

## 1.3 Thesis Statement

The high cost of mining has led to an increased usage of transaction fees as a means for miners to make a profit. This led to serious economic implications

for users, fee *overpaying* became the norm, and many fee estimators started to adopt higher fees than necessary [56].

We conjecture that by combining public data of Bitcoin with ML models, we can establish a *transaction inclusion pattern* for POW-based blockchains. This pattern allows users to predict transaction inclusion, optimize fees, and improve efficiency. By studying miners' decisions we aim to enhance trust, reliability, and utility in cryptocurrencies. It follows the thesis of this dissertation:

***Our thesis is that Bitcoin transaction fees can accurately be modeled and predicted using ML methods, improving utility and efficiency for clients using such cryptocurrencies, while maintaining a fair compensation for miners.***

To elaborate our thesis we initially conduct a longitudinal study on Bitcoin, so to evaluate a large amount of data, and how the system behaves in the event of network saturation, price fluctuations, and transaction fee variations. After building knowledge on POW systems at scale, we need to formally define our view on *transaction inclusion*, in order to use such insights to exploit a ML model at best.

To measure our scope's success, a thorough analysis and evaluation of the ML model needs to be carried out. For that, we will use statistic and probabilistic metrics, and we will define the evaluation set up used in this dissertation, so to make results easily replicable. Our thesis recognizes the central role of POW-based blockchains in matter of security, distributed governance, and cheap, instant transactions all over the globe, therefore our evaluations and results will consolidate the use of such systems, in cryptocurrency domain and elsewhere.

Furthermore, considering the inherent nature of POW-based systems, our inclusion pattern study will be easily adaptable to other POW-based blockchains, facilitating their use at scale, and helping users at not getting overburdened of fees.

## 1.4 Scope and Limitations

To focus on our thesis statement, we provide a clear and concise description of what the study aims to accomplish and outline the boundaries and constraints of the research. Following, we define research objectives, scope, time constraints,

limitations, generalization, and ethical considerations.

### 1.4.1 Research Objectives and Scope

Research objectives of this study include:

- Investigate the strategic integration of POW-based blockchains and ML models to develop a transaction inclusion pattern for improving utility and cost-efficiency in cryptocurrencies like Bitcoin.

- Explore the Bitcoin fee market and understand the interdependence between users and miners.

- Develop the BAS for acquiring, storing, and pre-processing a local dataset of the Bitcoin blockchain, utilizing various data acquisition methods and time-series data analysis.

- Create a comprehensive model for transaction inclusion in POW-based blockchain systems, emphasizing factors of revenue and fairness. Revenue serves as an incentive for miners, while fairness ensures equal opportunity for users upon paying an adequate fee.

- Construct an ML architecture consisting of an ingestion engine, pre-processing, and ML model to predict transaction inclusion, with a focus on feature extraction and data processing to generate a complete dataset.

- Evaluate the effectiveness of the ML model in predicting transaction inclusion, including accuracy, cost savings on transaction fees, and likelihood of inclusion.

- Enable Bitcoin users to make informed decisions by selecting suitable fees and predicting transaction inclusion with precision, contributing to the growth and adoption of cryptocurrencies.

The scope of this dissertation focuses on the model for transaction inclusion within POW-based blockchains, with a specific implementation and testing conducted solely on the Bitcoin network, and specifically, BTC. While the ML model has the potential for use on a global scale, it is important to recognize that its full adoption may bring changes in the way miners include transactions. However, its direct application and testing on a global scale are beyond the scope of this study. The scope includes an exploration of the Bitcoin fee market,

which also holds relevance for other POW-based solutions. By investigating transaction inclusion dynamics, the study aims to enhance user experience, contribute to the trust and reliability of cryptocurrencies, and ensure miners continue to receive transaction fee rewards.

### 1.4.2 Time Constraint and Limitations

The data collection period for the primary findings of this dissertation, involving data processing and refinement, was conducted from January 2021 to May 2021. Monthly information on Bitcoin price, transaction fees, and miner consumption was collected monthly to capture the historical trend of the key factors influencing the study. The research project, including literature review, hypothesis formulation, data collection, and system building, spanned from 2018 to 2021. Following, our focus shifted towards presenting our findings [57, 58], and subsequently compiling this dissertation.

#### Limitations

- In the free and decentralized market of Bitcoin we observe a transaction fee price uptrend, caused by the cost of mining and the fear of "51% attack". In such scenario, we assume that users ought to chose a desired fee, based on their transaction's total amount and network congestion, without fearing of being left out from miners. Therefore, we adopt a solution where users can select their own fee, while monitoring their transaction confidence of being accepted in the next mined block.

- A rational miner should prioritize transactions based mainly on its revenue. Considering that the reward for mining new blocks is halved periodically, we assume that miners will keep on enforcing this behavior in the long run. We therefore consider miners to be *rational agents* in a POW-based ecosystem, as they need to establish a *Nash equilibrium* [59] among themselves in order to approach complex decisions. Our solution works in the presence of such rational miners, which we conjecture to be present in every POW-based systems.

- A Nash equilibrium should be kept also between users and miners. In order to understand how users and miners interact to approach complex solutions, we assume that despite miners ought to be greedy as the network scales and mining costs rise, users should be deterred in leaving the system. We design for this purpose a model where transactions'

waiting time is taken into account, and miner's choices cannot depend by greediness alone.

- The public nature of blockchains facilitates data retrieval and analysis. For our purpose, while adopting ML models to focus on our thesis statement, we adopt a *supervised learning* approach, and therefore, we assume blockchain data to be always available and retrievable. In this way, the patterns we define will establish the guidelines for training ML models, while newer data will shape the model's outcome during time.

### 1.4.3 Generalization

The findings and conclusions of this research study hold implications for generalization. While the specific focus of the study is on the strategic integration of POW-based blockchains and ML models for transaction inclusion in Bitcoin, the insights gained from this research may have broader applicability. Although the study is conducted within the specific context of Bitcoin, the underlying principles and methodologies explored in this study can potentially be generalized to other POW-based blockchain systems. The examination of the Bitcoin fee market and the development of the transaction inclusion model contribute to a deeper understanding of the dynamics and factors affecting transaction inclusion in POW-based blockchains more broadly.

Each blockchain network have unique characteristics, and the specific implementations and considerations within different systems may vary. However, the insights gained from this research can serve as a foundation for further investigations and can inform the development of transaction inclusion strategies in other POW-based blockchain networks. The generalizability of the research findings beyond the specific case of Bitcoin will depend on various factors, including the similarities in the underlying blockchain architecture, consensus mechanisms, and transaction dynamics across different blockchain systems. Further studies and empirical validations in diverse blockchain environments are necessary to assess the extent to which the findings and models developed in this research can be generalized.

### 1.4.4 Ethical Concerns

Although we acknowledge the ethical concerns associated with POW and its potential environmental impact, our dissertation does not aim to question the applicability or sustainability of POW. Instead, our study focuses on a

widespread phenomenon related to blockchain technology, recognizing that alternative consensus mechanisms may exist that offer solutions to the ethical concerns associated with POW.

## 1.5 Methodology

The empirical approach of acquiring knowledge about a certain phenomenon, physical or ethereal, is the *scientific method*. This approach is characterized by careful observations and systematic study of the subject, followed by hypothesis formulation via *inductive reasoning*, experimental and measurement-based testing of *deductions*, and finally, refinement of the hypothesis based on the experimental findings. Conclusions reported at the end of the process are fundamental for hypothesis formulation in a new research cycle.

Natural sciences follow the *hypothetico-deductive model* [60], where the scientific inquiry is carried out by formulating hypothesis that can be logically contradicted by an empirical test. Debates on whether computing can be considered a science or not still animates many [61], and only recently was considered to be a natural science, and not only a subject of the artificial [62]. In 1989, the final report of the ACM Task Force on the Core of Computer Science [63] presented a new taxonomy for classifying computing as a science. They root the field's research in three main paradigms, *theory*, *abstraction*, and *design*.

**Theory** roots its fundamentals in *mathematical* sciences, and it describes objects or events whose properties can be defined using logical reasoning. It is characterized by four steps:

1. *Definition* of the studied objects.
2. Make a *theorem* on their possible relations.
3. *Proof* relations validity.
4. Interpret results.

A glaring example is the study of algorithms, where given an ample set of descriptions, hypothesis can be proven using logical reasoning.

**Abstraction** roots its fundamentals in *natural sciences*, where the notion of scientific progress is achieved by systematically verify and validate certain hypothesis, about a specific phenomena. It is characterized by four main steps:

1. Form a *hypothesis*.

2. Construct a *model*, and make *predictions*.
3. Collect data.
4. Analyze results.

The studied object can span from biological or chemical processes, to physical phenomena, down to the holistic behavior of a complex computer system. The abstraction paradigm goal is to construct accurate models of the rules and laws that govern the behavior of observable phenomena. The model is evaluated by comparing its predictions to experimentally collected data, and it can be used to predict certain behavior in circumstances that have not been observed yet.

**Design** roots its fundamentals in *engineering*, and it uses a systematic approach to construct a system that solves a given problem. It is characterized by three main steps:

1. Define *requirements* and *specifications* based on a series of observations.
2. Design and implement a *prototype system* based on such specifications.
3. Build a set of *experiments* to evaluate such system, by following the stated requirements.

Engineers expect to iterate these steps, and they share the notion that progress is achieved by designing a system that solves a posed problem.

In computing these three paradigms are often intertwined [63], and researchers generally resort to all three paradigms to varying degrees. The work presented in this dissertation initiates with a theoretical nature. The studied subject needs a formal definition before any abstraction or design fundamentals are applied. We use theory to define mathematically the Bitcoin market, and a possible miners inclusion pattern. Definitions must be rigorous and specific, before any hypothesis is expressed. We rely on well-established theory regarding economical principles and market in Bitcoin, including POW properties and limitations.

The rational and systematic approach used in this dissertation involves a *top-down* scheme where, once the broader theory is defined, we use abstraction to form hypotheses for narrowing down our subject of study. We make assumptions and construct a model that will be evaluated and analyzed after collecting and storing information. Big data analysis and longitudinal studies are key parts of this monograph, allowing us to focus our attention in a narrower perspective for building a ML-based system prototype, and establishing a *proof-of-concept* [64]

of it.

Theory and abstraction applied in earlier stages of this study set the backbone for our system prototype implementation. Based on collected data and the theoretical knowledge acquired, we apply design principles to define requirements of such system. We refine the proof-of-concept in order to build our ML-based prototype. Afterwards we construct a set of experiments to evaluate such system, including different metrics to verify its *performance* and yielding evidence for *usability* in a real world scenario, although its proof lay outside the scope of this dissertation. Such performance metrics include theory of pattern recognition, information retrieval, and classification in ML.

This dissertation focuses on deriving principles that govern POW-based markets and miners decisions, when such systems scale. Within our research, we use a top-down approach that focalize in building a prediction model for transaction inclusion. Results are subject of a process of continuous refinement, and the model we build is not final nor static. Empirical measurements and practical experiences might challenge initial assumptions when new network statuses or events occur. Ultimately, we aim to set the baselines for studying such systems at scale, by formalizing market fundamentals and a plausible inclusion model.

## 1.6 Research Context

This dissertation has been carried out in the context of CSG[2] at UiT. The project has been founded by the Research Council of Norway, together with BBChain[3] project, and Nofima.[4] Studies on blockchain security have been conducted in the context of Cryptology and Data Security Research Group at the University of Bern.[5] The dissertation here presented relates with previous scientific studies done in the CSG [65, 66], and to place this dissertation in the right context, a brief overview of previous works is surveyed.

The CSG is investigating fundamental system problems rooted in practical application domains. The group undertakes high-impact interdisciplinary research and innovation at the intersection of computer science, law, sports science,

2. Cyber Security Group at UiT, Norway `https://site.uit.no/arcsecc/`
3. BBChain at University of Stavanger (UiS) `https://bbchain.no`
4. The Norwegian food research institute `https://nofima.com`
5. Cryptology and Data Security Research at University of Bern, Switzerland `https://crypto.unibe.ch`

psychology, statistics, and medicine, and it is now also focused on blockchains and big data analysis. Early works of the CSG include creating streaming infrastructure for football [67], devising a mobile agent middleware architecture for supporting distributed applications in a wide-area network [68], optimizing adaptive streaming and video composition over HTTP [69], and proposing a mechanism for expressing and enforcing security policies for shared data [70]. The cutting-edge and innovative nature of CSG, allowed to explore P2P and early-blockchain domain since 2006 with Fireflies [71], a leaderless BFT consensus protocol. The group research focuses also on AI solutions. One example is monitoring and surveillance in privacy-sensitive and unstable offshore environments. For that purpose, systems for executing distributed AI applications on the edge has been built [72, 73]. Further works using AI have been deployed, Dorvu [74] is a digital platform for real-time privacy-preserving sustainability management in the domain of commercial fishery surveillance operations, and it implements distributed artificial intelligence algorithms on mobile. The group expertise in ML solutions is fundamental for the purpose of this research.

The BBChain project aims to combine blockchain and biometrics to build a privacy-preserving and fault-tolerant public database of digitally authenticated documents. This to enable academic degree certificates to be issued and verified from any place in the world with a high degree of trust [75]. They also use a permissioned blockchain to form verifiable contracts between clients and storage providers [76]. Their knowledge in the blockchain domain is the key for a valuable background education and backbone knowledge for this dissertation.

Nofima is a leading food research institute that explores and develops for the aquaculture, fishing, and food industries. Their projects include using blockchain technology for traceability in the food industry [77, 78, 79], and studying blockchain applicability for enterprises dealing with aquaculture, fisheries, and agriculture, providing a farm-to-consumer holistic view. Their competence in blockchain technology applied in real world scenarios exhibits an indispensable resource of this dissertation applicability.

During the exchange in Bern, at the Cryptology and Data Security Research Group, we surveyed the Avalanche protocol and analyzed its security [80]. The group research is notorious for addressing cryptographic protocols [81], distributed consistency, consensus [82, 83, 84], and cloud-computing security [85], with applications to blockchains [86], distributed ledger technology, cryptocurrencies [87, 88], and their economics. The group's theoretical knowledge in the area of blockchain consensus mechanisms and cryptography, is fundamental to deepen security constraints of such technology, and to understand

protocol limitations even under non-optimal circumstances.

## 1.7 Impact

This research has far-reaching implications for the rapidly evolving field of cryptocurrencies and the broader financial landscape. By providing a detailed understanding of the transaction fee mechanism in Bitcoin and developing a ML model that accurately predicts transaction inclusion, our work contributes to enhancing the trust, efficiency, and utility of cryptocurrencies for end-users. The insights gained through this research have the potential to improve user experiences, enabling them to make more informed decisions about fee selection and increasing their confidence in the likelihood of transaction inclusion in the next mined block.

Furthermore, our findings may guide future research, policy-making, and the development of practical applications, ultimately fostering the growth and adoption of cryptocurrencies in various sectors of the global economy. This study, therefore, represents a significant step towards bridging the gap between the theoretical understanding and practical application of cryptocurrencies, paving the way for a more accessible and efficient financial ecosystem.

## 1.8 Summary of Contributions

The major contributions of this dissertation are based on the publications listed in Appendix B. From a longitudinal study on Bitcoin [65, 66], we made assumptions and conjectures about *correlation* between transaction fees and latency. We refined our linear regression approach to a more accurate ML-based one [57]. After that we formalized and defined a pattern for transaction inclusion [58], and gathered information in our dataset with a mechanism based on block-epochs [89], useful for increasing prediction accuracy. Following, is a brief summary of each contribution:

### Longitudinal Study and Initial Analysis

We identified three main issues of POW-based blockchains as (1) *scalability*, (2) *performance*, and (3) *costs*. We conducted a longitudinal analysis on Bitcoin to study relations between transaction *fees* and *latency*. We showed how scalability

affects performance, then how costs and fees are dependent on them both. Using polynomial interpolation we defined two functions for characterizing fee/latency relation. We stated that applications can improve messaging latency by paying transaction fees, although overpaying does not always improve transaction latency. In our future works we investigated the reasons for that, thus opening our research to a careful study on Bitcoin market ecosystem, and a more thorough approach on prediction models.

## Machine Learning Approach

Using data from previous longitudinal studies, we explored the Bitcoin market ecosystem and made some conjectures on what could cause the latency to drastically increase. We analyzed the *first-price* auction market in Bitcoin, and presented a novel ML model solving a binary classification problem, that can predict transaction fee volatility in the Bitcoin network so that users can optimize their fees expenses and the approval time for their transactions. A feature that we included provides information on how many bytes were already occupied by other transactions in the mempool, assuming they are ordered by fee density in each mining pool. With such information, the ML model could predict transaction inclusion with an accuracy of 86%.

## Model Formalization

In order to be more accurate in predicting transaction latency, we formally defined a novel inclusion model that describes the mechanisms and patterns governing miners decisions to include individual transactions in the Bitcoin system. We abstracted and defined concepts like *fairness* and *revenue*, adding new definitions and approaches for increasing prediction accuracy. We also defined a new method for storing local dataset of the Bitcoin blockchain. The approach we followed is based on a block-epoch collection of transactions. Each transaction has time-based information according on when it was observed. And the time metric used is the block creation time (or block epoch). Using this model and data collected, we devised a novel ML approach to predict transaction inclusion, with an overall accuracy of 91%.

## Dataset Definition

The dataset we built stores part of the Bitcoin blockchain. Blocks are sampled every month and information about transactions and blocks were separated to

save disk space and avoid redundancies. This dataset was used to generate a ML model that predicts transaction inclusion. Information is stored to generate all the necessary features for the ML model, and one transaction can be represented as a multivariate time series, based on the block-epoch approach we have previously described.

### Security Analysis

Our study on blockchain technologies adjourns with an orthogonal project whose aim is to study security of a newer protocol. We inspect the DAG-based chain of Avalanche [24]. Theoretical studies outlined how Avalanche lacks a complete abstract specification and a matching formal analysis. To address this drawback, we presented a detailed formulation of Avalanche through pseudo-code. Furthermore, we performed an analysis of the formal properties fulfilled by Avalanche in the sense of a generic broadcast protocol that only orders related transactions. And finally, the security analysis revealed a vulnerability that affects protocol liveness. Despite the considerable investment of time and effort dedicated to researching the security of Avalanche, culminating in a published paper [80], the content of this research is not incorporated into the main body of this dissertation. Instead, the paper and its findings can be found in Appendix B, accompanied by a concise introduction to DAG-based blockchains in Section 2.2.2.

## 1.9 Outline

In this dissertation, we first provide a background on cryptocurrencies, blockchains, and ML in Chapter 2, which lays the foundation for the subsequent chapters. Following this, Chapter 3 discusses the principles and rules governing the Bitcoin ecosystem at scale, specifically focusing on the interdependence between users and miners, as well as the emergence of a fee market in POW-based blockchains. This chapter establishes the importance of understanding the fee market for formalizing a transaction inclusion pattern.

In Chapter 4, we present the Blockchain Analytics System (BAS), which we developed for acquiring and storing a local dataset of the Bitcoin blockchain. We explain the data acquisition methods and techniques, as well as the structuring and pre-processing of the data for further analysis. In Chapter 5, we discuss our approach using time-series data analysis as a tool for predicting future trends, specifically focusing on the factors of revenue and fairness in a comprehensive

model for transaction inclusion in POW-based blockchain systems.

Chapter 6 presents the ML architecture used in our study, covering the ingestion engine, pre-processing stage, and the ML model itself. This chapter details how raw data is transformed and processed to be suitable for analysis, including feature extraction and training set generation. In Chapter 7, we evaluate the ML model and discuss the datasets used for training and testing, the evaluation metrics employed, and the results of the analyses. The findings of this study demonstrate the efficiency of our ML model in predicting transaction inclusion and its potential as a powerful tool for end-users, offering significant savings in transaction fees.

Chapter 8 delves into a discussion of our findings, exploring the implications and potential applications of our study. We reflect on the limitations of our work and suggest areas for future research to further refine and expand upon our model. In the final chapter, Chapter 9, we present our concluding remarks, summarizing the key takeaways from the research and emphasizing the significance of our ML model for predicting transaction inclusion in the Bitcoin blockchain. Our study not only contributes to the understanding of the fee market and transaction dynamics but also showcases the potential benefits for end-users in terms of transaction fee savings.

# 2

# Background

This chapter provides an overview of blockchain technologies and their applications in cryptocurrencies. The history of blockchain technology will be discussed, including the transition from centralization to decentralization and distribution. The various types of Distributed Ledger Technology (DLT) will be compared and the advantages and disadvantages of using blockchains in different business sectors will be examined. The consensus protocol of Bitcoin will be discussed, along with its limitations at scale and alternative consensus mechanisms used in cryptocurrencies. Additionally, the role of ML in this research will be explained, including the specific ML models that have been adopted.

## 2.1 Blockchains

It is important to note that the terms blockchain and cryptocurrency are often used interchangeably, but they refer to distinct concepts. A distinction between the two can be made as follows:

A *blockchain* is a DLT that allows multiple nodes to maintain and share a consistently replicated and verifiable record of data, without the need for central administration or governance.

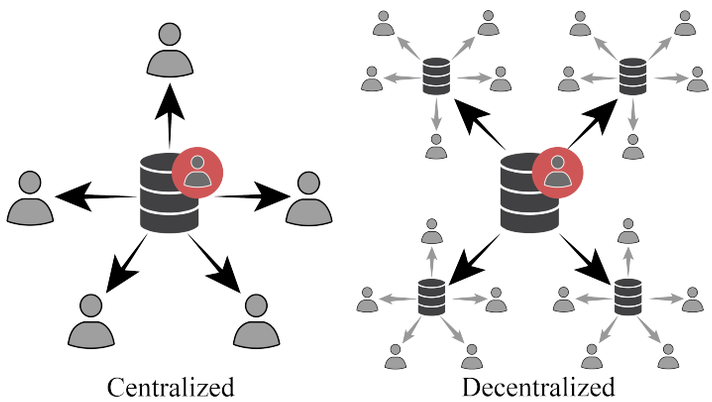


**Figure 2.1:** In a centralized database system, data is stored on a single point and all workload is placed on a single node. The authority to manage the database is held by a single entity (red user). On the other hand, in a decentralized database system, a consistent and replicated view of the data is maintained across multiple nodes, allowing for users to be geographically distributed. However, the governance of the decentralized database is still centralized.

A *cryptocurrency* is a decentralized digital currency that is used as a medium of monetary exchange through a network of computers. It is not controlled by any central authority.

Blockchain technology enables the creation of systems for storing distributed data without relying on a central trusted authority. Cryptocurrencies utilize this technology to facilitate the exchange of information based on the principle of distributed trust inherent in blockchains.

### 2.1.1 Centralization and Decentralization

Before discussing DLTs and blockchains, it is useful to provide an overview of centralized and decentralized systems (showed in Figure 2.1), particularly databases, as the main function of blockchains is to securely and permanently store data while maintaining eventual consistency.

**Centralized** A centralized database is stored and maintained on a single location, often used by an organization or institution that also holds governance over it. Data can be added, modified, or deleted by the central authority. Users must connect to the sole available node to access the database, which has the advantages of less duplication, data integrity, and ease of organization.

**Decentralized** A decentralized database is a system in which data is stored and replicated across multiple physical locations. This architecture provides increased fault tolerance by eliminating a single point of failure. The central authority maintains governance rights in a manner similar to that of a centralized database. This type of system has the potential to accommodate a larger number of users, even those who are geographically dispersed, as depicted in Figure 2.1.

The governance of distributed systems refers to the process of establishing and maintaining the legitimacy of decision-making within the system [16]. In traditional centralized and decentralized systems, this process is typically carried out by a trusted authority or small group of reliable parties, with hierarchical structures and control maintained through legal systems. In a distributed environment, governance is distributed equally among participants, following rules established by the consensus algorithm.

### 2.1.2 Distribution and DLTs

The primary characteristic of DLTs is distribution. This refers not only to the Peer-to-Peer (P2P) gossip-based substrate messaging protocol, but also to the governance and decision-making process for preserving data consistency and integrity. An illustration of the distribution of governance in a DLT network is shown in Figure 2.2.

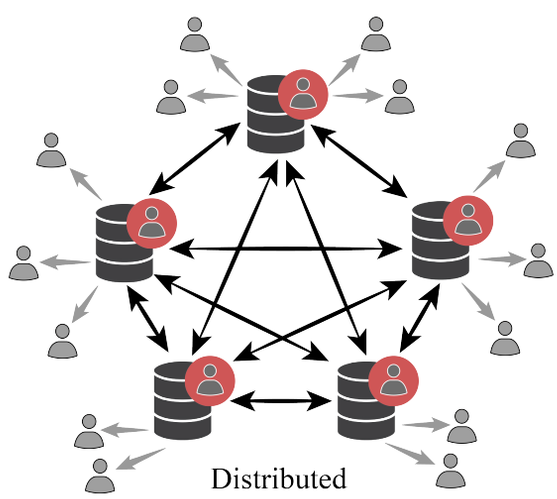


**Figure 2.2:** Distribution in DLTs. The governance is distributed, and the consistency is maintained by a consensus algorithm that enables each party to observe the same order of events.

**Distributed** A distributed ledger, or DLT, is a type of digital database that, like a decentralized one, is replicated, shared, and synchronized among multiple geographic sites, countries, or institutions. Its consistency and integrity are maintained through a consensus mechanism that enables parties to trust each other despite operating in a potentially untrustworthy environment. Unlike centralized and decentralized databases, there is no central administrator or trusted authority in a distributed ledger.

In a DLT, each replica maintains a copy of the ledger and independently updates itself. When an update occurs, every node constructs an updated view of the ledger, and each participant in the consensus process votes on which copy is correct. Once a consensus has been reached, all other nodes update themselves with the new, accurate copy of the ledger [90]. Finally, security is ensured through the use of cryptographic keys and signatures.

DLTs can be classified based on their data structure and consensus mechanism, each of which have their own advantages and disadvantages. Figure 2.3 presents three common implementations of DLTs: blockchains, DAGs, and hashgraphs.

**Blockchains** are a linear linked list data structure in which each block is totally ordered. In the event of conflicts, the longest chain prevails, as

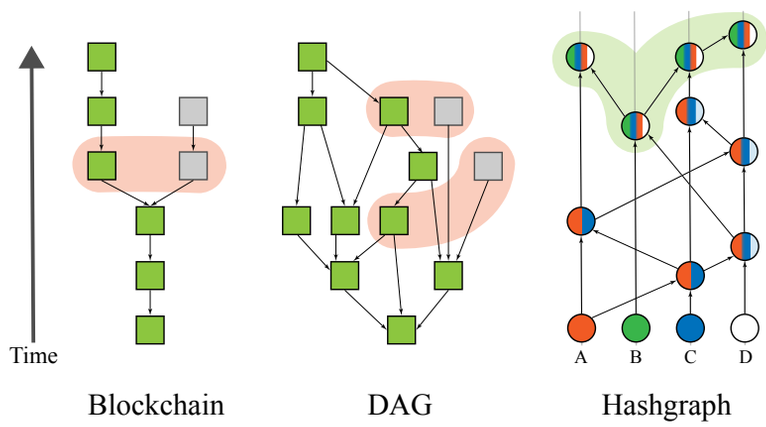


**Figure 2.3:** A comparison of the data structures of different DLTs. Blockchains use linked lists to connect blocks with cryptography, while DAGs and Hashgraphs use a Directed Acyclic Graph. In the first two diagrams, the green blocks represent accepted blocks, while the red sets represent conflicts or instances of double spending. The third diagram illustrates that all parties should eventually agree on the same order of events (shown as the green set).

depicted in Figure 2.3. The first widely implemented blockchain technologies, Bitcoin [8] and Ethereum [91], were introduced in 2008 and 2014, respectively. Bitcoin uses a POW consensus mechanism, while Ethereum recently switched to Proof-of-Stake (PoS), with validators referred to as miners and minters, respectively. These solutions (especially POW) offer high reliability and security, but have low throughput and high energy consumption at scale.

**DAGs** are tree-like data structures in which the total ordering of transactions is not necessarily important, unless conflicts arise. In Figure 2.3, one of the two conflicting blocks (red set in DAG) is discarded, and therefore it does not have any child blocks. Systems that implement a DAG-based chain emerged in 2018 with IOTA [92] and in 2019 with Avalanche [24]. While implementing a DAG is more complex than creating a blockchain, it is more efficient in terms of scalability, although its reliability and security are not necessarily proven to be as strong as those of POW systems.

**Hashgraphs** are a type of DLT that utilize a DAG as their core data structure. Transactions in hashgraphs are stored in parallel among all validators and the order of these transactions is not based on timestamps but rather on the occurrence of events. In hashgraphs, events are generated through a process called *gossip about gossip*, [93], in which validators reach agreement on the order of events. Each event contains one or more transactions, a timestamp, a digital signature, and cryptographic hashes of two earlier events. The hashgraph technology was first introduced in 2016 [93], and a cryptocurrency implementation called Hedera [94] was released in 2019. Hedera utilizes an asynchronous Byzantine Fault-Tolerant (ABFT) consensus algorithm. Hashgraphs are known for their scalability and speed compared to other DAG-based technologies, but the correctness of the entire protocol has faced criticism [95] and their use typically requires a private chain or a closed consortium of voters.

This dissertation focuses on a specific type of DLTs, known as blockchains. In particular, we examine the most widely used one of Bitcoin, which utilizes a POW-based consensus mechanism. Additionally, in our recent publication [80], we provide a brief security analysis of Avalanche, a DAG-based DLT solution.

### 2.1.3 Elements of Blockchains

Blockchains are distributed ledgers characterized by linked lists of blocks that contain information about transactions between parties. These blocks are cryptographically linked to create an immutable ledger with an append-only structure. The *access policy* of a blockchain determines who can read the information, leading to a classification as either public or private. The *control policy* determines who can participate in the advancement of the blockchain and how new blocks can be appended, resulting in classification as either permissioned or permissionless. The *consensus policy* regulates the progression of the protocol.

In 1979, Merkle introduced the concept of using a cryptographic hash to link information in an immutable chain, a structure now known as a *Merkle hash tree* [96]. Each data node in the tree is hashed ($H$ function in Figure 2.4) and the resulting Merkle leaves are paired and hashed together to form branches, eventually leading to a root hash that includes the information from every other node in the tree. This allows for the authentication of a set of messages stored in the data nodes using a unique signature (the Merkle root) without disclosing the other information. The verifier only needs to fetch a small portion of the tree (green nodes in Figure 2.4) to reconstruct the hashes up to the Merkle root, which can then be compared with the root from a trusted source to verify

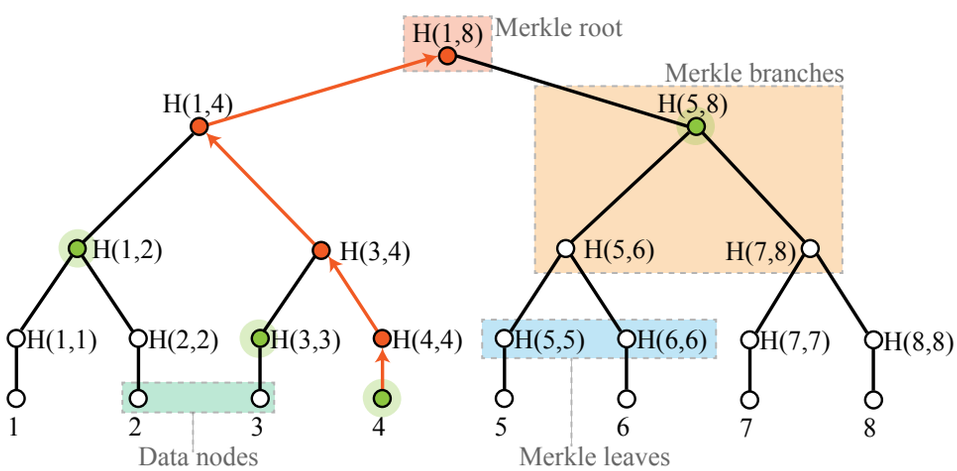


**Figure 2.4:** Illustration of a Merkle tree with 8 data nodes. The data nodes are hashed to create the merkle leaves, and the merkle leaves are then hashed together in pairs to form higher nodes in the tree. To verify the authenticity of the data contained in node 4, a verifier must retrieve the nodes in green and use them to reconstruct the tree from the data to the root. The rebuilt nodes are marked in red, and the root is used for verification.

the authenticity of the data. Similarly, in blockchains, the latest records or blocks contain the history of the entire chain. Such data structure is adopted by Dynamo [97], the efficient key-value storage system of Amazon. In fact, it minimizes the amount of data that needs to be transferred for synchronization and it reduces the number of disk reads performed during the anti-entropy process.

Access policies refer to the rules that determine which parties have the ability to access information stored on a distributed ledger. *Public* blockchains are accessible to anyone with an Internet connection, while *private* blockchains are restricted to certain organizations or consortiums and can only be accessed by parties who have been granted access. There is a range of control policies that can be implemented in blockchain protocols [98], which determine the ability to write information on the ledger and define the blockchain as either *permissioned* or *permissionless*. These control policies have an impact on the governance of the system. Permissionless blockchains allow anyone with an Internet connection to become a validator of the network and participate in the consensus process that drives the progression of the blockchain. In contrast, permissioned blockchains place restrictions on the ability to append data to the ledger.

Blockchains are defined by the structure of an append-only linked list of records that are secured using cryptography. However, the choice of control and access policies gives rise to different consensus mechanisms. These mechanisms describe the procedure by which network validators reach agreement on a single data value among distributed processes. A consensus mechanism should be fault-tolerant and provide security guarantees of termination, finality, and consistency for any decision under stated assumptions. Verification of validators may be required to increase trust, but this also reduces anonymity for nodes. The trade-off between security and speed, as well as the decision to require node verification or not, results in a variety of combinations of public and private, permissioned and permissionless blockchains, as depicted in Figure 2.5.

As mentioned above, various control and access policies determine their inherent consensus mechanisms:

**Public / Permissionless** Public and permissionless blockchains allow any participant to join the consensus mechanism without verifying their identity. This type of blockchain can provide a high level of anonymity, but it also requires a higher level of trust and may have slower overall performance and higher cost due to the use of POW consensus mechanisms like Bitcoin. Public and permissioned blockchains that require node verification are

faster than POW, but do not offer anonymity and their security assumptions are weaker compared to POW systems. These blockchains often use consensus protocols such as PBFT or Federated Byzantine Fault Tolerance (FBFT), as implemented by cryptocurrencies such as Ripple [21] and Stellar [23].

**Public / Permissioned** Permissioned blockchains require that nodes satisfy certain conditions to participate in the consensus process. These conditions may include verification requirements or the need to put money at stake as an incentive to act honestly. These systems are typically faster than POW systems, but there is a higher risk of having a small number of wealthy validators control the network. Ethereum, which was originally a POW system, has transitioned to a POS system [16]. Another example of a permissioned blockchain is Avalanche [24], which uses a POS protocol.

**Private / Permissionless** Hybrid blockchains are private systems that allow access to only a select group of restricted members, but also implement permissionless features and are controlled by a single organization or consortium. These systems provide the level of oversight performed by

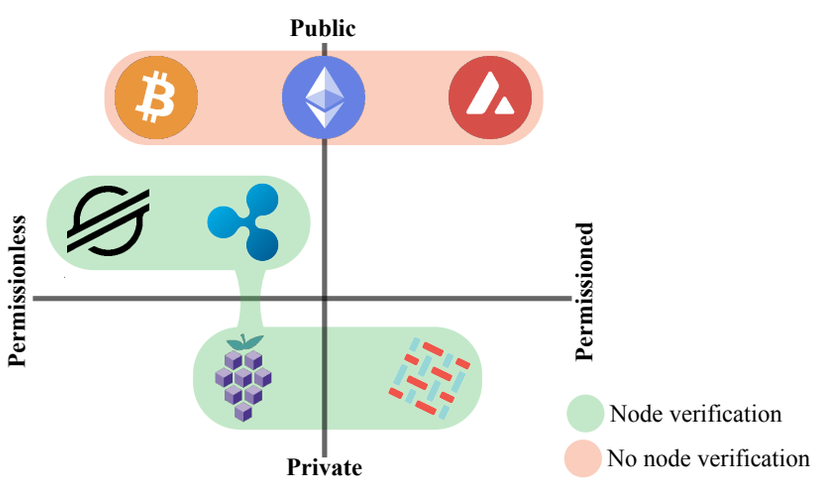


**Figure 2.5:** Public and permissionless blockchains allow anyone to participate in the consensus mechanism. Some examples of this type of blockchain include Stellar and Ripple, which may require node verification, and Bitcoin, which does not. Permissioned but public blockchains impose some restrictions on participation in the consensus process, with examples including Avalanche and Ethereum. Private and permissioned blockchains are controlled by a single organization, such as Hyperledger Fabric. Private and permissionless blockchains, such as IBM Food Trust, are hybrid solutions that are controlled by a single entity but implement permissionless functionality.

public blockchains for transaction validation, while also preserving a level of privacy. An example of a hybrid blockchain is IBM Food Trust [99], which uses the private and permissioned blockchain of Hyperledger Fabric [100] as its core.

**Private / Permissioned** Private and permissioned blockchains are controlled by a single entity, with the central authority determining which individuals or entities can act as validators. While such systems may be efficient in terms of throughput, they are only partially decentralized and do not fully embody the decentralized nature of blockchains. An example of this type of blockchain is Hyperledger Fabric.

In our opinion, the most significant impact of blockchain technology lies in its ability to create a fault-tolerant, tamper-proof, immutable, and verifiable system with decentralized governance. Therefore, the focus of our dissertation is on permissionless and public blockchains, specifically Bitcoin. In the following sections, we will discuss the history of blockchains, the POW consensus mechanism of Bitcoin, and the POS scheme of Avalanche. In the next chapter, we will examine the fee market that has emerged as a result of the scalability limitations of POW systems.

### 2.1.4 History of Blockchains

A proposal for a blockchain system was first presented in 1982 by Chaum [101, 11], in which he described the design of a distributed computer system that could be established, maintained, and trusted by groups that do not necessarily trust each other. This system implemented a public record-keeping solution with group membership consistency, utilizing cryptographic primitives such as symmetric and asymmetric encryption, cryptographic hash functions, and digital signatures. It is worth noting that Chaum's system predates the concept of permissioned and permissionless blockchains, and therefore does not clearly fit into either of these categories [102].

The problem of reaching consensus among unreliable or fallible processes, known as the Byzantine Generals problem, has garnered significant attention from researchers and academics. In 1982, Lamport et al. [103] introduced this problem, and in 1984 Schneider [104] proposed a solution that laid the foundation for consensus mechanisms in permissioned blockchains. Protocols such as PBFT as presented by Castro and Liskov [105] in 2002 and Paxos introduced by Lamport [106] in 1998 serve as the basis for achieving Byzantine agreement in open networks with node verification, such as Ripple and Stellar.

In 1993, Dwork and Naor [107] introduced a computational method for addressing junk mail in their publication. Their approach involves requiring users to perform computationally difficult, but not impossible, functions in order to gain access to resources, thus preventing frivolous use. In 1997, Back proposed the concept of *Hashcash* [12], a mechanism designed to address the systematic abuse of unmetered Internet resources such as email and anonymous remailers, without being aware of Dwork and Naor's earlier work on the subject.

The main idea behind Hashcash is to use a pricing function to create strings that, when processed through the SHA-1 hash algorithm, result in a string with the first $N$ bits equal to zero, where $N$ is typically around 20-30. An example of this process is illustrated in Figure 2.6, which shows an Hashcash token with a 28-bit collision ($N = 28$). The hexadecimal output has 7 leading zeros, corresponding to 28 bits in binary.

This concept of a cost function is similar to the one used by Finney [13] in 2004 to develop the first POW scheme, called Reusable Proof-of-Work. In this system, Hashcash is used as a POW token, and in exchange, RSA-signed tokens, or RPOW-tokens, are created. These tokens can be transferred from one person to another and are as rare and valuable as the Hashcash used to create them, but they are reusable, unlike Hashcash. These primitives are computationally expensive, as they require a proof of computation, but they offer high security and resistance to Sibyl attacks [108]. This foundation for establishing consensus in permissionless and public blockchains that do not require user verification is known as the POW protocol and is used in Bitcoin and previously in Ethereum. It allows for consensus to be reached in a distributed and untrusted environment, and it ensures a high level of security based on computational power rather than the number of participants.

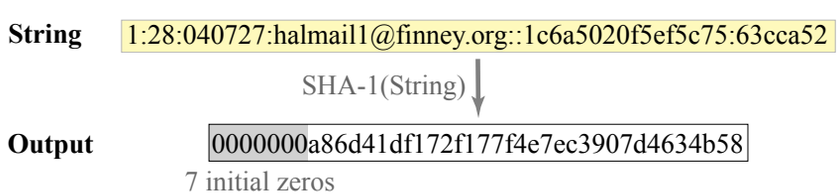


**Figure 2.6:** The Hashcash cost function maps a string using the SHA-1 hashing algorithm, ensuring that the first 28 bits of the output string are equal to zero as per the specified rule.

## 2.2 Cryptocurrencies

Cryptocurrencies, are generally not considered to be currencies in the traditional sense, and are instead treated as a separate asset class in practice [109, 110]. Cryptocurrencies do not have any inherent or legislated value and their worth is determined by the supply and demand in the market. Despite having an initial value of less than half a cent in 2009 (when Laszlo Hanyecz used 10,000 Bitcoins to purchase two pizzas, an event now known as Bitcoin Pizza Day on May 22 [111]), cryptocurrencies have gained popularity for their decentralization, anonymity, and cost-effectiveness, leading to an increase in the overall market capitalization from one billion dollars in 2013 to almost three trillion dollars in 2022.[1]

Following the release of Bitcoin, many other cryptocurrencies have been developed and, at present, there are approximately 23,000 different cryptocurrencies that can be traded on more than 250 exchanges.[2]

### 2.2.1 Bitcoin and Proof-of-Work

In 2008, a person or group using the pseudonym Satoshi Nakamoto published a paper on Bitcoin [8] and released the open-source software for the cryptocurrency. Bitcoin was the first successful application of blockchain technology that used POW as a consensus mechanism. It timestamps transactions by hashing them into a chain of hash-based POW, making it difficult to alter the recorded information without redoing the POW and rebuilding the chain from scratch. Since the longest chain is generally considered to be the correct one, as long as the majority of the computing power is controlled by honest nodes, they will be able to generate the longest chain and outpace any attackers.

#### Transactions

According to Nakamoto [8], an electronic coin can be represented as a *chain of digital signatures*. In Figure 2.7, we observe that each owner transfers a coin to the next by signing the hash of the previous transaction with their private key and including the next owner's public key. The recipient of the coin can verify the signature (signed by the previous owner) using the previous owner's public key. While this system allows for the transfer of ownership of a single

1. According to Coinmarketcap `https://coinmarketcap.com`
2. Coinmarketcap `https://coinmarketcap.com/rankings/exchanges/`

coin, it does not prevent double spending. In fact, the recipient cannot know if the previous owner has signed any earlier transactions. To address this issue and prove the authenticity of transactions without relying on a central trusted authority, transactions must be publicly announced and participants must reach consensus on the order of transactions.

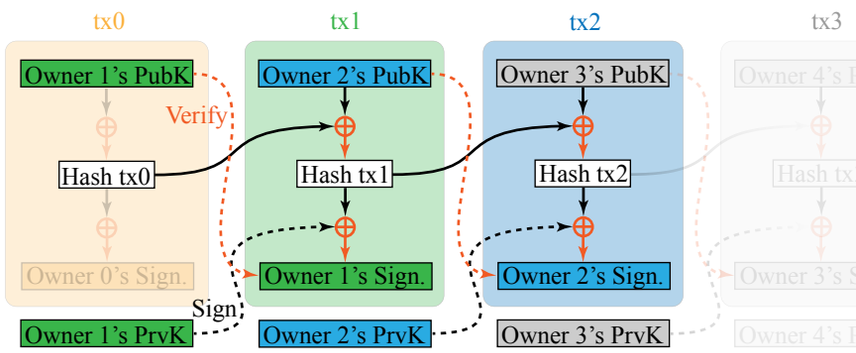


**Figure 2.7:** Bitcoin Transactions. In the context of Bitcoin, the concept of ownership of a particular coin is established through a sequence of digital signatures. An example of coin transfer is depicted in green as Transaction 1 (tx1), is made from Owner 1 (green) to Owner 2 (blue). This transfer is facilitated through the creation of a hash that incorporates Owner 2's public key (PubK), and the previous transaction hash (Hash tx0). The validity of the transfer can be confirmed through the utilization of Owner 1's private key (PrvK) to sign Hash tx1, which can then be verified by Owner 2 using Owner 1's public key. Subsequent transfers of the coin, such as the transfer to Owner 3 (gray), result in the formation of a chain of digital signatures.

## Blocks

To address the double spending problem, Nakamoto's initial solution was to implement a *timestamp server* that creates a hash of a block of transactions that need to be timestamped and publishes this hash as proof of the transactions' existence at that time. For efficiency and security purposes, each transaction in the block is represented by a leaf in a Merkle tree, and the root of this tree is used to generate the timestamp (block) hash. As shown in Figure 2.8, a single block hash contains information about the previous hash, time, and Merkle root. This allows every transaction to be publicly announced, and if any of the transactions are tampered with, the entire block hash will be changed. Furthermore, each block includes the previous block's hash in its own hash, forming a chain where each additional timestamp strengthens the ones before it and makes manipulations visible at any point in the chain, unless the entire chain is rebuilt. Once transactions have been proven to be publicly announced,

a distributed timestamp server is needed to reach consensus among validators (called miners in Bitcoin) on a single record history. This is achieved through the use of a POW implementation similar to that proposed by Hashcash [12].

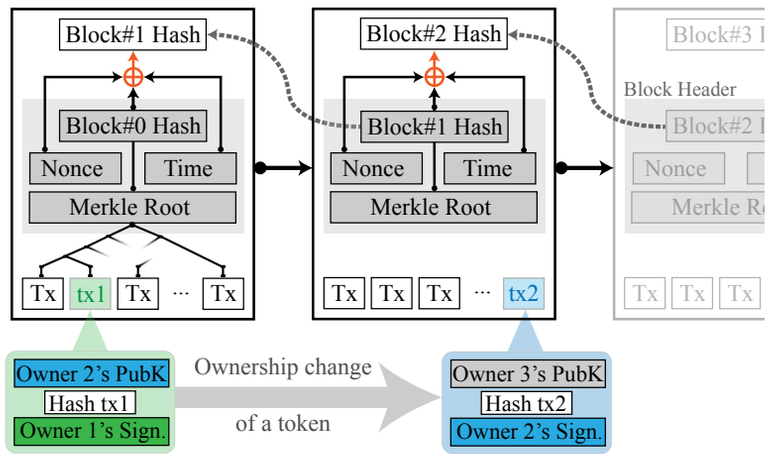


**Figure 2.8:** Blocks are linked together through a chain of hashes. Each transaction in a block is represented by a leaf in the generated Merkle tree, and the root of this tree is included in the block header. The block header also includes the time, nonce, and hash of the previous block. These values are used to generate the hash of the new block, which is then linked to the previous block through its hash. The chain of digital signatures depicted in Figure 2.7 can be contextualized in terms of blocks, where tx1 and tx2 represent a change in ownership or a particular token.

### Proof-of-Work

In Bitcoin, validators reach consensus on a single record history by verifying that newly created blocks are valid. When a block is deemed valid, it indicates that a peer has successfully solved the POW puzzle associated with it, demonstrating that a certain amount of work has been done. This peer becomes the leader for this round and proposes a new block. To solve the POW puzzle, a miner must find a block hash with a specified number of leading zeros that is below a certain target value. This target value is determined by the network difficulty, as described in Section 2.1.4.

The SHA-256 algorithm is used to hash the block header twice, and the nonce (a number used only once) is incremented by one for each failed attempt. The probability of finding the target value (shown as the yellow box in Figure 2.9) through this process is low, requiring a significant amount of trial and error. The

solution can be verified quickly by re-hashing the block header and comparing it to the posted block hash.

In a POW-based system, the individuals responsible for validating blocks are called *miners*, and the process of solving the POW puzzle is called *mining*. Once a block has been mined, it is immutable and cannot be altered without building a longer chain starting from the tampered block. Therefore, the more hashing power the network has, the harder it is for an individual or group to overtake the original chain and confirm the tampered block. POW was originally developed to combat spam emails and DDOS attacks, but Bitcoin was the first system to use it for both mining (where validators are compensated when they find a new block) and achieving consensus [102]. In summary, POW involves finding the nonce that, when hashed twice with the rest of the block header using the SHA-256 algorithm, produces a block hash with a specified number of leading zeros. The main drawbacks of using POW are the high energy consumption required for mining and the low transaction throughput due to block size and time constraints for producing new blocks [58].

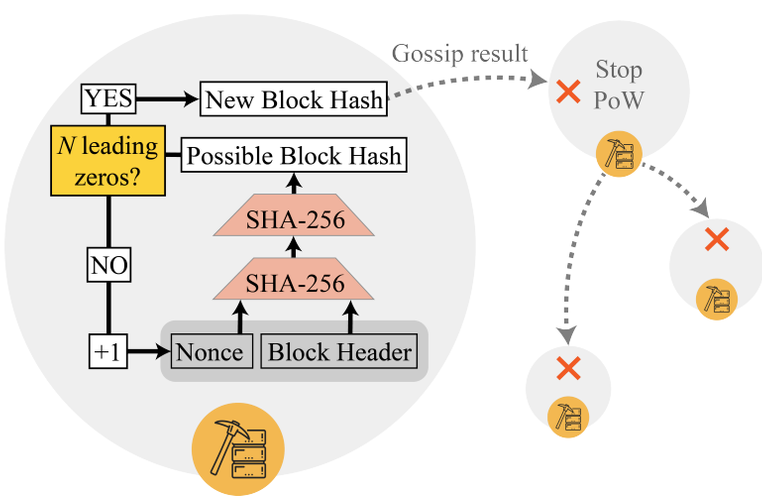


**Figure 2.9:** For each attempt, the nonce is incremented and the block header is hashed twice using the SHA-256 algorithm. The first miner to solve the puzzle broadcasts the solution to other peers. If the proposed hash is valid, each peer aborts their current POW and begins a new one with a new set of transactions and a new Merkle root to hash.

### Difficulty

In relation to POW, *difficulty* refers to the measure on how hard is to find a hash below a specified target. This difficulty can be increased or decreased by modifying the target value according to the scheme in Figure 2.10. Difficulty serves to maintain a consistent block creation frequency, despite variations in Bitcoin's overall hashing power over time. The desired block creation time in the Bitcoin network is set at 600 seconds, which is determined by the core algorithm and design of the network. The difficulty level of mining is adjusted approximately every 2,016 blocks, equivalent to around 14 days. This adjustment ensures that the network maintains a consistent block creation rate. The calculation of the difficulty adjustment involves normalizing the mean creation time of the past 2,016 blocks. This mean creation time is denoted as $\mathcal{T}'$ and can be calculated using Equation 2.1:

$$\mathcal{T}' = \frac{\sum_{i=1}^{2016} \mathcal{T}_i}{2016} \tag{2.1}$$

In this equation, $\mathcal{T}'$ represents the average block creation time, which is obtained by summing the creation times of the past 2,016 blocks and dividing the sum by 2,016. This normalization process helps adjust the mining difficulty to maintain the desired block creation time. The difficulty value at a specific block height,[3] denoted as $x$ (where $x$ mod 2016 = 0), is represented

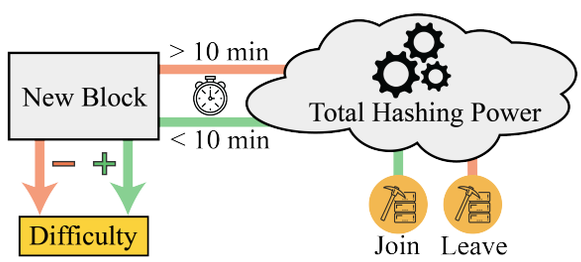


**Figure 2.10:** In the Bitcoin network, the difficulty of creating new blocks adjusts in response to changes in the overall hashing power of the network. When a miner joins, the overall hashing power increases, leading to the likelihood of faster block generation and an increase in difficulty to maintain a stable block creation time. Conversely, when a miner leaves, the difficulty decreases to compensate for the decrease in hashing power. While the illustration shown depicts the creation of a single new block, in the Bitcoin network, the difficulty is actually adjusted every 2,016 blocks.

3. The height represents the number of blocks that have been added to the blockchain from its inception. The condition $x$ mod 2016 = 0 indicates that the height of the block is a multiple of 2,016, which typically corresponds to the point at which the network adjusts the mining difficulty.

by Equation 2.2.

$$d_x = \begin{cases} 1 & \text{if } x = 0 \\ d_{x-1}\frac{\mathcal{T}}{\mathcal{T}'} & \text{if } x > 0 \end{cases} \tag{2.2}$$

At every block creation, the miner or pool of miners who successfully completes POW with a given difficulty will be compensated with a *coinbase* transaction. This transaction is included as the first transaction in every block and consists of the sum of transaction fees plus a block reward of newly mined Bitcoins, which is periodically halved every 210,000 blocks.

### 2.2.2 Avalanche and Proof-of-Stake

In 2018, a group of scientists, initially referred to as Team Rocket, published a novel metastable consensus protocol family for cryptocurrencies [24]. These protocols provide a high level of probabilistic safety in the presence of Byzantine adversaries and are claimed to be both fast and environmentally friendly, as they do not rely on POW-based blockchains. The protocol family includes a naïve implementation known as *Slush* and a more sophisticated consensus algorithm called *Snowball*, which serves as the backbone of the Avalanche protocol.

**Slush** Slush introduces the concept of *metastability* and serves as the foundation for this protocol family. It allows for the eventual reaching of consensus by choosing between two conflicting colors (blue and red in Figure 2.11) in $m$ rounds, where $m$ is a sufficiently large value. This algorithm is almost memoryless meaning that a node retains no state between rounds other than its current color and does not maintain a history of interactions with other peers. Each round involves randomly sampling a small, constant-sized group of $k$ nodes from the network, and once the querying node collects $k$ responses, it checks the color of the fraction $\geq \alpha k$, where $\alpha > 0.5$. The querying node adopts the winning color as its own and re-issues the query with a different set $K$. Even if peers are divided in a 50/50 split, the network will eventually reach a decision within $m$ rounds. However, Slush is not tolerant to Byzantine faults, as an adversary could attempt to flip nodes to the opposite color decision in an effort to maintain balance within the network. Figure 2.11 (1–2) shows the first of $m$ cycles for a blue-queried node (1), while Figure 2.11 (3–4) represents the second cycle for $m = 2$.

**Snowflake** Snowflake extends the Slush protocol by adding a *counter* that tracks a node's conviction about a particular color choice. This counter

stores the number of consecutive samples of the network that have all yielded the same color. Snowflake introduces BFT through the use of the parameter $\beta$, which indicates the counter threshold required to reach consensus. At every color change, the node resets $\beta$. Whenever a successful query ($\geq \alpha k$) occurs, the node increments the counter. Consensus is reached when the threshold $\beta$ is reached. The protocol preserves liveness, but it can be significantly delayed, as there is no finite counter $m$ present and $\beta$ can be reset every time there is a disagreement, leading to an ephemeral notion of state in Snowflake [24].

**Snowball** Snowball augments Snowflake by incorporating *confidence counters*. Each validator stores in memory its confidence level for each color. Mul-

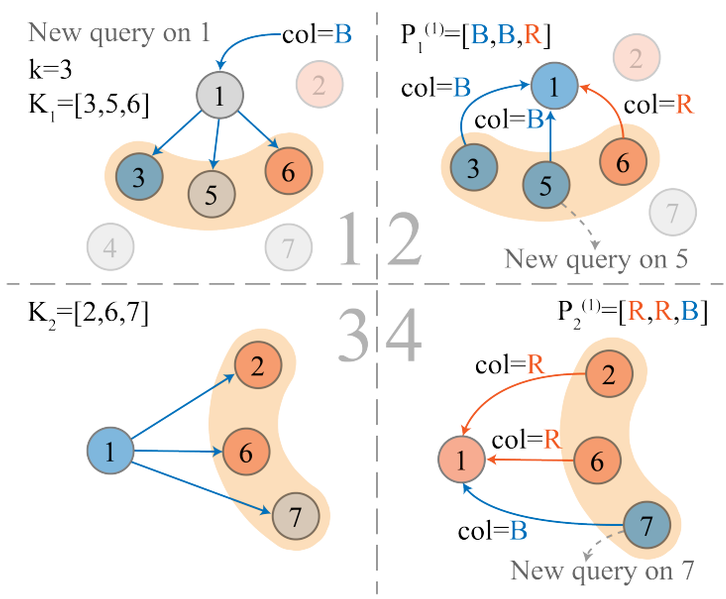


**Figure 2.11:** In the Slush protocol, during the first frame, node (1) is queried with the color blue. Node (1) then selects $k$ random nodes and sends its decision to choose blue. In the second frame, node (3) has already decided on blue, node (6) has been confirmed as red, and node (5) has not yet made a decision. Node (3) and node (6) reply with their preferred colors, while node (5) becomes blue and issues a new query with blue as the preferred color. The pool for node (1) at step $m = 1$, $P_1^{(1)}$, contains two blue and one red answer, so node (1) becomes blue. In the third frame, the $m = 2$ cycle is represented, and a new set $K_2$ is selected. Node (1) sends its blue view to the $k$ chosen nodes. In the final frame, node (1) turns red as its pool for node (1) at $m = 2$, $P_2^{(1)}$, has a majority of reds, while node (7) turns blue and issues a new blue query. The algorithm continues until the $m^{th}$ cycle.

tiple counters track the number of queries that have yielded a result of $\geq \alpha k$ for their corresponding color. Whenever a successful query occurs, the node increments its confidence counter for that color. A node will switch colors when the confidence level for its current color becomes lower than that of the other color. When a counter reaches the threshold of $\beta$, the current color is accepted. Snowball is more resistant to attack than Snowflake and serves as the backbone of the Avalanche protocol.

**Avalanche** Avalanche generalizes Snowball by implementing a dynamic, append-only DAG of all known transactions. Each DAG vertex contains a collection of items starting from the *genesis vertex*. The DAG structure offers two main benefits: (1) increased efficiency, as a single vote on a vertex implicitly means voting for all transactions on the path to the genesis vertex; and (2) improved security, as the DAG intertwines the history of transactions, making it difficult for an attacker to reverse a decision without the approval of the correct nodes, similar to the Bitcoin blockchain.

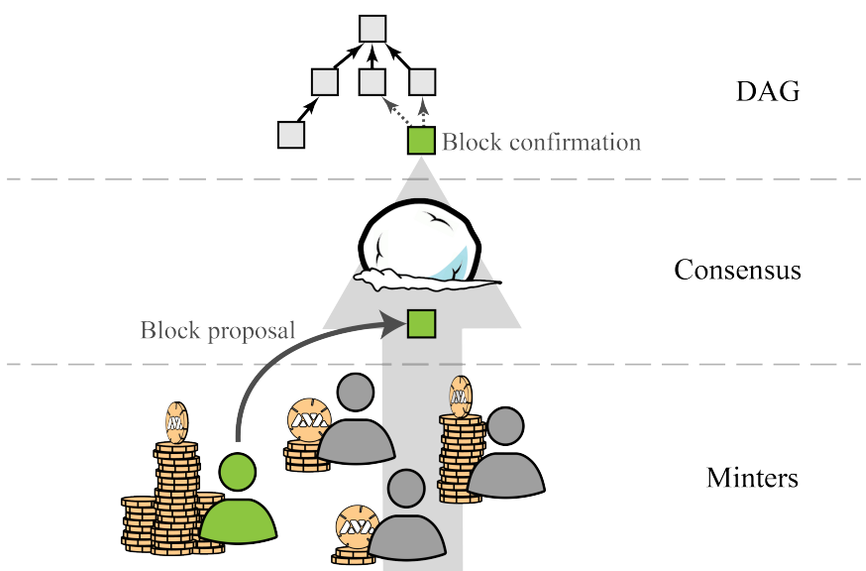


**Figure 2.12:** In Avalanche, Proof-of-Stake is used to determine the selection of a minter to propose a new block. The minter is chosen based on the amount of funds they have staked. Once the block is proposed, the minters must reach consensus on the solution using the Snowball consensus process. Upon successful consensus, the new block is added to the DAG.

### Proof-of-Stake

Proof-of-Stake is a consensus mechanism that reduces the computational cost of POW by requiring validators to put their funds at risk while participating in the consensus process. Miners in POS systems are referred to as minters, and the verification of nodes is not necessary due to the amount of stake held by the minters. In POS, the honest majority of computational power is replaced by the honest majority of stake values. To maintain the integrity of the single history of records in POS systems, minters must honestly verify new blocks to avoid having their stake slashed or destroyed. A pool of minters is selected at each round to review newly proposed blocks, with the validators chosen based on the amount of their stake. If a validator submits fraudulent transactions, their stake will be destroyed and they will no longer be able to participate in the system. On the other hand, honest minters are rewarded with additional coins.

Avalanche consensus does not solely rely on POS, but it also incorporates the substrate BFT-based-based consensus protocol earlier described, Snowball. POS is utilized in Avalanche to prevent Sybil attacks and preserve the anonymity of validators, while the stake of each minter plays a role in determining who will lead the BFT consensus at each round. Typically, validators with larger stake are more likely to be selected for block proposal, making it difficult for dishonest actors to execute a Sybil attack without risk of losing their funds. One major concern with POS is the potential for centralization, particularly when stake is based on financial resources. This can lead to a situation where the wealthy become even wealthier, making it financially prohibitive for many individuals to become validators and undermining the decentralization of governance. In Avalanche, the minimum required stake for a validator is 2,000 AVAX,[4] which is equivalent to $ 30,000 in May 2023.

### Directed Acyclic Graph

In contrast to a blockchain, DAGs do not impose a total ordering on transactions, instead providing a partial ordering of decisions. DAGs are constructed using a similar chain of cryptographic links logic as used in blockchains. For example, in Avalanche, each vertex in the DAG contains information about transactions, the chain ID, a list of parent IDs, the epoch, and the version. This information is hashed using SHA-256 to create a new vertex ID. The use of DAGs significantly

4. From Avalanche documentation at `https://docs.avax.network/nodes/validate/staking`

increases the frequency of block creation, as non-conflicting transactions can be included simultaneously in two separate vertices that have a common parent, as illustrated by the vertices *b* and *c* in Figure 2.13. At each vertex creation, the consensus mechanism establishes a shared view of the updated DAG.

### Consensus Comparison

To summarize, Table 2.1 presents a comparison of the characteristics of various consensus mechanisms. Ethereum was initially developed as a POW system. It then adopted a hybrid approach, using both POW and POS, where POW was used for more critical operations and POS was employed for the remainder. At the time of writing, Ethereum has fully transitioned to using POS. Avalanche implements both POS and BFT solutions. Finality in POW systems takes longer to achieve compared to Avalanche POS systems. In Bitcoin, for example, a transaction is considered finalized once it has been included in six consecutive blocks in the blockchain. However, the time it takes to create these blocks is relatively slow in POW systems. POS and BFT are generally faster and more environmentally friendly solutions, while POW offers a more robust system through the use of hash rate-based leader selection.

## 2.3 Machine Learning

ML algorithms are able to analyze large datasets and outperform humans in classifying new data based on what they have previously learned. In contrast to

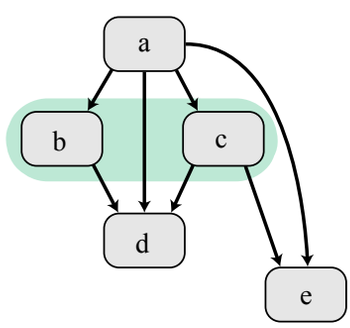


**Figure 2.13:** When DAGs are used as a blockchain, we can establish a partial ordering of the vertices. For example, we can determine that vertex *a* comes before vertex *c*, vertex *c* comes before vertex *e*, and therefore vertex *a* comes before vertex *e*. However, we have no information about the relative ordering of vertices *b* and *c*.

| Consensus mechanism comparison | | | |
|---|---|---|---|
| | **POW** | **POS** | **BFT** |
| **Leader selection** | Hash rate | Stake amount | Trust |
| **Energy consumption** | Significant | Negligible | Negligible |
| **Speed (txs/s)** | Poor | Good | Good |
| **Finality** | Poor | Good | Immediate |
| **Applications** | Bitcoin, Ethereum. | Ethereum, Cardano, Algorand, Avalanche. | Avalanche, Hyperledger Fabric, Ripple, Stellar. |

**Table 2.1:** A summary of various consensus mechanisms.

traditional programming, which uses predetermined patterns to process data and generate output, ML aims to create patterns by combining input data with its corresponding output. In this section, we will explore the key elements of ML and various types of ML models, with a focus on identifying the model that potentially is best suited for our classification task. We will also consider how large amounts of data available through public blockchains can be used to formally define patterns for inclusion, given that miners follow certain criteria for selecting transactions.

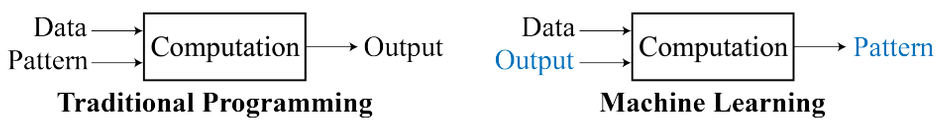


**Figure 2.14:** Traditional programming and ML.

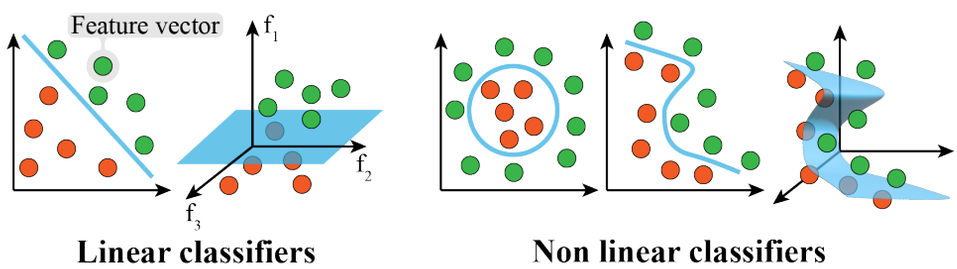


**Figure 2.15:** This figure illustrates linear and non-linear classifiers, with measurements for features depicted on different axes ($f_1$, $f_2$, $f_3$). Each point, depicted as either green or red, represents a labeled feature vector.

### 2.3.1 Elements of Machine Learning

ML is a discipline focused on developing and understanding algorithms that are able to learn from and improve their performance on a given task through exposure to data [112]. ML has a wide range of applications, including data clustering [113, 114], data transformation, and transfer learning [115]. In this thesis, we utilize ML as an automated classification machine. Given a dataset, our ML model must be able to label data that it has not seen before. In order to achieve optimal classification performance, it is important to select the most appropriate input features, which can be represented as a feature vector that uniquely identifies a single object. A set of feature vectors constitutes a training set, which is derived from the initial dataset and used to train the ML model for future predictions on new data. In order to solve a classification task, we can envision a classifier as a decision boundary that separates different classes, as depicted in Figure 2.15. In some cases, linear classifiers such as the perceptron, linear Support Vector Machines (SVM), or Least Squares Methods (LSM) can be used when the classes are linearly separable in two or more dimensions [39]. However, not all problems are solvable through linear methods, so other techniques such as k-means, Random Forest (RF) [116], kernel SVM, or Neural Network (NN) [117] may be employed.

For the purpose of this study, features such as transaction fee and size may be important, and a specific Bitcoin transaction can be represented as a feature vector belonging to a specific class. Based on the complexity and variety of features derived from the non-deterministic interaction of miners and users in the Bitcoin ecosystem, a solution that can address a wide range of tasks is required. Literature suggests that using a non-linear classifier is a safer option in terms of solvability for non-linear problems, as it is generally injective (i.e., if a problem is linear, it can also be solved as a non-linear problem, but not vice versa). Therefore, our approach follows this principle.

### 2.3.2 Types

The availability or scarcity of data plays a significant role in determining the methodology employed by a ML model for classifying data. When a set of labeled training data is available, the classifier is designed to utilize this prior knowledge to train itself in a pattern recognition task called supervised learning. When such information is not available, the given non-labeled training set is used to identify underlying similarities and cluster similar feature vectors together. This type of classification is known as unsupervised learning, and it is applicable to a variety of fields, including social sciences and engineering, such

as remote sensing, image segmentation, and image and speech coding [39]. Different algorithms can be used to implement each type of pattern recognition task, with variations in complexity, speed, or efficiency. Careful selection of the appropriate model algorithm can significantly impact the outcome of the clustering task.

**Supervised learning** The ML task of learning a function that maps an input to an output based on example input-output pairs is known as supervised learning [118]. In this approach, a function is inferred from labeled training data in order to map new, unlabeled examples. This is an optimal solution when the training set is representative of the overall distribution. Supervised learning models include SVM, k-Nearest-Neighbors (KNN), perceptrons, and Artificial Neural Network (ANN).

**Unsupervised learning** The ML task of learning patterns from unlabeled data is known as unsupervised learning. Unsupervised methods have the ability to self-organize and capture patterns as probability densities [119]. This approach is particularly useful when the training data is limited. Unsupervised learning models include clustering, k-means, and the Expectation–Maximization (EM) algorithm. An example of an unsupervised clustering task is shown in Figure 2.16.

Blockchains are public ledgers of data that can be accessed and read by anyone, resulting in a large amount of data that is always available and retrievable. Therefore, it is assumed that labeled data is always available and that the training set is representative of the overall distribution, with no missing data. Based on these assumptions, the classification task at hand requires a non-linear classifier and a supervised approach. As a result, ANNs, specifically Deep Neural Networks (DNNs), were chosen as the model of choice, as ML theory suggests that they are the most suitable solution for this problem.

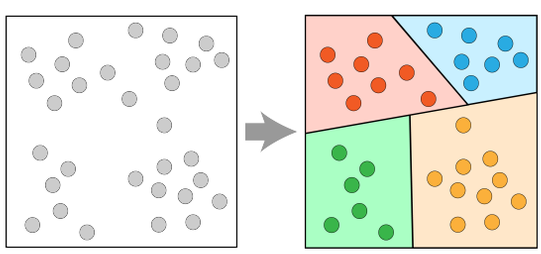

**Figure 2.16:** This figure illustrates a clustering task, in which unlabeled data is grouped into clusters based on a pattern that minimizes errors for feature vectors belonging to the same guessed cluster, using methods such as euclidean distance, probability density, or nearest neighbors.

### 2.3.3 Artificial Neural Networks

Artificial Neural Networks (ANN), or Neural Networks (NN) for short, are models inspired by the structure of the brain, including biological neurons and synapses. NNs are defined by Hopfield [120] as networks or circuits of biological neurons, or, in a technological context, as being composed of artificial neurons (or nodes). Each artificial neuron is a computational structure with multiple inputs and a single output. The building block of an NN model is the artificial neuron, and the simplest NN implementation consists of a single artificial neuron with a set of inputs and a single output.

#### Artificial Neuron

An artificial neuron, also known as a perceptron, is an algorithm used to learn a binary classifier, or *linear discriminant function*, that takes in a feature vector as input and produces a value $\psi(a)$ as output, where $a$ is the result of the weighted features plus the bias, and $\psi$ is an activation function that activates the neuron and forwards the final output. Figure 2.17 illustrates the feature vectors $\mathbf{f}$ and weights $\mathbf{w}$. The input to the activation function $\psi$ is then the dot product $\mathbf{f} \cdot \mathbf{w}$ plus the bias $w_0$, which is formalized in Equation 2.3. The bias term $w_0$ is a randomly initialized value that shifts the discriminant and increases the neuron's ability to classify inputs. If the number of features is $n$, then $a$ is given by:

$$a = \sum_{i=0}^{n} \mathrm{f}_i w_i + w_0 \tag{2.3}$$

The activation function is a non-linear function that is used to introduce non-

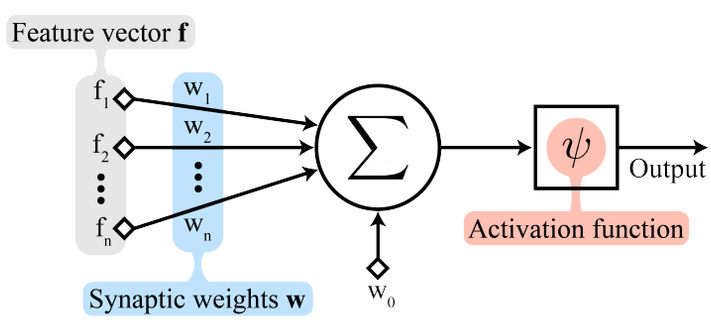


**Figure 2.17:** An artificial neuron, also known as a perceptron, receives a feature vector $\mathbf{f}$ as input and applies a set of weights $\mathbf{w}$ and a bias term $w_0$. The resulting output is then passed through an activation function $\psi$.

linearity into NNs. Without an activation function, a NN with $N$ layers can be reduced to a single linear layer, which is the linear combination of all the other layers. The activation function determines how information is propagated through the network. Some commonly used activation functions include:

**Unit step function** It sets the value to either 0 or 1, to elements that comes before, or after a certain threshold. This function works well with binary classifiers, but it is less suitable for problems concerning more than two classes. Formally $(a < 0) \rightarrow \psi(a) = 0$, and $(a > 0) \rightarrow \psi(a) = 1$. The neuron can either be active or non active, as the function can fire or inhibit the neuron.

**Sigmoid function** One of the most commonly used activation function. It is easy to analyze and to compute, and it provides a *soft* transition between 0 and 1, with a threshold of 0.5. The most used sigmoid function type is the *logistic function*: $\psi(a) = {}^{1}/_{1+e^{-a}}$. The resulting curve is more steep towards 0, meaning that $a \rightarrow 0$ values are mapped in a significantly distant space from each others. On the other hand, values for $a \rightarrow \pm\infty$ are mapped not far enough for the neuron to change its activation, and consequently, it will learn slowly or not learn at all. This is know as the *vanishing gradient problem*. The output is a continuous value.

**Rectified Linear Unit** The Rectified Linear Unit (ReLU) activation function is defined as the positive part of its argument: $\psi(a) = a^{+} = max(0, a)$. It is widely used because it is computationally efficient, as only comparison, addition, and multiplication are involved. It offers a better gradient propagation, with fewer vanishing gradient problems compared to sigmoidal activation, as ReLU only activates after a certain threshold, and not in both directions [121], it is scale-invariant, as $max(0, ba) = b\, max(0, a)$ for $b \geq 0$.

**Softmax function** The softmax function is often referred to as normalized exponential function, and it is a generalization of the logistic function to multiple dimensions. It is also commonly used as the *last* activation function of a NN. The softmax function is used for multi-class classification in ANN, and it normalizes the network output to a probability distribution for every predicted class.

The implementation discussed in this dissertation utilizes a DNN with softmax and ReLU activation functions.

### Deep Neural Networks

The NN architecture consists of multiple artificial neurons that are connected together. Each neuron utilizes algorithms to process mathematical equations, such as multi-dimensional polynomials (as described in Equation 2.3). Figure 2.18 illustrates a multi-layer NN with one hidden layer, input features ($f_1$ and $f_2$), and two potential outputs (green and red). In this model, the neurons are organized into layers, with each layer fully connected to the preceding one. The output of each artificial neuron in the previous layer serves as an input for each neuron in the subsequent layer, as depicted by the arrows in Figure 2.18. This type of ANN is referred to as a fully connected NN.

A NN model learns through the process of training. The resulting trained NN model is representative of the specific dataset it was trained on, so it is important that the training set accurately reflects the desired pattern for the classification task. Each input in the NN has a weighted parameter, allowing for the classification impact of each input to be controlled and adjusted as necessary. Every layer in the NN handles dependencies by calculating the values of adjacent inputs, creating both weak and strong paths through the network based on the activation functions. It is challenging to represent the information contained within a NN model, and it is common for two NN models trained on the same dataset to have different content.

The perceptron employs a discriminant function to linearly separate classes.

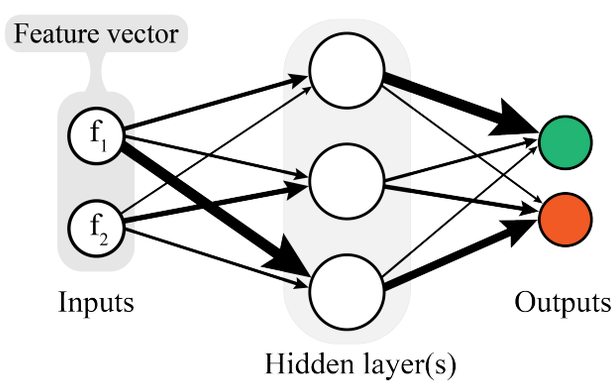


**Figure 2.18:** A fully connected Artificial Neural Network is depicted, with inputs, one hidden layer, and outputs represented. Each input constitutes a feature vector, and the hidden layer(s) can consist of one or multiple layers. The connections between the various components of the ANN are weighted according to the strength of the relationship between a particular feature and its corresponding outcome.

In cases where this is not possible, and the classes are not linearly separable, an arbitrary number of neurons (and therefore discriminant functions) can be added to separate the classes. An example of this can be seen in Figure 2.19, which depicts the OR and XOR problems plotted on a two-dimensional plane. While the OR task can be solved with a single neuron (shown on the left plane in Figure 2.19), due to its linear separability, the XOR problem requires a non-linear classifier. The right plane of Figure 2.19 illustrates that two discriminant functions can be used to efficiently classify the elements, meaning that two perceptrons arranged in parallel (forming a layer of neurons) can be utilized to solve this classification task.

Neural Networks are considered deep if they consist of more than one hidden layer. Each layer trains a distinct set of features, which are determined by the output of the previous layer. The hidden layers can be understood as an ensemble of perceptrons that are arranged in parallel in order to solve nonlinear classification tasks, and in series in order to combine previous information with a new classification task. The use of weight calculations and dot products limits the input data to be either floating point or integer values. In cases where the points in the multidimensional space are widely scattered, it is often necessary to employ *normalization* techniques.

Backpropagation is a key component of NNs. It calculates weight gradients, allowing the network to be trained by minimizing the loss function. This is achieved through backward passes, updating the weights to bring the output closer to the target [122]. The frequency of backpropagation depends on the batch size of the training set. Negative gradients are propagated and weights are adjusted to reduce errors within each batch. Training occurs over multiple passes (epochs) of the entire dataset. The required training time is indeterminate, as it depends on the distance the weights must move to

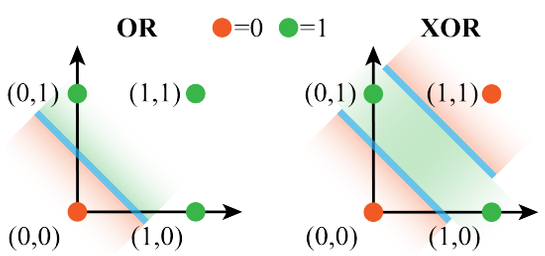


**Figure 2.19:** The OR and XOR problems demonstrate that a single perceptron is unable to effectively distinguish between ones and zeros when plotted on a two-dimensional plane using the XOR operation. However, the OR problem can be solved through linear means.

reach a solution. The minimum number of neurons, layers, and weights is also indeterminable.

### Residual Neural Networks

Residual Neural Network (ResNet) implements skip connections in NN. The construction of DNN using this technique is provided in a way to bypass certain layers of the network. In a standard DNN, each layer is connected to the subsequent layer such that the input to a given layer is the output of the preceding layer. In contrast, skip connections allow the input to be passed directly to a layer that is further down the network, effectively creating a shortcut. This way, the network can learn not only from the output of the preceding layer but also from the input itself, resulting in better training and more accurate predictions.

Skip connections were first introduced in the ResNet architecture in 2015 [123]. Since then, they have become a popular technique in neural network design, particularly for DNNs with many layers. By providing a way for information to flow directly through the network, skip connections can help prevent the vanishing gradient problem that can occur in very deep networks. This can lead to improved performance and faster convergence during training, despite their effectiveness may depend on the specific problem being addressed. In our study, it has been determined that the implementation of the ResNet architecture is more effective and useful than standard DNN models.

## Summary

This chapter provided a comprehensive overview of blockchain technologies and their applications in cryptocurrencies. It covered the historical development of blockchain, and the advantages and disadvantages of using blockchains in various business sectors are explored. The chapter focused on explaining POW and POS consensus mechanisms applied to cryptocurrencies such as Bitcoin and Avalanche. The consensus protocol of Bitcoin is discussed, highlighting its limitations at scale and alternative consensus mechanisms employed in cryptocurrencies. Furthermore, a brief introduction to ML is provided, and its role in this research is explained, including the specific ML models that have been adopted.

# 3

# The Fee Market in Bitcoin

In this chapter we unravel principles and rules governing the Bitcoin ecosystem at scale, focusing on user-miner equilibria and showing how these parties depend on one another. We explain how miners make profits, what are their resulting costs, and how such factors are crucial for transactions inclusion. We discuss how a fee market emerges in PoW-based blockchains, describing the auction schemes that miners could adopt, and how this can lead to fee dynamism in Bitcoin. Notions of cryptocurrencies and PoW explained in Section 2.2 are useful for understanding mechanisms and reasons behind main issues in Bitcoin, including expensive fees, low throughput, and high energy consumption. In this dissertation, we focus on high fees and overpaying, we study how miner's criteria for transactions inclusion changes over time, and how these regime shifts are dictated by the mass adoption of Bitcoin and its inner throughput limitations, favoring a fee market to emerge. The study of such market is fundamental for our purpose of formalizing a transactions inclusion pattern.

## 3.1 Profits in Proof-of-Work

In this section, we investigate mining revenue and costs. We formalize the profit equation and calculate the cost of mining with and without fees. For that

we take into account various parameters, such as electricity and Bitcoin prices and individual and total hash rates. As we discuss in Section 2.2.1, the security of the Bitcoin network increases as the number of miners grows. However, we also show that the individual cost of mining rises in tandem with the total hash rate, prompting rational miners to develop strategies for optimizing their profit. This makes their critical role in securing the network more expensive than originally intended, and therefore, it is essential to explore the sources of profit for the sustainability of the system.

### 3.1.1 Formalization

In Section 2.2.1, we discussed coinbase transactions and explained that the concept of *creatio ex nihilo* does not apply to digital tokens, as a certain amount of computational work is required to secure the network. The coinbase transaction enables miners to generate revenue from two sources: (1) transaction fees, denoted as $M$; and (2) block reward, denoted as $R$. However, explaining miners' profit solely in terms of coinbase transactions is overly simplistic. Rizun [9] formalizes miners' profit, denoted as $\langle \Pi \rangle$, as the difference between revenues $\langle V \rangle$, and costs $\langle C \rangle$, as shown in Equation 3.1.

$$\langle \Pi \rangle = \langle V \rangle - \langle C \rangle \tag{3.1}$$

The expected cost for a single miner, denoted as $\langle C \rangle$, is formally defined in Equation 3.2 as the product of its hardware's price per hash, denoted as $\eta$, its hash rate, $h$, and the time required to mine a block, denoted as $\mathcal{T}$.

$$\langle C \rangle = \eta h \mathcal{T} \tag{3.2}$$

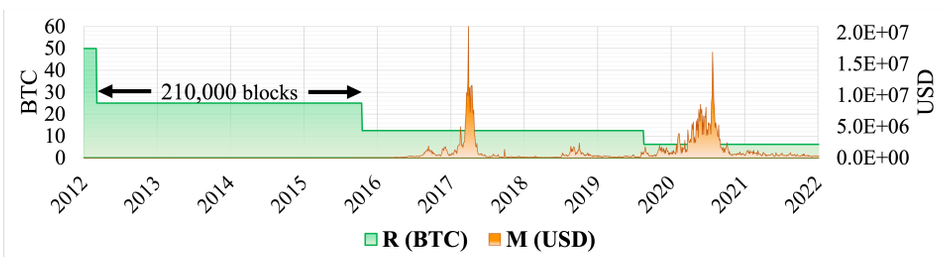


**Figure 3.1:** Block reward $R$ (BTC) and transaction fees $M$ (USD) are represented respectively on the left y-axis, and on the right y-axis. Public data of Bitcoin fetched from blockchain.com at `https://www.blockchain.com/explorer/charts`

The expected revenue from mining is given by the earnings from the coinbase transaction, denoted as $M+R$, multiplied by the probability of orphaning,[1] based on the individual miner's hashing power relative to the total hash rate of the Bitcoin network, denoted as $H$. The expected revenue, denoted as $\langle V \rangle$, is formalized in Equation 3.3.

$$\langle V \rangle = (R + M)\frac{h}{H}(1 - \mathbb{P}_{orphan}) \tag{3.3}$$

Replacing equations 3.2, 3.3, and A.1, with Equation 3.1, the *miner's profit equation* is defined as:

$$\langle \Pi \rangle = (R + M)\frac{h}{H}e^{-\frac{\tau}{\mathcal{T}}} - \eta h \mathcal{T} \tag{3.4}$$

A rational miner's goal is to maximize $\langle \Pi \rangle$, which is inversely proportional to the total hashing power of the Bitcoin network, but directly related to three main factors: (1) the reward and transaction fees ($R + M$), (2) the individual hashing power ($h$), and (3) the probability of *not* orphaning the block just mined ($1 - \mathbb{P}_{orphan}$). The individual hashing power's margin for increasing revenue is minimal, as it is normalized with the total hash rate of Bitcoin. Additionally, reducing the probability of orphaning a block would require reducing the orphaning rate of the network, which a miner cannot directly control. Considering that factors (2) and (3) have a diminishing effect on a miner's potential earnings, it can be concluded that a rational miner can earn additional revenue solely from factor (1). Figure 3.1 illustrates the proportion of miners' earnings over time. As the mining reward is periodically halved every 210,000 blocks, *transaction fees become the main source of revenue for miners in the long run.*

### 3.1.2 Calculations

To support our previous statement, we analyzed real-world miners' profit using the revenue and cost equations above. We observed that with a zero-fee policy, miners struggle to make any profit and instead lose money unless the electricity price is near zero. To conduct this analysis, we assume that miners are using Antminer S19 Pro, which has a hashing rate of 110 TH/s and a Miner Power Efficiency (MPE) of 29.55 J/TH. We then examine electricity prices ($e_p$) for countries with low (Qatar with 0.032 $/kWh), medium (U.S. with 0.162 $/kWh), or high (Denmark with 0.469 $/kWh) costs. Finally, we adapt Rizun's equations

1. Detached or orphaned blocks are valid blocks that are not part of the main chain. They can occur when two miners produce blocks at the same time, and one block gets discarded because of higher propagation delay. See Appendix A.1

to calculate the daily profit assuming a block creation time of ten minutes, a Bitcoin price of $15,000, and minimum and maximum fees of $1 and $70, respectively. We ignore the orphaning rate as it was recorded to be 0.31 % of blocks mined per day from 2014 to 2017[2], and Shahsavari et al. [124] measured it to be even lower at 0.09 %, resulting in a negligible decrease in daily revenue if the block size is kept at 1.1 MB. We calculate the daily profit $\langle \Pi \rangle_{\text{day}}$ as:

$$\langle \Pi \rangle_{\text{day}} = \langle V \rangle_{\text{day}} - \langle C \rangle_{\text{day}} \tag{3.5}$$

if $s = 86{,}400$ seconds in one day, we have:

$$\langle V \rangle_{\text{day}} = g_B \frac{h}{H} B_{\text{day}} \qquad g_B = (R \times \text{BTCP}) + M \qquad B_{\text{day}} = \frac{s}{\mathcal{T}}$$

$$\langle C \rangle_{\text{day}} = e_p \eta_{\text{day}} \qquad \eta_{\text{day}} = s\eta h \qquad \eta = \frac{\text{MPE}}{3.6 \times 10^{12}}$$

Since 1 W = 1 J/s, the cost per hash in kWh/TH can be calculated by dividing the MPE by 60 seconds/minute × 60 minutes/hour and then by 1,000 W/kW. Since $\eta$ is represented in kWh/hash, it is further divided by $10^{12}$.

Figure 3.2 shows profit calculations for miners using Antminer S19 Pro in different countries. It is evident that, with the selected Bitcoin price of $15,000 and a reward of ₿6.25, it is not feasible to expect low fees. In fact, with a uniform fee of $1, mining is only profitable for individuals where the electricity price is near zero. With the current Bitcoin hash rate, it is not possible to profit with a uniform fee of $1 in the U.S., and a rational miner should not try to recover from this loss by increasing their individual hash rate, as this will only increase their mining costs. Looking at the first U.S. plot in Figure 3.2 and fixing the x-axis value at the current Bitcoin hash rate while moving along the y-axis, we can observe a downward profit trend as the individual hash rate increases.

As shown in Table 3.1, the price of Bitcoin also plays an important role in determining profit. However, this price cannot be controlled by miners, and the uncertainty associated with it means that adopting a uniform fee of $1 will lead to a loss of profit in many different scenarios, such as changes in the Bitcoin price, increases in the total hash rate, or shifts in electricity prices. Table 3.1 also considers the upcoming scenario of halving the reward. It shows that even with a uniform high fee of $70 per transaction, miners will have little profit unless the Bitcoin price increases again above $30,000.

2. According to data stored in blockchain.info at `https://www.blockchain.com/explorer/charts/n-orphaned-blocks`

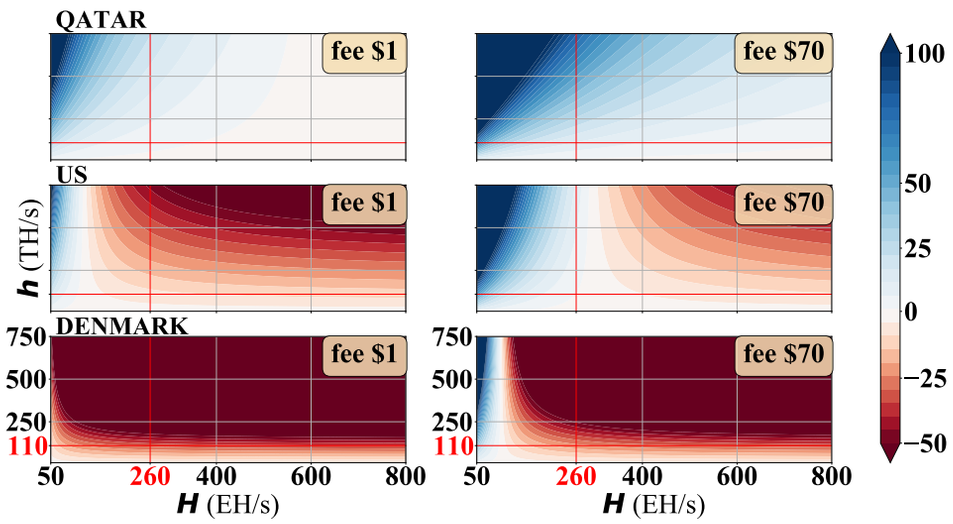


**Figure 3.2:** The profitability of Bitcoin mining operations is influenced by several factors, including the miner's individual hashing power (e.g., 110 TH/s per second for the Antminer S19 Pro) and the overall hash rate of the Bitcoin network (currently 260 EH/s). In this analysis, the cost of electricity is considered for three countries: Qatar, the United States, and Denmark, with average fees ranging from $1 to $70. The daily profit for these miners is estimated to fluctuate between a loss of $50 and a gain of $100, depending on the specific market conditions.

| $e_p$ ($/kWh) | Daily profit in U.S. dollars with $1 fee | | | | | |
|---|---|---|---|---|---|---|
| Bitcoin price ($) | 1000 | 10000 | 15000 | 30000 | 60000 | 100000 |
| Qatar : 0.032 | -1.99 | 1.43 | 3.33 | 9.04 | 20.47 | 35.7 |
| US : 0.162 | -12.13 | -8.7 | -6.8 | -1.09 | 10.33 | 25.56 |
| DK : 0.469 | -36.08 | -32.65 | -30.75 | -25.04 | -13.61 | 1.61 |
| | Daily profit in U.S. dollars with $70 fee | | | | | |
| Qatar | 6.41 | 9.84 | 11.74 | 17.45 | 28.87 | 44.1 |
| US | -3.72 | -0.3 | 1.6 | 7.31 | 18.73 | 33.96 |
| DK | -27.67 | -24.25 | -22.34 | -16.63 | -5.21 | 10.01 |
| | Daily profit with $70 fee and halved $R$ | | | | | |
| Qatar | 6.22 | 7.93 | 8.88 | 11.74 | 17.45 | 25.07 |
| US | -3.91 | -2.2 | -1.25 | 1.06 | 7.31 | 14.92 |
| DK | -27.86 | -26.15 | -25.2 | -22.34 | -16.63 | -9.01 |

**Table 3.1:** The profitability of the Antminer S19 Pro mining operation is influenced by fluctuations in both the market price of Bitcoin and the cost of electricity. At present, the Bitcoin network's hash rate is measured at 260 EH/s.

#### Why do fee-markets emerge?

As Bitcoin's popularity grew, the number of miners and total hash rate increased, resulting in a significant loss in miners' revenue. This popularity also translated into more transactions being submitted per second, leading to increased competition for inclusion due to the inherent throughput limitations of POW (1 block every 10 minutes). As discussed in Chapter 3.1.2, rational miners cannot rely on the price of Bitcoin for revenue, and they should not attempt to compensate for the loss of profit due to the rise of the total hash rate ($H$) by increasing their individual hashing power ($h$). Their mining power would be outperformed by $H$ regardless of any individual boost, and the total costs would increase. The only rational way for miners to continue profiting is to change their behavior towards transaction inclusion in a profit-oriented manner, focusing on *fees* and *transaction size*.

## 3.2 Auction Market Types

This section presents different auction schemes that can be adopted by miners when fee markets emerge in POW-based blockchains. In an auction market, buyers and sellers enter competitive bids simultaneously, and the good trades when the highest bidding price matches the lowest selling price. This competitive bidding process helps determine the equilibrium price at which the market clears and the trade is executed. For POW-based cryptocurrencies, miners act as auctioneers while users are bidders. The users are *buying space in the next mined block*, while the miners are *selling their block space availability* as competition increases. In the largest blockchain implementations of Bitcoin and Ethereum, miners have adopted different inclusion schemes over time, including the well-known First-Price Sealed-Bid Auction (FPSBA), Uniform-Price Auction (UPA), and Second-Price Auction (SPA).

### 3.2.1 First-Price Sealed-Bid Auction

A FPSBA is a common type of auction in which all bidders simultaneously submit sealed bids, unknown to other participants. The highest bidder pays the submitted or truthful price. For POW-based blockchains governed by miners who use FPSBAs, users propose their transaction fees without knowing the bids of other users. If their transactions are included in a block, the submitted bids will be paid. While Bayesian Nash equilibrium (BNE) (see Appendix A.3) is efficient for FPSBAs with identical items and symmetric bidders, these equilibria

are unlikely to occur in practice. The result is a strategic bidding scheme in which transactions initially bid low and then increase their fee if approval is taking too long. This scheme leads to fee instability in Bitcoin, particularly when the number of transactions to be processed increases and bidders fear being left out of the next mined block. Figure 3.3 shows different outcomes for two bidders. The first bidder, who submits tx1, overpays for their space in the block due to incorrect assumptions about other sealed bids, while the second bidder, with tx2, is able to be included with a minimal fee increment.

### 3.2.2 Uniform-Price Auction

The UPA scheme, as depicted in Figure 3.4, charges each bidder with the price paid by the lowest included bid. The concept behind this approach is that any bidder can offer as much as they believe their transaction is worth, regardless of the size of their bid. This means that a bidder's bid may be high, but they will not necessarily have to pay that amount unless every other offer is equally high. This scheme allows bids to affect only their inclusion in the next block, and not the price paid (non-truthfulness concept).

If a bidder offers a price of $x$ for a transaction $t_x$ and that transaction is included in a block, the bidder will pay a fee that is less than or equal to $x$. If the minimum price required for inclusion in the block is higher than $x$, the

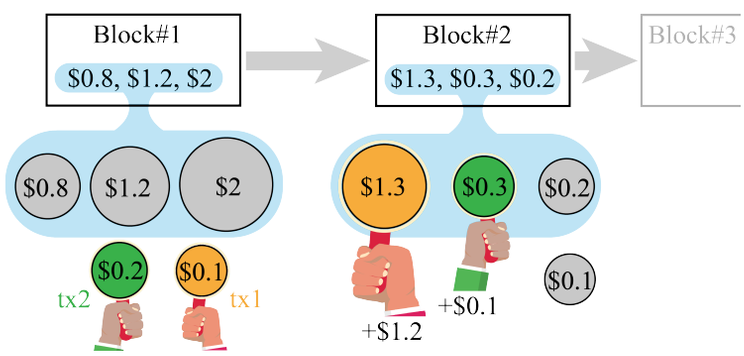


**Figure 3.3:** In this scenario, Users 1 and 2 submit transactions tx1 and tx2, respectively, but the fees they have paid are insufficient to be included in Block 1. User 1 then proposes a new bid using the average of all fees in Block 1. However, the other bids in Block 2 are considerably lower, resulting in User 1 overpaying for their transaction. User 2 instead decides to slightly increase their fee without taking into account the fees of previous transactions, and in this particular case, this strategy is successful. When miners adopt the FPSBA scheme, fee unpredictability is common.

transaction will not be included since the bidder is not willing to pay more than $x$.

Despite this solution generally preventing overpayment, in a fee market governed by rational and profit-oriented miners, it can result in two major weaknesses: (1) a block proposer can include their own transactions in a block in order to increase the clearing accepted price (as illustrated by the red $ 2 transaction in Figure 3.4); (2) a block proposer could collude with some portion of bidders, asking them to submit higher offers and then refunding them through a separate channel. These attacks are possible because a bidder can substantially boost a miner's revenue by making only a slight increase in their bid. In contrast, the FPSBA does not exhibit this vulnerability.

### 3.2.3 Second-Price Auction

Even though the FPSBA method discourages auctioneers from including their own transactions, bidding the true valuation can at times hinder the achievement of Nash equilibrium. An alternative solution, known as the SPA, or Generalized Second Price (GSP), is a non-truthful bidding method for multiple items. In this scheme, each bidder places a bid and, if there are more bids than available slots ($N > K$), the slots are assigned from the highest to the lowest bid. Unlike the FPSBA, the highest bidder pays the second-highest bid, the

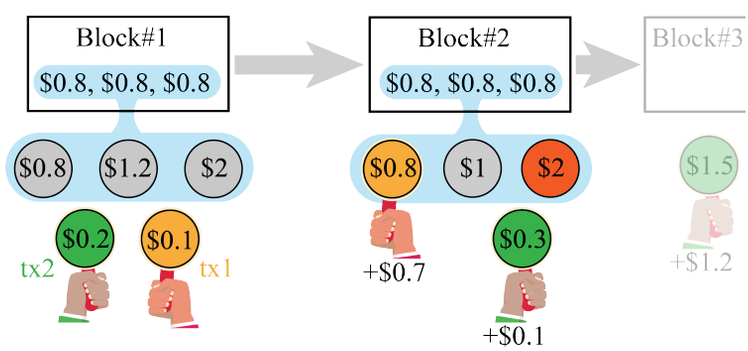


**Figure 3.4:** In this scenario, Users 1 and 2 submit transactions tx1 and tx2, respectively, but the fees they have paid are insufficient to be included in Block 1. User 1 then offers the previously accepted fee of $ 0.8, while User 2 slightly increases their fee. Although User 1 does not overpay, a rational and profit-oriented miner may still choose to exclude User 2's transaction and include one of their own transactions instead (e.g., the red $ 2 one) in order to raise the clearing price to $ 0.8 rather than receiving a uniform compensation of $ 0.3, as no other bidder was offering more.

second-highest bidder pays the third-highest bid, and so on. This is illustrated in Figure 3.5, where each bidder, if their bid is among the top $K$ bids (top 3 in Figure 3.5), pays the highest bid before their own. In this example, tx1 is among the top 3 bids for Block 2 with $k = 2$, and therefore it pays the $k = 3$ bid.

Designing a mechanism to improve the FPSBA in Bitcoin is challenging, as an SPA scheme can easily be manipulated by miners who can submit fake transactions after observing the fees in the mempool. Miners can use any criteria for including transactions and can manipulate the results of the auction after learning the proposed fees, which can lead to overpayment as shown in Figure 3.6.

## 3.3 Evolution of Transaction Fees

The policies that miners follow for the inclusion of transactions in blocks are not publicly known, making it difficult to determine the adopted auction scheme and the preferred patterns used by validators. However, it is known that transaction fees in the Bitcoin network have evolved from a mining-based structure to a market-based ecology [125]. The distributed nature of Bitcoin and the absence of a central authority contribute to a dynamic fee structure that can be unpredictable due to a range of endogenous and exogenous factors.

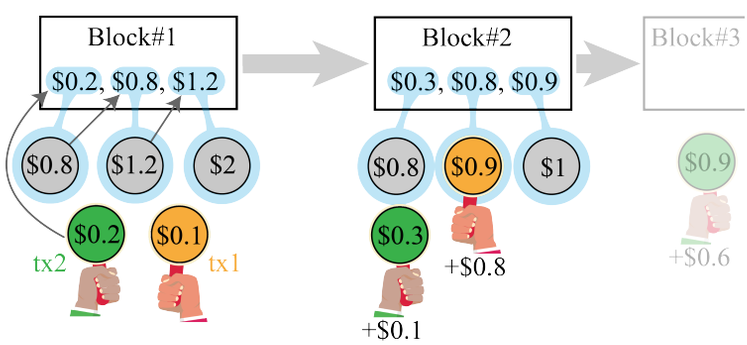


**Figure 3.5:** In this scenario, Users 1 and 2 submit transactions tx1 and tx2, respectively, but the fees they have paid are insufficient to be included in Block 1. Despite this, tx2's fee is used to pay for the last bid included in Block 1. User 1 then offers a higher fee of $ 0.9, while User 2 only slightly increases their fee without being aware of the auction scheme adopted by miners. As a result, User 1's transaction is included in Block 2 at position $k = 2$, with a fee pool of [1, .9, .8, .3]. This means that User 1 pays the bid of the user in position $k = 3$, which is $ 0.8.

This section discusses the implications of these changes and provides an overview of previous research on high fees, POW limitations in terms of scalability and throughput, and the factors that influence miner behavior. Early works in 2014 [126, 127] anticipated the high fee issue before it occurred, and later research in 2017 [65, 57] examined the relationship between transaction fees and latency. Understanding the evolution of transaction fees in Bitcoin is important as it can provide insight into the potential evolution of fee markets in other POW-based systems at scale.

### 3.3.1 Donations for Miners

The Nakamoto [8] paper states that Bitcoin is designed as a low-cost payment scheme, with occasional fees serving as an incentive for miners:

> "*The incentive **can also** be funded with transaction fees.*"
>
> Nakamoto [8]

The quote suggests that miners can often ignore transaction fees. Furthermore, in the official online documentation of Bitcoin before 2014 [126], we read:

> "*At the moment, many transactions are typically processed in a way where no fee is expected at all, but for transactions which draw coins from many bitcoin addresses and therefore have a large data size, a small transaction fee is usually expected.*"

While such statements may be true in relatively small environments, they do not take into account global Bitcoin adoption. Already in 2014, the study of Kaskaloglu [126] discussed the issue of high fees. The author argues that an increase in transaction fees in Bitcoin is inevitable, transforming the so-called *donations* into real fees. Donations are financially unsustainable in the long term for two reasons: (1) the cost of mining, and (2) mitigating the 51 %attack. The cost of mining depends on electricity prices and the variation between individual mining power and the total hash rate. To mitigate the 51 % attack, a majority of hashing power must remain honest, leading security in Bitcoin to follow the principle of *the more miners the merrier*, which in turn increases mining costs.

Bitcoin is also highly energy inefficient by design, and to prevent Sybil attacks, the work required to secure blocks must be difficult for miners but easy to verify for any verifier, as a form of nondeterministic polynomial time (NP) decision problem. The predetermined parameter $\mathcal{T}$ makes it impossible to speed up

the mining process, and as the total network hash rate increases and costs rise, miners must find new ways to generate profits. Other exogenous factors such as difficulty, Bitcoin price, and cost of mining can change in a dynamic ecosystem of miners, investors, and users, resulting in an unpredictable scenario for determining fees and prices.

Distributed governance enables Bitcoin to transition from its current operational mode, where transaction fees are mostly a voluntary tip to miners, to a situation where a *fee market* effectively regulates all traffic. With such a fee market, low-fee transactions may potentially remain pending for hours, days, or even weeks while waiting for approval and inclusion by a miner. As the energy demands of the Bitcoin network increase and mining becomes more costly, the transition to a fee market becomes more evident. Despite being designed as a low-cost payment scheme, the system has become expensive for all parties involved.

### 3.3.2 Fee is Mandatory

Later studies began to examine miners' behavior with respect to transaction fees. In 2015, Möser and Böhme [127] acknowledged the role of fees as a critical factor in the stability of the system. The study provided empirical evidence of agents' behavior regarding payment of transaction fees, along with several regime shifts caused by changes in the default client software. The research demonstrated the trend of a long-established POW-based blockchain moving towards a fee-oriented market. Two years later, Bitcoin experienced a significant scalability issue with regard to transactions. Blocks became saturated and miners started to reject zero-fee transactions, in what appeared to be a fixed price auction scheme.

In 2017, we conducted a study [65] that investigated the relationship between fees and waiting times. Our findings suggest that latency and fees are inversely related, although spending more than 300 sat/byte was found to be ineffective.

In 2019, Easley et al. [125] examined endogenous and exogenous features of Bitcoin. Endogenous properties, which can be changed internally by users or miners, include transaction fees and the voluntary inclusion of transactions by miners. In contrast, exogenous properties, which are imposed by the Bitcoin protocol, include factors such as block size, network difficulty, and block reward. Although waiting time is influenced by both endogenous and exogenous factors, not all external factors affect transaction inclusion. For example, block reward

($R$) does not impact waiting time. If delays are reasonable, a FPSBA scheme may be effective, as transactions carrying a minimum fee will eventually be included. However, as the number of transactions per second increases, FPSBA has been shown to be a costly solution for users.

### 3.3.3 Overpaying

Figure 3.6 illustrates the average transaction fee per transaction in Bitcoin from 2016 to 2022. From this data, we can observe that the scheme adopted by miners led to excessive fee payments, particularly when blocks were saturated in 2017 and 2022. The FPSBA scheme has failed to provide users with stable prices for their services, and historical analysis shows that Bitcoin users could have saved $ 272,528,000 in transaction fees, while miners could have reduced the variance of fee income by an average factor of 7.4 times [128]. Clearly, an FPSBA market is unsuitable for large-scale POW blockchains. The market does not provide stable coin prices, resulting in unpredictable transaction fees and enormous variance. Additionally, capacity and demand do not always align, forcing users to overpay for space in the block.

In 2018, Ethereum co-founder Vitalik Buterin proposed improving how miners in Ethereum are paid by adopting the UPA scheme [129], which benefit both miners and users. As discussed in Section 3.2.2, the proposed solution mitigates overpayment as no transaction affects the fee paid by other transactions. However, it also has major drawbacks, such as the potential for malicious miners to increase the fee paid by every bidder.

The study of Messias et al. [130] reveals that miners in practice deviate from

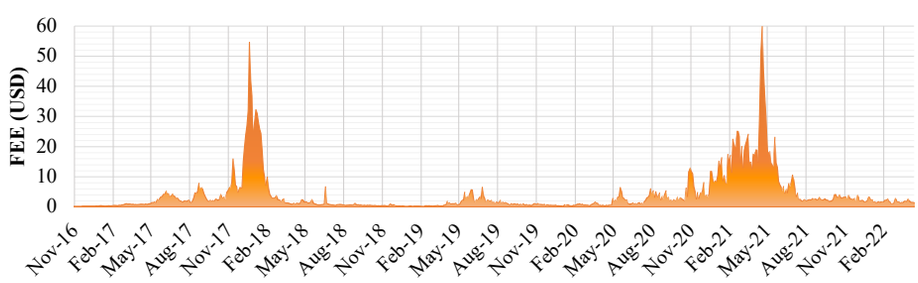


**Figure 3.6:** The chart shows the daily average of Bitcoin transaction fees in USD from 2016 to 2022, with significant unexpected spikes that result in excessive fee payments for users. Data source: blockchain.com at `https://www.blockchain.com/explorer/charts/fees-usd-per-transaction`.

the FPSBA scheme and instead adopt alternative strategies. A commonly used approach by many fee estimators is to adopt the *fee-per-byte* dequeuing policy, where transactions are ordered by their feerate (fee per byte) rather than by their fees. This has significant economic implications for users, as overpayment is the norm. Messias et al. [130] demonstrate that in June 2019, more than 30% of transactions offered a feerate that was two orders of magnitude higher than the minimum recommended.[3]

Basu et al. [128] introduce a mechanism inspired by the GSP, where each transaction is assigned a value. Every bidder knows their assigned value and the number of bidders, but not the values assigned to other bidders. Prices are paid using a UPA, where all bidders pay the $(K+1)^{th}$ bid. This could be a potential solution for Bitcoin if miners could commit to an auction form and the protocol could use bids to resolve payments. Another variant of the GSP auction model is presented by Li et al. [131, 132], where they employ a novel *rank-by-cost* rule to order transactions. The cost is calculated using the user-submitted fee and the waiting time. With this approach, they show that the daily saved fees for users can reach an average of ₿ 24.5985. Our model for transaction inclusion does not rely on a single auction scheme. Instead, we group the possible $K$-slots available at every block epoch and use a novel ranking system based on *feerate*, *waiting time*, and *current space available in the block* to generate a scheme that is likely followed by miners.

### 3.3.4 Miners and Users Equilibria

Figure 3.7 compares the evolution of transaction fees with exogenous factors such as the total hashing rate in Bitcoin and the number of new incoming transactions in the mempool. The first plot shows that the hashing rate, which affects difficulty, does not appear to have a significant impact on transaction fees. Drops in the total hashing power are caused by miners leaving the network (e.g., May-June 2021), as they no longer have incentives to continue mining due to low fees or high mining costs. The overall hashing rate has followed a monotonically increasing trend, indicating that it has always been profitable for miners to mine. The second plot in Figure 3.7 shows that the mempool count and transaction fees follow a similar trend. Although we acknowledge that correlation does not imply causation, an understanding of POW ecosystems can help us make educated conjectures about miner behavior. We observe that when the rate of incoming transactions is low, fees tend to be lower. However, as the mempool starts to fill, the equilibrium shifts, and only high-fee transactions

3. $10^{-5}$ BTC/kB $\equiv$ 1,000 sat/kB $\equiv$ 1 sat/byte, according to Bitcoin Core

are included by miners. In May 2017, the influx of new incoming transactions saturated the mempool, resulting in high fees (in BTC) but low relative USD value due to the favorable BTC-USD conversion rate for USD fees.

The transaction fee equilibria between miners and users must take into consideration a range of factors, such as the price of Bitcoin, the cost of electricity, and network difficulty, which exhibit strategic complementarity. Often, such equilibria are Pareto-ranked,[4] as transaction fees can lead to user non-participation, and conversely, low fees can cause miners to exit the market. The unpredictability of POW-based blockchain systems at scale, coupled with the insecurity stemming from the uncertain non-inclusion of transactions, can result in overpayment. Increasing transaction fees may attract more miners, but it also raises the difficulty level, thereby increasing the costs of mining. This demonstrates that higher revenue does not necessarily equate to higher profits. Figure 3.8 presents the calculation of the revenue over time for a single miner using Antminer S7 from 2015 to 2017, Antminer S9 from 2018 to 2020, and Antminer S19 Pro from 2020 under the assumption that no fees are paid by users. It should be noted that the profit is also influenced by changes in electricity prices, Bitcoin hash rate, Bitcoin price, and block rewards over time. Our analysis shows that revenue was particularly high when the Bitcoin price

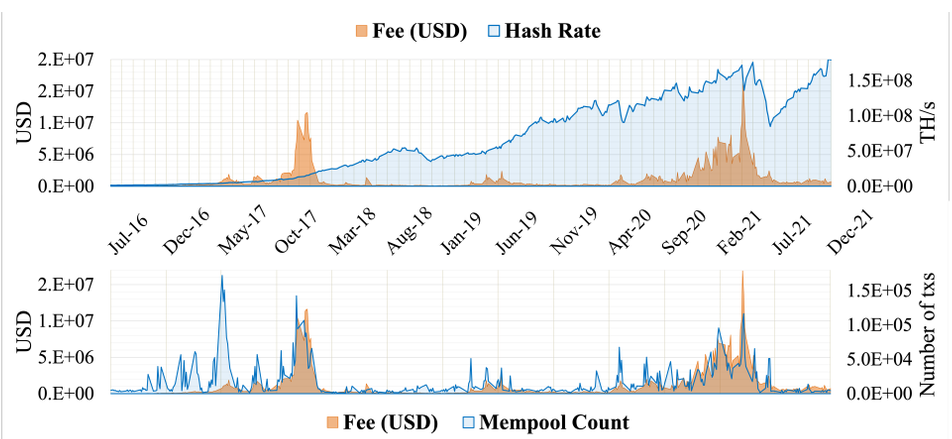


**Figure 3.7:** Factors that may contribute to high fees in Bitcoin are represented by the sum of transaction fees (in USD) paid daily from 2016 to 2021. This value is compared first with the total hashing rate in Bitcoin and then with the daily mempool count, which is the number of new incoming transactions submitted to Bitcoin each day. Open and available data of Bitcoin are fetched of blockchain.com.

4. No improvements can be made to at least one participant's well-being without reducing any other participant's well-being

increased in late 2017. However, despite the fact that the Bitcoin price was even higher in 2020, revenues were lower due to an increase in the total hash rate. We also observe that revenues began to increase again after January 2021, possibly due to a decrease in the number of miners on the network (as indicated by the drop in hash rate in Figure 3.7). Determining a pattern for transaction inclusion poses a dynamic challenge for the evolving Bitcoin blockchain, where transaction fees cannot solely determine inclusion. Our approach offers an alternative by considering fees as a significant factor in transaction inclusion, but not the only one.

## Approach

Our objective is to address two key challenges arising from the fee market in Bitcoin: (1) unpredictability of fees and (2) instances of users overpaying. For this, we propose to construct a model that employs ML techniques, such as a multi-layer NN, to define a pattern for the inclusion of transactions in the Bitcoin network. The model considers both the block size and the mempool size, which sets it apart from traditional FPSBA predictors. Additionally, we incorporate features that are not fee-based so that our model is not solely dependent on a SPA scheme for its predictions.

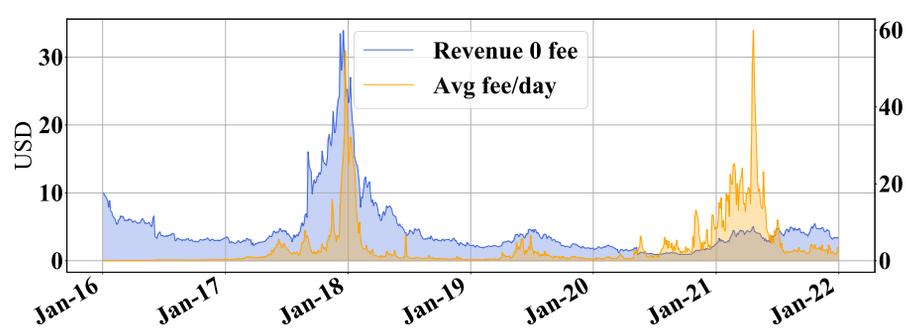


**Figure 3.8:** The calculation of revenues without fees takes into account the total hash rate of Bitcoin, its price, and historical electricity prices in the United States from 2016 to 2022 for each point. The block reward decreases from a starting value of ₿ 50 to ₿ 6.25, and it is assumed that a miner will switch from using the Antminer S7 (released in 2015), Antminer S9 (released in 2017), to the Antminer S19 Pro as mining hardware advances. We derived the revenue using open data of Bitcoin about total hash rate, transaction fees, and Bitcoin price, fetched on blockchain.com at `https://www.blockchain.com/explorer/charts/fees-usd-per-transaction`.

The utilization of ML models for the identification and prediction of patterns within large datasets has been widely adopted across various fields. For example, in the field of hydrology studies such the one by Diez-Sierra and del Jesus [133] have employed large amounts of data to recognize patterns and trends. Similarly, within the domain of network security, research such as Nanda et al. [134] have leveraged these models to detect and prevent cyber-attacks. Additionally, the work of Yazdinejad et al. [135] has demonstrated the efficacy of ML techniques in identifying cryptocurrency malware threats.

When analyzing patterns related to transaction inclusion, a significant volume of heterogeneous data is often encountered, which necessitates organization and structured analysis. An ML-based approach, in this case, allows for predictions and decisions to be made using a subset of the data (i.e., training data) and has been widely adopted across multiple industries, including education [136, 137], business and marketing [138, 139], healthcare [140, 141], financial services [142, 143], and transportation [144, 145]. As was demonstrated in our previous study [57], the utilization of ML techniques to analyze and identify patterns in large datasets is a viable approach, and the transparent and readily available Bitcoin blockchain serves as an excellent source for this purpose.

## Summary

This chapter delved into the principles and rules that govern the Bitcoin ecosystem at scale, with a specific focus on the interdependence between users and miners. We explored how miners generate profits, the associated costs they incur, and the crucial role these factors play in determining transaction inclusion. We also presented mining profit calculations for corner case countries with an high, medium, and low electricity price, and show how mining can be profitable or not. The emergence of a fee market in POW-based blockchains, including miners' auction schemes, is discussed, emphasizing its impact on fee dynamics in Bitcoin. Understanding this market is crucial for formalizing a transaction inclusion pattern.

In the upcoming chapter, we outline our data acquisition and organization methodology. We discuss essential elements for proper model functioning and explore unnecessary elements. We cover different data acquisition methods, such as using the Bitcoin core client software and external APIs. The effectiveness of our approach relies on optimizing and organizing the dataset to meet our objectives.

# 4

# Blockchain Analytics System

In this chapter, we present the methods and techniques used for data acquisition from the Bitcoin blockchain, as well as the structure of our dataset. Our study employs a combination of web scraping, APIs, and direct access to the blockchain using dedicated Bitcoin Core software, to acquire relevant data. The acquired data is structured and pre-processed to be suitable for the analysis in the following chapters. The system we designed and implemented to automate these tasks is referred to as the Blockchain Analytics System (BAS). This chapter provides an overview of the data acquisition process and the structure of the dataset, including any cleaning or pre-processing steps taken, which will be used in the subsequent analysis.

## 4.1 Data Sources

The Bitcoin blockchain is a rich source of information that can be used to gain valuable insights into the workings of the Bitcoin network and its underlying technology. Despite the availability of this data, the process of acquiring and storing it in a manner that is suitable for analysis requires a comprehensive understanding of the underlying technology as well as the various methods and

tools available for data collection. The sheer volume of data generated by the Bitcoin network can exacerbate the difficulty of this task. Effectively collecting and storing data from the Bitcoin blockchain necessitates a combination of technical expertise and careful planning to ensure that the data is acquired in a manner that is both efficient and rigorous. In this study, three distinct methodologies are employed to acquire blockchain data: utilization of web sockets and APIs offered by blockchain.com, utilization of the Bitcoin Core client software, and implementation of web scraping techniques.

### 4.1.1 Web Sockets and APIs

The `blockchain.com` website offers web socket APIs as a service.[1] While we have not extensively utilized this service, we found it useful for real-time monitoring of the Bitcoin mempool. Specifically, it allows for the observation of the number of pending transactions awaiting confirmation. To monitor pending transactions, we subscribed to a designated endpoint and implemented a process to periodically update a local file at regular intervals. This file stores the hash of each retrieved unconfirmed transaction. Through this method, we were able to compare instances of unconfirmed transactions to the contents of the file and subsequently identify those that have been confirmed, allowing for their removal from the list.

Pseudo-code in Algorithm 1 demonstrates how to use web socket APIs to fetch unconfirmed transactions in the Bitcoin network. We assume that the `WebSocketAPI` class has implemented methods for subscribing, fetching data, and unsubscribing. Our `processData()` function is available to process the fetched data, and to manage the storage of unconfirmed transactions on a local level. This includes periodically updating the unconfirmed transactions at a specified `timer` interval and removing transactions that have been approved upon the creation of new blocks.

BAS primarily obtains stored information from the blockchain.com[2] platform by utilizing their RESTful APIs. BAS includes a function dedicated to the retrieval of block information, `FetchBlocks()` in Algorithm 2, utilizing RESTful API endpoints (e.g., the RAW BLOCK endpoint listed in Appendix C.1) to fetch and store said information within a locally maintained dataset.[3] The `FetchBlocks` function in Algorithm 2 takes three parameters: the hash of the block where

1. connection URL: `wss://ws.blockchain.info/inv`
2. blockchain.com at `https://www.blockchain.com/explorer/api`
3. Raw block endpoint at height 600000: `https://blockchain.info/rawblock/600000`

**Algorithm 1** Retrieve unconfirmed transactions using web sockets.

```
1: procedure FetchUnconfirmedTxs(timer, sub, unsub)
2:     ws ← WebSocketAPI(sub, unsub)
3:     ws.subscribe()          ▷ subscribe at {"op":"unconfirmed_sub"}
4:     while True do                  ▷ time listening the socket is arbitrary
5:         sleep(timer)
6:         unconfirmed_txs = ws.fetchData()
7:         processData(unconfirmed_txs) ▷ manipulate data, store it locally
8:     ws.unsubscribe() ▷ unsubscribe at {"op":"unconfirmed_unsub"}
```

the retrieval should start, if it is not provided, it will try to read from a previous stored file; the number of blocks to be fetched; a boolean read flag, that if set to `True`, it will read from a previous stored file. The function uses a `getJson()` procedure to fetch the JSON data of the first block (starting from the provided hash or height) and converts it into a Block and Transaction objects. On each iteration, the JSON data of the current block is obtained, parsed into a Block object, and appended to the previously initialized block dataset ($ds_b$ in Algorithm 2).

Additionally, a transaction dataset ($ds_t$ in Algorithm 2) is initialized and populated with transaction objects extracted from the current block. The iteration proceeds by updating the hash to the next block, until the specified number of blocks have been downloaded. The function ultimately returns both the block and transaction datasets.

### 4.1.2 Bitcoin Core

Bitcoin Core is the reference open source implementation of the Bitcoin protocol.[4] That provides functionality for full node participation were the entire history of the Bitcoin blockchain is downloaded and maintained on the user's device. Bitcoin Core is considered the most secure implementation of the Bitcoin protocol but also requires a significant amount of storage and memory to run. In our case, we hosted a full node on Azure, which is currently maintaining a storage capacity of over 400 GB for the purpose of holding blockchain data. The process of retrieving data from the Bitcoin Core platform can be challenging in terms of efficiency and time. One specific example is the calculation of transaction fees, which requires the examination of spent outputs across multiple transactions, as a result of the Unspent Transaction Outputs (UTXO)

4. https://bitcoin.org/en/bitcoin-core/

**Algorithm 2** Retrieve block information using RESTful API.

```
1:  procedure FetchBlocks(hash, n, read)
2:      ds_b ← Pandas.DataFrame()                    ▷ initialize block dataset
3:      if read is True then
4:          ds_b, ds_t ← readDS()                    ▷ read last stored dataset instance
5:      else
6:          for 0 to n do
7:              data ← getJson(RAW BLOCK + hash)     ▷ raw block endpoint
8:              b ← Block(data)                      ▷ create a Block instance
9:              ds_t ← Pandas.DataFrame()            ▷ initialize transaction dataset
10:             for all tx in b do
11:                 t ← Transaction(tx, b)           ▷ create Transaction instance
12:                 append(t, ds_t)                  ▷ append row to ds_t
13:             append(b, ds_b)                      ▷ append row to ds_b
14:             hash ← b.next_block
15:         return ds_b, ds_t
```

model implemented by Bitcoin.

During our experiments we have observed that Algorithm 3 results in an average retrieval time of 30 seconds for fee information within a single block. In contrast, utilizing APIs for data retrieval can provide the same amount of fee information across 10 blocks within the same time frame, illustrating a significant improvement in efficiency.

**Algorithm 3** Obtaining information about one transaction fee in Bitcoin Core.

```
1:  procedure getTxFee(t)
2:      s_in, s_ou ← 0                   ▷ sums of transaction inputs and outputs
3:      for inp in t.vin do              ▷ for each input in t
4:          index ← inp.vout             ▷ index of the spent output in inp
5:          tx_in ← getRawTransaction(inp.txid) ▷ local call using bitcoin-cli
6:          v_in ← tx_in.vout[index].value   ▷ current input value
7:          s_in ← s_in + v_in           ▷ update transaction input
8:      for out in t.vout do             ▷ for each output in t
9:          v_ou ← out.value             ▷ current output value
10:         s_ou ← s_ou + v_ou           ▷ update transaction output
11:     return s_in - s_ou               ▷ return transaction fee
```

The function detailed in Algorithm 3 is utilized to calculate the transaction

fee of a given transaction in JSON format. The algorithm iterates through the transaction inputs, `t.vin`, of the transaction and retrieves corresponding information by utilizing the `getRawTransaction` command provided by the Bitcoin-cli (Appendix A.1). The sum of all inputs, $s_{in}$, is then computed. Subsequently, the algorithm iterates through the transaction outputs, `t.vout`, and computes the sum of all outputs. The transaction fee is calculated as the difference between the sum of inputs and the sum of outputs. The function then returns this value as the transaction fee.

### 4.1.3 Web Crawling

The use of web crawling for data acquisition, presents a significant challenge due to the need for a comprehensive analysis of each individual HTML page. This process cannot be easily fully automated, and thus requires manual examination of each page. In our study, we utilize web crawling only in specific instances where alternative methods of data retrieval are not feasible. One example is the identification of miners utilizing their names rather than IP addresses, as this information may not be readily available through alternative means. The class representation of the web crawler, as depicted in Figure 4.1, illustrates the inheritance relationship between the classes `TransactionPage`, `BlockPage` and the parent class `Page`. The former two classes implement specific methods, namely `get_latency()`, `get_fee()`, and `get_miner()`, which extract and parse relevant information such as the latency of a transaction in seconds, the transaction fee in satoshi,[5] and miner information, from the content of an HTML web page of a certain transaction, or block, on the Bitcoin blockchain. Algorithm 4 is an example of how the crawler methods work. The helper function `findHTML()` takes in a page content string, a starting substring, and an ending substring as input. It finds the first occurrence of the starting

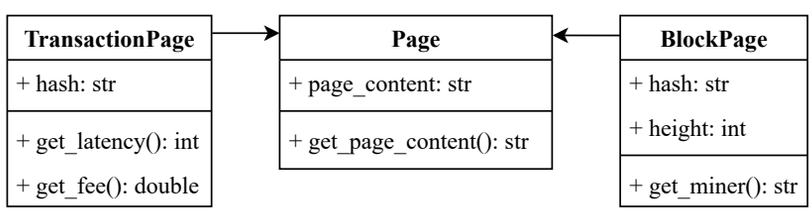


**Figure 4.1:** A class diagram representing the entity-relationship model for web crawler classes, with the `TransactionPage` and `BlockPage` classes inheriting from the `Page` class, and implementing methods for obtaining transaction latency, fees, and miner from the web page content.

5. satoshi, or sat, is the unit of Bitcoin, 1satoshi = 0.00000001 BTC

substring in the page content and finds the first occurrence of the ending substring after it. It then returns the substring of the page content between these indexes, or an empty string if either substring is not found.

**Algorithm 4** Retrieving transaction fee from an HTML page.

```
1: procedure GET_FEE
2:     p ← find 'Fees' in page content and returns a portion
3:     p ← findHTML(p, '">', 'BTC</')                ▷ start and end char
4:     fees ← re.findall("\d+\.\d+", p)                    ▷ find float
5:     fees ← float(fees[0]) ×10^8                  ▷ from BTC to satoshi
6:     return fees
```

## 4.2 Data Structure

Once the data is retrieved, it is stored locally in the following structure:

```
dataset
└── Mmm-yy : samples for a specific month and year
    ├── blocks
    │   ├── info.txt : metadata for block files
    │   └── 𝒟_B : block dataset, partitioned every 30 MB
    └── transaction
        ├── info.txt : metadata for transaction files
        └── 𝒟_T : transaction dataset, partitioned every 30 MB
```

Our approach to data storage involves separating blocks and transactions, and storing their respective information in separate datasets. This design mitigates redundancies and conserve storage space, as certain information pertaining to blocks is deeply ingrained within every transaction, and would otherwise be repeated numerous times within a single block. Hence, we categorize the datasets containing raw transactions and raw blocks, referred to as $\mathcal{D}_T$ and $\mathcal{D}_B$, respectively, as those in which information is stored in its original format as it was fetched, prior to any processing or feature engineering. The data is organized by month, for facilitating the construction of ML models and the evaluation process in the future. To mitigate the potential issues associated with handling large files, the transaction dataset is partitioned into smaller files with a maximum size of 30 MB. The file structure of the dataset is depicted above and a portion of the dataset have been made publicly available on the Dataverse platform as referenced in [89].

### 4.2.1 Blocks

For each month the `block` folder contains the metadata file, `info.txt` (Appendix C.2), and the data. The former serves as a means to store key information about the dataset, such as the start and end date, start and end hash, and the number of blocks retrieved. The latter comprises information about the blocks that occurred during that month. The Block class in Figure 4.3, is a representation of a single block in the blockchain, and is instantiated with a block in JSON format. It comprises various attributes, both raw data, which are saved as they are retrieved, such as the block hash, height, hashes of previous and subsequent blocks, or block size. Processed data derives from various attributes or is acquired from external sources when those attributes are not available within the JSON object, for instance, the block creation time.

The Algorithm 5 defines two methods for calculating processed data. The `get_miner()` procedure uses the web crawler defined in Section 4.1.3 to retrieve information about a miner associated with a block. The `get_bct()` procedure calculates the block creation time by fetching the previous block from the analyzed block's epoch.

**Algorithm 5** Block's methods.

```
1: procedure GET_MINER                    ▷ using web crawler to get miner info
2:     return BlockPage(self.hash).get_miner()
3: procedure GET_BCT                                        ▷ block creation time
4:     prev_b ⟵ getJson(RB + prev_b)                        ▷ fetch previous block
5:     return self.epoch − prev_b.epoch
```

### 4.2.2 Transactions

Similarly to that of the block files, the `transaction` folder comprises the metadata file, referred to as `info.txt`, as well as the corresponding data. The representation of the Transaction class is illustrated in Figure 4.3, and, similar to the block files, it encompasses both raw and processed data. Algorithm 6 outlines the methodology utilized to calculate the processed features for each retrieved transaction. The calculation of the transaction fee is accomplished by utilizing information regarding the inputs and outputs of the transaction, as described in Appendix C.3. As this information, present in the JSON response, is not germane to our research objectives, it is not retained in our local dataset $\mathcal{D}_T$.

**Algorithm 6** Transaction's methods.

```
1: procedure GET_TL
2:     return self.b_epoch − self.epoch
3: procedure GET_DELTA                          ▷ transaction waiting time
4:     prev ⟵ self.b_epoch − self.bct           ▷ previous block epoch
5:     return prev − self.epoch
```

### 4.2.3 Data Processing Pipeline

Figure 4.2 illustrates the data processing pipeline in the BAS system, starting with the retrieval of data from various sources, as described in Section 4.1. Most of data exchanged between the sources and the ingestion engine is through JSON messages. Processed data is stored locally using the Pandas library [146]. The ingestion engine performs pre-processing, selecting, and extracting relevant features, which are saved in the form of NumPy text files [147] for use as training sets for the ML model. The chosen ML model is implemented using a TensorFlow [148] backend with Keras [149] modules. The rationale behind the selection of features is discussed in the next chapter.

The illustration presented in Figure 4.3 depicts the relationship between the datasets designated as $\mathcal{D}_B$ and $\mathcal{D}_T$. This relationship is established through a many-to-one association, utilizing the block hash (called $ha$) as a unique identifier, denoted as $r : \mathcal{D}_T \rightarrow \mathcal{D}_B$. It can be inferred that for every element, $ha'$, within the dataset $\mathcal{D}_T$, there exists a corresponding element, $ha''$, within the dataset $\mathcal{D}_B$, such that $ha' = ha''$. The resulting dataset, referred to as the

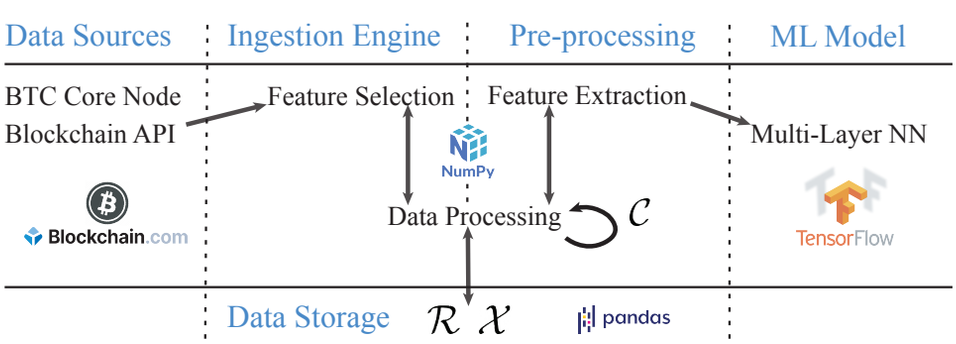


**Figure 4.2:** In BAS, data flow is facilitated from the blockchain to the ML framework. In this process, various datasets are utilized, denoted as $\mathcal{R}$, $\mathcal{C}$, and $\mathcal{X}$. Specifically, dataset $\mathcal{R}$ represents raw data extracted from the blockchain, dataset $\mathcal{C}$ represents a comprehensive dataset utilized during runtime, and dataset $\mathcal{X}$ encompasses all data utilized for training purposes.

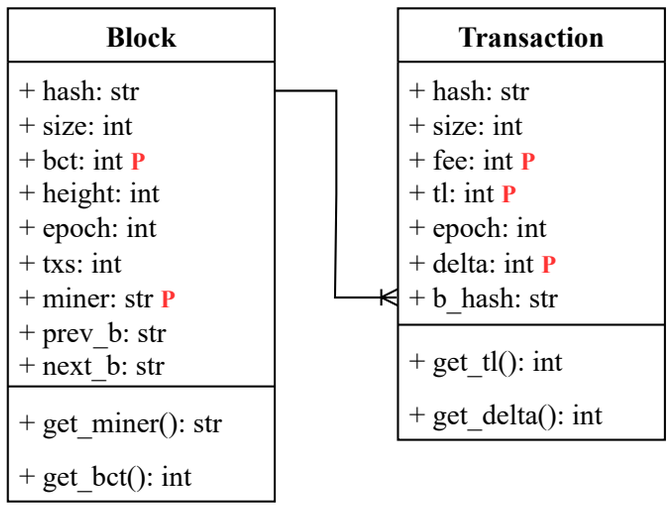


**Figure 4.3:** Structure that organizes the preservation of information related to both $\mathcal{D}_B$ and $\mathcal{D}_T$. The red P serves as an indicator to signify that the corresponding data has undergone processing as opposed to being obtained directly.

*raw dataset* and denoted as $\mathcal{R}$.

## Summary

The chapter discussed data retrieval and storage methods for analyzing the Bitcoin blockchain. It mentioned three approaches for data acquisition: using web sockets and APIs for real-time and historical monitoring, utilizing the Bitcoin Core client software, and employing web scraping in specific cases. Data storage involved separating blocks and transactions into separate datasets to reduce redundancies. The data processing pipeline involved retrieving data, storing it locally, and performing pre-processing for feature selection. Efficient data handling was crucial for analysis and future modeling.

Chapter 6 will provide a comprehensive explanation of the three datasets, while in the next Chapter we formalize the transaction inclusion model based on our conjectures.

# 5

# Transaction Inclusion Model

Time-series data analysis has been widely recognized as a valuable tool for predicting future trends in various fields, including finance [150], physics [151, 152], and economics [153, 154, 155]. In this study, we adopt a time-series observational approach to analyze transactions in a blockchain system. Our methodology is based on the collection of time-series data, where transactions are sampled on a monthly basis with a fixed interval. We also incorporate a notion of relative time, represented by the block creation epochs.

In this chapter, we present a comprehensive model for the inclusion of transactions in a POW-based blockchain system. In Section 5.1, we explain the rationale behind our choice, and how transaction data is analyzed. The time-series approach allows accurate analysis of the dynamics of transaction inclusion. Building on this foundation, we define and analyze two main factors that can affect the inclusion of transactions in a blockchain system. These factors are referred to as *revenue* and *fairness*. In Section 5.2, we examine the concept of revenue and its impact on transaction inclusion. Revenue is a critical factor as it serves as an incentive for miners to participate in the network and validate transactions. Section 5.3 explores the notion of fairness in the context of transaction inclusion. Fairness implies that all users have an equal opportunity to

have their transactions included in the blockchain, regardless of their computational power or resources, upon paying an adequate fee value. Our model takes into account both revenue and fairness as complementary factors for an accurate study and prediction of transaction inclusion. A holistic view of the inclusion process must be sought through the consideration of both revenue and fairness concepts.

## 5.1 Observational Approach

The present study adopts a time-series-based methodology that considers the sequential arrangement of transactions and their status at the point of each block creation. The conceptual framework is explicated in the subsequent section and formalized in the one that follows.

### 5.1.1 Block-Epoch-Based Collection

The idea behind our observational approach is that a transaction carries different information throughout the time it is pending in the network. This phenomenon arises from the inherent supply and demand dynamics in the blockchain domain, which continually change every time a new block is appended to the blockchain. The approach uses a block-epoch-based collection, meaning that a transaction can potentially change its worth to miners every time a new block is created. As a result, we define the time interval as the time between two consecutive block creation epochs.

Each transaction is uniquely identified in each time frame by a pair of values $ha_t$ and $be_x$. Here, $ha_t$ is the hash of transaction $t$ and $be_x$ represents the block epoch at block height $x$. The transaction at a specific block height is referred to as $t^{(x)}$, representing an instance of the transaction during the time slot between block creation epochs $be_x$ and $be_{x+1}$.

The goal of this study is to gain insights about network saturation and waiting times at each block epoch by tracking transactions over time. To accomplish this, three concepts are defined: (1) *timeline set*, which represents the set of all block time epochs; (2) *lifespan*, which represents the time interval between a transaction's first and last occurrence in the dataset; (3) *number of occurrences*, which represents the number of times a transaction appears in the dataset. These concepts allow us to describe and analyze the state of the network at specific points in time and how transactions are behaving within it.

### 5.1.2 Formalization

**Definition 5.1.1: Timeline set**

The timeline set, identified as $\mathbb{T}$, is a set that contains all the block-time epochs, defined as:

$$\mathbb{T} = \{be_x | 0 \leq x \leq \xi\} \tag{5.1}$$

□

Where $be_x$ is the block time epoch at height $x$ and $\xi$ is the maximum block height. This set is used to delineate the time slots used for the analysis of transactions in our system.

**Definition 5.1.2: Lifespan**

The lifespan of inclusion of a transaction $t$, represented as $\mathcal{L}(t)$, is a range in epoch time, that starts when the first node sees the transaction to when it is included in a mined block. More formally, if $t$ is included at height $x$, a transaction lifespan is defined as:

$$\mathcal{L}_t^x = [ep_t, be_x] \tag{5.2}$$

□

Here, $ep_t$ is the time the first node sees the transaction and $be_x$ is the block-time epoch at which the transaction is included in the blockchain. Understanding lifespan helps unravel its inclusion dynamics and determines how many occurrences can be counted in the complete dataset (denoted with $C$ and explained in Chapter 6.2.3).

**Definition 5.1.3: Occurrences of $t$**

The number of occurrences (or cardinality) of a transaction $t$ in a dataset, represented by $\gamma_t$, is identified by $(ha_t, be)$ pairs with same $ha_t$ but different $be$ as follows:

$$\gamma_t = |(ha_t, be)|_{\forall be \in \mathbb{T}} \tag{5.3}$$

□

This equation sums the number of times the transaction $t$ occurs in the dataset, where $n$ goes from $\texttt{min}(be \in \mathcal{L}(t))$ to $\texttt{max}(be \in \mathcal{L}(t))$, and a value is summed if $be \in \mathbb{T}$. The occurrence value defines how many times a transaction appears to the miners before it is included in a block, and as such it is a measure of the network saturation and waiting time at each block epoch. A transaction $t$ has as many occurrences in $C$ as the number of blocks appended to the blockchain before its inclusion. In Table 5.1 we represent $\gamma$ occurrences of the same transaction before its approval. The waiting time differs at each block epoch. As we will demonstrate in subsequent sections, the inclusion of additional features allows for a more comprehensive understanding of how network conditions affect the transaction's waiting time at each block epoch.

| | **hash** | **be** | **w time** |
|---|---|---|---|
| **1** | 49baa25... | ...22049 | -958 |
| **2** | 49baa25... | ...23235 | 38 |
| **...** | | | |
| $\gamma$ | 49baa25... | ...27793 | 5399 |

**Table 5.1:** Representation of one transaction in a block-epoch-based collection.

## 5.2 Revenue for Miners

As seen in Chapter 2.2.1, Bitcoin's mining difficulty is determined by the total hashing power on the network ($H$). When the total hashing power grows, of difficulty of mining also increases, making it more expensive for miners to scale their operations.[1] As long as the honest nodes have more computational power than the malicious nodes, the blockchain will be secure. A high total hashing power is therefore preferable for the security of the network, but yields higher operational expenses for the miners to maintain their operations. Hence, transaction fees tend to correlate with hashing power. High security on the blockchain may be desirable for the integrity of the network, but it also comes with a cost that ultimately affects the miner's profit.

1. The adjustment of difficulty levels in a blockchain network is contingent upon the speed at which the collective pool of miners can solve the Proof-of-Work puzzle. An increase in the number of miners results in higher consumption levels, even though the frequency output of blocks remains unchanged.

### 5.2.1 Revenue Optimization Strategies

To mitigate a loss of revenue as the total hashing power ($H$) grows, a miner can adopt one of the following four strategies:

1. reduce its mining costs,
2. increase its hashing power $h$,
3. reduce the chances of block orphaning ($\mathbb{P}_{orphan}$),
4. increase the sum of transaction fees $M$ and reward it receives $R$.

Reducing costs is challenging as the exogenous properties $\mathcal{T}$ and $\eta$ cannot be altered, since they are normally distributed with a fixed known mean (600 seconds in Bitcoin). Therefore, reducing hashing power ($h$) would be in conflict with the second strategy. Furthermore, as previously discussed in Chapter 3.1.2, augmenting the individual hashing power does not always result in a higher revenue, as the associated costs may outweigh the benefits gained from the increased $h$. The probability of block orphaning depends on the block propagation delay, which is impacted by the block size [156]. In theory, a rational miner could reduce the orphaning rate by making its blocks lighter and faster to disseminate, but this only partially increases revenue as fewer transactions would also lead to less fees and decrease the overall network throughput. Additionally, the occurrence of orphaning has been calculated to happen only 3 times in every 1,000 blocks, and thus has limited impact on miner revenue [156].

Since the block reward $R$ is halved every 210,000 blocks, transaction fees $M$ are the only remaining source of profit. Most miners are assumed to act rationally [157] and implement individualized policies for transaction inclusion that maximize their profits. Because miners can arbitrarily select transactions, their main endogenous source of profit is *transaction fee*, and it is assumed that a transaction's inclusion is highly dependent on its fee and is selected rationally.

### 5.2.2 Feerate

Miners increase their potential revenue with each transaction they include, but simultaneously reduce their block propagation rate, thus reducing the probability of earning a reward. The time required for the propagation of blocks and achieving consensus among participants depends on the block size [158], which is generally fixed at 1 MB in the case of Bitcoin. Miners may attempt to optimize their revenue by including the maximum number

of transactions paying higher fees within the fixed block size by calculating the feerate ($\rho$), defined as the ratio of transaction fee and transaction size as follows:

$$\rho = \phi/q \tag{5.4}$$

The dequeueing feerate policy is the commonly accepted norm among miners [130], and it forms the foundation of their revenue. However, many fee estimators that incorporate the feerate still result in overpayment.[2] Analyses indicate that on average, between 50 % and 70 % of transactions offer fee rates that are two orders of magnitude higher than the recommended minimum,[3] and that 88 % of all Bitcoin transaction inputs pay higher fees than necessary [130]. Thus, we contend that revenue is not the only metric to consider, and that a miner must also consider *fairness* by allocating space for transactions that have been waiting for a longer period of time, as long as they are offering fair fees, in order to sustain the overall system.

## 5.3 Fairness for Users

The concept of fairness in transactions encompasses the idea that a transaction, upon payment of a fee, should not be subjected to unjustified delay as a result of the arrival of newly submitted transactions with higher fees. In other words, the scheduling of transactions should ensure that no transactions are left in a state of starvation. It is essential to incorporate fairness into our model, as transactions should not be left in a state of indefinite waiting, especially after the payment of an *expected fee*. The expected fee is a value that is deemed reasonable by both parties to secure prompt processing of a transaction. The concept of fairness ensures that, once a fee is paid, a transaction should not experience undue delay due to the presence of transactions with higher fees that arrived after it.

To provide a clearer understanding of fairness, we introduce the concepts of Epoch Before Inclusion (EBI) and Relapsed Pending Transactions (RPTs). Additionally, we provide a definition for the expected fee value, which represents the fee that a transaction ought to pay in order to receive prompt processing and inclusion within reasonable time.[4] These concepts serve to form a basis for evaluating the fairness of transactions within the system.

2. E.g. bitcoinfees `https://bitcoinfees.earn.com`
3. Recommended minimum feerate is $10^{-5}$ BTC/kB ≡ 1, 000 sat/kB ≡ 1 sat/byte, according to Bitcoin Core
4. By reasonable time we refer to a timeframe typically ranging from a few minutes to a few hours

### 5.3.1 Epoch Before Inclusion

EBI represents the epoch of the most recent block mined prior to the inclusion of a given transaction $t$. This value can be expressed formally through the Equation 5.5 as $\beta_t$, where the latest block epoch is represented by $be_\xi$, and $\xi$ is the height of the last block mined.

**Definition 5.3.1: Epoch before inclusion**

For a transaction $t$ at height $x$, denoted as $t^{(x)}$, if $t$ has yet to be included, the Epoch Before Inclusion (EBI) is defined as ${\beta_t}^{(x)} = be_x$, where $[be_x, be_{x+1}]$ represents the time slot at height $x$.

$$\beta_t = \begin{cases} be_{x-1} & \text{if } t \text{ is included in block at epoch } be_x \\ be_\xi & \text{if } t \text{ is yet to be included} \end{cases} \tag{5.5}$$

□

### 5.3.2 Expected Fee

The expected fee value determines the appropriate fee for a given transaction based on its size. The value is calculated by multiplying the feerate (denoted as $\rho^*$ in the equation) by the size of the transaction (denoted as $q$).

**Definition 5.3.2: Expected fee**

The feerate must be greater than or equal to 1 sat/byte, which is the minimum feerate required for a transaction to be processed. The expected fee value is expressed as:

$$\mathbb{E}[f] = \rho^* q, \text{ where } \rho^* \geq 1 \,\text{sat/byte}. \tag{5.6}$$

□

In this equation, $\mathbb{E}[f]$ represents the expected fee value, and the condition $\rho^* \geq 1$,sat/byte ensures that the fee rate is sufficient to meet the network's minimum fee requirements.

### 5.3.3 Relapsed Pending Transaction

Next we introduce the concept of Relapsed Pending Transaction (RPT).

**Definition 5.3.3: Relapsed pending transactions**

Given a block height $y$, $\mathcal{P}^{(y)}$ represents the set of RPTs at that height. The set includes transactions that have not been included in any block until height $y$, have experienced at least one block creation in their lifespan, have not been included up until height $y$, and have a fee equal to or greater than the expected fee. The conditions are specified in Equation 5.7.

$$\begin{aligned} \mathcal{P}^{(y)} = \{\ t | & ep_t - {\beta_t}^{(y)} < 0 \quad \wedge \\ & be_y < be_x, \text{ if } \mathcal{L}(t) = \mathcal{L}_t^x \quad \wedge \\ & \phi_t \geq \mathbb{E}[f_t]\ \} \end{aligned} \tag{5.7}$$

□

We say $t$ is a RPT at height $x$, if $t^{(x)} \in \mathcal{P}^{(x)}$. The more generic definition of $\mathcal{P}$ is obtained by taking the union of all block-epoch-based $\mathcal{P}$ sets as $\bigcup_{i=0}^{\xi} \mathcal{P}^{(i)}$. We conjecture that a transaction appearing multiple times in $\mathcal{P}$ has a higher chance of being included in the next mined block.

## 5.4 Model Formalization

A successful transaction inclusion framework must consider the pivotal notions of RPTs, EBI, and the lifespan of each transaction. Additionally, it is critical that the framework continuously monitors the current status of the network during both the training and testing phases. To attain this goal, it is crucial to accurately record the moment of inclusion of each analyzed transaction into a newly generated block. In support of this objective, we propose the definition of a set of Temporarily Approved Transactions (TATs) which incorporates the previously mentioned key concepts.

### 5.4.1 Temporarily Approved Transaction

To understand the transaction inclusion process in a block-epoch-based time division, we must determine each transaction's status in each time frame. The

set of TATs offers valuable information regarding the inclusion prospects of each transaction, serving as a valuable resource during both the training and testing phases. This set allows for a comprehensive understanding of the specific moments at which a transaction is slated for inclusion in the blockchain. We formalize the set $\mathcal{A}$ of TATs in Definition 5.4.1.

**Definition 5.4.1: Temporarily approved transactions**

Let us define the set $\mathcal{A}^{(y)}$ as the collection of Temporarily Approved Transactions at height $y$. This set comprises all transactions that are selected for inclusion at height $y$ during the time interval $[be_y, be_{y+1}]$ and are eventually included at height $y+1$. We shall refer to a transaction $t$ as a TAT at height $y$ if $t^{(y)} \in \mathcal{A}^{(y)}$. This set can be mathematically represented as defined in equation (5.8).

$$\mathcal{A}^{(y)} = \{\ t | \mathcal{L}(t) = \mathcal{L}_t^{y+1}\ \} \tag{5.8}$$

□

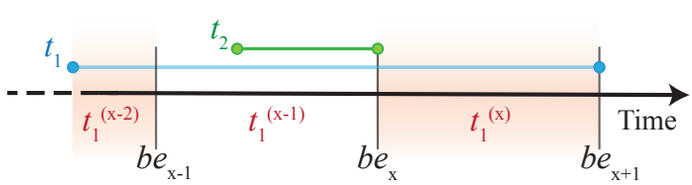


**Figure 5.1:** Two distinct transactions, denoted as $t_1$ and $t_2$, are initiated at a different time, respectively $ep_{t_1}$ and $ep_{t_2}$. The transaction $t_1$ is recorded in the block at height $x+1$, whereas $t_2$ is immediately recorded in the block at height $x$ following its initiation in the same block-epoch time frame. The number of occurrences for $t_1$ can then be represented as $\gamma = 3$, and for $t_2$ as $\gamma = 1$.

Figure 5.1 depicts two instances of block-epoch-based transactions, designated as $t_1$ and $t_2$. The information conveyed by $t_1$ varies based on its location and is therefore named differently, such as $t_1^{(x-2)}$, $t_1^{(x-1)}$, and $t_1^{(x)}$. The membership of $t_1$ and $t_2$ in sets $\mathcal{A}$ and $\mathcal{P}$ changes over time, which is formalized in Equations 5.9 and 5.10. Given that the lifespan of $t_1$ is defined as $\mathcal{L}(t_1) = \mathcal{L}_{t_1}^{x+1}$, it follows that:

$$\begin{aligned} t_1^{(x-2)} &: \notin \mathcal{P}^{(x-2)} \wedge \notin \mathcal{A}^{(x-2)} \\ t_1^{(x-1)} &: \in \mathcal{P}^{(x-1)} \wedge \notin \mathcal{A}^{(x-1)} \\ t_1^{(x)} &: \in \mathcal{P}^{(x)} \quad \wedge \in \mathcal{A}^{(x)} \end{aligned} \tag{5.9}$$

In a similar manner, the lifespan of $t_2$ is defined as $\mathcal{L}(t_2) = \mathcal{L}^x_{t_2}$, resulting in the following equation:

$$t_2^{(x-1)} : \notin \mathcal{P}^{(x-1)} \wedge \in \mathcal{A}^{(x-1)} \tag{5.10}$$

### 5.4.2 Ordered Pending Transactions

It follows the definition of the Ordered Pending Transaction (OPT) set.

**Definition 5.4.2: Ordered pending transactions**

We define $S$ at a given block height $x$ as the set of the OPT, denoted as $S^{(x)}$. The set includes all non-approved transactions whose lifespans end in a block height greater than $x$ and whose inceptions occur before $be_{x+1}$. The set is ordered in ascending order based on the transactions' feerate, $\rho_t$, as follows:

$$\begin{aligned} S^{(x)} &= \{\ t | \mathcal{L}(t) = \mathcal{L}^y_t \wedge ep_t < be_{x+1}\ \} && \forall y > x \\ S^{(x)} &= [t_1, t_2, \dots t_n] && \text{is an ordered set} \\ \text{where } & \rho_{t_1} \leq \rho_{t_2} \leq \cdots \leq \rho_{t_n} \end{aligned} \tag{5.11}$$

□

Miners play a crucial role in verifying and confirming transactions. Their incentive to do so is driven by the reward of block subsidies and transaction fees. As mentioned in Section 5.2, it is widely acknowledged that miners seek to maximize their profit by including transactions with the highest feerate (or $\rho$) first. This behavior is rational as it leads to the greatest financial reward for the miner. Given this reality, it is imperative that the transaction inclusion model takes into account the miners' priority of selecting transactions with the highest feerate. To this end, we introduce the concept of an ordered set of pending transactions, $S$, which prioritizes transactions based on their feerate. This concept is formally defined in Definition 5.4.2. By incorporating this principle, our proposed transaction inclusion model is better aligned with the financial incentives of the miners and the widely accepted norm in the blockchain ecosystem.

The proposed model employs information garnered from sets $\mathcal{P}$, $\mathcal{A}$, and $S$ in order to make informed decisions regarding the inclusion of transactions. Understanding the impact of revenue and fairness (as described in Sections 5.2-

5.3) on sets $\mathcal{P}$ and $S$ is crucial in determining the dynamic membership of a transaction within set $\mathcal{A}$. This information is utilized to generate new features through a feature extraction process (as detailed in Section 6.1.1).

Figure 5.2 illustrates the evolution of the $\mathcal{P}$ $\mathcal{A}$ $S$ ecosystem over time, taking into account four transactions with varying feerate values. It can be observed in Figure 5.2 that transaction $t_1$, initiated within the block-epoch time frame of $be_{x-2}$, is included in the first block created at epoch $be_{x-1}$, and thus it is present in $\mathcal{A}^{(x-2)}$ and not in $\mathcal{P}$ at any time. On the other hand, transaction $t_2$, which was also initiated during the block-epoch time frame of $be_{x-2}$, has a lower feerate, implying that it could potentially remain in a pending state for a longer duration. As a result, it appears in both $\mathcal{P}^{x-1}$ and $\mathcal{P}^{(x)}$. The same criteria apply to transactions $t_3$ and $t_4$, initiated in the block-epoch time frame of $be_{x-1}$, and ultimately included in the blockchain, with the former being included immediately and the latter after a single block creation. The lifespan of $t_4$ is shown in the figure and can be represented as $\mathcal{L}_{t_4}^{x+1}$.

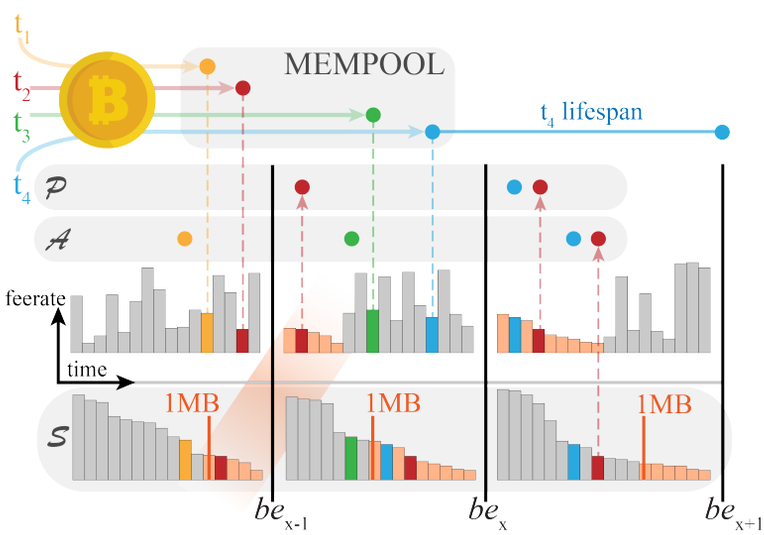


**Figure 5.2:** We examine a selected group of transactions, denoted as $t_1, \ldots, t_4$, spanning from time $be_{x-2}$ to $be_{x+1}$, in order to graphically demonstrate their progression towards inclusion and their designation within the $\mathcal{P}$, $\mathcal{A}$, and $S$ sets. Upon creation, transactions are inserted into the mempool and possess information regarding their feerate. Throughout various time epochs, these transactions may or may not belong to the aforementioned sets. The $S$ set orders transactions based on feerate, the $\mathcal{P}$ set provides a temporal view of their waiting period, and finally, transactions are part of the $\mathcal{A}$ set when they are imminent for inclusion.

## Summary

In this chapter, we have established a formalized perspective on the transaction inclusion model, emphasizing the notions of fairness for users and revenue for miners. Additionally, we have introduced our observational approach, which is based on the consistent evaluation of pending transactions by miners during each block creation. This emphasized the significance of utilizing a block-epoch-based collection methodology for our research goals. These foundations are crucial as they lay the groundwork for the selection and extraction of relevant features, enabling the generation of the necessary training set.

In the subsequent section, the methodology for data retrieval, processing, and feature engineering will be explained, and the model for transaction inclusion will be developed and evaluated.

# 6

# Machine Learning Architecture

This chapter outlines our methodology for constructing training datasets, focusing on the ingestion engine and pre-processing stages. The ingestion engine utilizes locally stored data, selects relevant features, and performs data processing and storage. The pre-processing stage involves features extraction and data processing to generate a comprehensive dataset with relevant and non-redundant features. Throughout these stages, we ensure the training dataset adheres to principles of fairness and revenue, previously described. This chapter also introduces the ML model, employing the ResNet architecture to forecast future trends in the Bitcoin blockchain market. The model's optimization includes the use of the ReLU activation function, resulting in improved accuracy and faster training times.

## 6.1 Ingestion Engine

The ingestion engine processes and transforms raw data obtained from the blockchain into a format suitable for further analysis and storage. Data analysis libraries like Pandas and NumPy are used to perform various data processing tasks such as filtering, aggregation, and transformation. For instance, Pandas

is used to read raw data from the blockchain into a data frame, perform data cleaning and pre-processing, and then write the transformed data into a storage system such as a database or a file. NumPy is used for numerical computations and analysis, such as calculating various statistics or performing matrix operations on the data. With the ingestion engine, we extract relevant information from the Bitcoin blockchain and prepare this data for further analysis.

### 6.1.1 Features Selection

The process of feature selection begins by downloading data from the blockchain and storing it locally. Only relevant[1] data is retrieved, allowing us to maintain a partial local copy of the Bitcoin blockchain with the necessary data for fast access. This results in an average disk space savings of 68% comparing to store the full blockchain.[2] The space saving are achieved by eliminating redundancies, preserving only the information needed for prediction, separating blocks and transactions data, and incorporating newly extracted features. The features selected for analysis are initially listed in Section 4.2 and summarized again in Tables 6.1-6.2. To construct the block-epoch-based collection discussed in Section 5.1.1, it is necessary to select features that include information about the creation time epoch of a block (`bepoch`), the inception time epoch of a transaction (`tepoch`), and the block height. Additionally, gathering data on

| Block $b^{(x)}$ | | | |
|---|---|---|---|
| **Feature** | **Symbol** | **Type** | **Processed** |
| `bhash` | $ha$ | `string` | False |
| `bsize` | $Q$ | `int` | False |
| `bct` | $\mathcal{T}^{(x)}$ | `int` | True |
| `height` | block height | `int` | False |
| `bepoch` | $be_x$ | `int` | False |
| `n_txs` | $t_B$ | `int` | False |
| `miner` | block's miner | `string` | True |
| `prev_block` | previous block's hash | `string` | False |
| `next_block` | next block's hash | `string` | False |

**Table 6.1:** Features of blocks within $\mathcal{R}$.

1. Data that are useful for the purpose of our research, like transaction data about fee or size, while information related to security and block/transaction verification are omitted
2. We store 1.3 GB of information from the actual Bitcoin blockchain, in only 0.4 GB. We refer to Table 7.1 and 7.2 for more information

transaction fee (`fee`), transaction size (`size`), and transaction latency (`tl`) is important for obtaining information on miners' revenue.

| Transaction $t$ | | | |
|---|---|---|---|
| **Feature** | **Symbol** | **Type** | **Processed** |
| `hash` | $ha_t$ | `string` | False |
| `size` | $q$ | `int` | False |
| `fee` | $\phi$ | `int` | True |
| `tl` | $l_t$ | `int` | True |
| `tepoch` | $ep_t$ | `int` | False |
| `delta` | $\Delta\mathcal{P}$ | `int` | True |
| `bhash` | $ha$ | `string` | False |

**Table 6.2:** Features of transactions within $\mathcal{R}$.

The processed column of the tables above indicates whether any manipulation, editing, or other form of processing has been applied to the data prior to storage in our local dataset instance. The value of features, such as the block creation time (bct), is not directly recorded in the Bitcoin blockchain; instead, it must be derived during the data processing phase to define the time frame of each block-epoch-based transaction instance (as described in Section 6.2). Additionally, some newly engineered features (e.g., `delta`) require further aggregation and transformation, as we will explain in Section 6.2.2. Careful feature selection is necessary to construct the sets $\mathcal{P}$, $\mathcal{A}$, and $S$ discussed in Chapter 5.

### 6.1.2 Data Processing and Storage

The features subjected to data processing prior to storage encompass transaction fee, transaction latency, feerate, and bct. Notably, feerate is computationally straightforward to derive during runtime, and its omission from saving it locally can save space. Nonetheless, we choose to include it within the stored features in our locally stored raw blockchain, $\mathcal{R}$, for ease of analysis.

#### Transaction Fee and Feerate

Transaction fee and feerate are revenue-based features that we use to identify inclusion patterns. The fee is computed using function $f_\phi$, which is listed in Algorithm 3 and is based on the inputs and outputs of transactions. When a

transaction $t$ involves $n$ inputs and $m$ outputs, the transaction fee is calculated using Equation 6.1, where $\phi$ represents the transaction fee, $inp_i$ represents the $i$-th input of the transaction, and $out_j$ represents the $j$-th output.

$$\phi = \sum_{i=1}^{n} inp_i - \sum_{j=1}^{m} out_j \tag{6.1}$$

Finally, we define the fee-function $f_\phi$ as:

$$(inp, out) \mapsto \phi = f_\phi(inp, out)$$

The feerate-function $f_\rho$ is designed to acquire information pertaining to transaction feerate,[3] in keeping with the revenue principle. Feerate is calculated using Equation 5.4, which gives us the function $f_\rho$ as follows:

$$(\phi, q) \mapsto \rho = f_\rho(\phi, q)$$

### Transaction Latency

The function for transaction latency computes the duration from the initiation of a transaction $t$ or its first sighting by a miner until its approval. Transaction latency is calculated as showed in Equation 6.2, if $be$ is the epoch of the block that includes $t$.

$$l_t = be - ep_t \tag{6.2}$$

Then the function for calculating transaction latency can be identified as $f_l$, where:

$$(be, ep_t) \mapsto l_t = f_l(be, ep_t)$$

### Block Creation Time

In our block-epoch-based approach, the unit of measurement is represented by the block creation time, which refers to the duration between the creation of one block and the subsequent block. The formalization of the function that computes bct is presented in Equation 6.3.

$$\mathcal{T}^{(x)} = be_x - be_{x-1} \tag{6.3}$$

The function is denoted as $f_\mathcal{T}$, which is defined as a mapping that takes the block epoch $be_x$ and the previous block epoch $be_{x-1}$ as input parameters

3. as previously described, the feerate represents the ratio between the transaction fee and its size

and outputs the computed value $\mathcal{T}^{(x)}$. The function and its mapping can be expressed as follows:

$$(be_x, be_{x-1}) \mapsto \mathcal{T}^{(x)} = f_{\mathcal{T}}(be_x, be_{x-1})$$

### Raw Dataset

In Section 4.2.3, we briefly outlined the procedure for generating the raw dataset $\mathcal{R}$, which involves utilizing the datasets $\mathcal{D}_B$ and $\mathcal{D}_T$ to perform a join operation over the block hash $ha$, which can be expressed as:

$$\mathcal{R} = \mathcal{D}_B \bowtie_{ha} \mathcal{D}_T$$

Each row in $\mathcal{R}$ represents a transaction $t$ at the time of its approval, while each column corresponds to a specific feature. The dataset $\mathcal{R}$ is used to store information locally, perform real-time data processing, and generate additional datasets, as depicted in Figure 4.2.

Algorithm 7 illustrates the process of generating the dataset $\mathcal{R}$. The algorithm employs the Pandas library routines to parse the datasets $\mathcal{D}_B$ and $\mathcal{D}_T$ and generate the resulting dataset $\mathcal{R}$. The algorithm begins by reading the metadata files corresponding to the transactions and blocks and instantiates runtime objects for $\mathcal{D}_T$ and $\mathcal{D}_B$. Subsequently, for each block and transaction file in their respective directories, the algorithm combines the block and transaction instances. Finally, the two instances are merged based on the block hash, yielding the dataset $\mathcal{R}$ as the output.

**Algorithm 7** Reads $\mathcal{D}_B$ and $\mathcal{D}_T$ and produces $\mathcal{R}$.

```
1:  procedure READ_ALL
2:      info_b, info_t ← read(info files for txs and blocks)
3:      df_t, df_b ← empty dataframes
4:      for bf in info_b.files do                    ▷ bf is block file name
5:          df*_b ← read(bf)
6:          df_b ← concat(df_b, df*_b)        ▷ concatenates two Pandas datasets
7:          for tf in info_t.files do                ▷ tf is transaction file name
8:              df*_t ← read(tf)
9:              df_t ← concat(df_t, df*_t)
10:     return merge(df_b, df_t)                              ▷ on block hash
```

## 6.2 Pre-Processing

The pre-processing phase is a crucial step in preparing the data stored in $\mathcal{R}$ for training the ML model. This involves a series of steps that transform the raw data into a suitable form for the subsequent analysis. The first step involves dividing the transaction information into a block-epoch-based collection, which facilitates the analysis of the current network state based on the time period.

The second step extracts new features that are related to fairness and revenue. This step aims to enhance the discriminatory power of the data and improve the accuracy of the model.

Finally, the complete set $C$ is assembled to serve as the input for the generation of the training set $X$, and to proceed with the subsequent training phase of the model. The effectiveness of the pre-processing phase is important for the overall performance of the ML model, impacting both the accuracy and reliability of the predictions.

### 6.2.1 Feature Vector and Complete Transaction

Next, we detail the representation of a transaction and its associated features in a block-epoch-based format, and represent a feature vector in the context of the dataset $C$. Once the selection of features has been made, we establish their structure in the data set $\mathcal{R}$, so that they can be used in a systematic manner by the ML model. Our ingestion engine and pre-processing phases create a temporary, locally generated version of $\mathcal{R}$ referred to as $C$. Each row of $C$ constitutes an instance of a feature vector $\mathbf{t}$, which identifies a transaction within a specified time frame, as described in Chapter 5.1.2. Subsequently, the block-epoch-based representation of a transaction $t \in \mathcal{R}$ is defined as $\boldsymbol{T}$, which encompasses all information pertaining to the transaction over its entire lifespan.

**Definition 6.2.1: Feature vector $\mathbf{t}$**

A feature vector $\mathbf{t}$ is a list of features that identify a block-epoch-based transaction $\boldsymbol{T}$ in a specific time slot, and it is defined as: $\mathbf{t} = [k_1, k_2, \ldots, k_n]$ with $|K| = n$. □

**Definition 6.2.2: Complete transaction $T$**

A Multivariate Time Series (MTS) $\boldsymbol{T} = [\boldsymbol{t}_1, \boldsymbol{t}_2, \ldots, \boldsymbol{t}_\gamma]$ is an ordered set of feature vectors $\mathbf{t}$, and consists on $\gamma$ different univariate time-series with $\mathbf{t} \in \mathbb{R}^n$, $\forall \mathbf{t} \in \boldsymbol{T}$, and $|K| = n$. □

The information contained within $\boldsymbol{T}$ can be utilized to extract novel features (e.g., `delta`) that convey contextual information over distinct temporal intervals, in our case, block epochs. Such information is leveraged by the pre-established set $S$ to create a feature, denoted as *offset*, which is explained further in the subsequent paragraph.

### 6.2.2 Features Extraction

The procedure of feature extraction entails the creation of engineered features that are used for a supervised classification in a DNN model. The feature we are using are rooted in the notions of fairness and revenue, and computed using the pending transactions function and the offset function, as will be described below.

#### Pending Transaction Function

This fairness-based function evaluates the extent to which a transaction $t$ belongs to the set of the relapsed pending transactions $\mathcal{P}$, and consequently ascertain the probability of it being included in the set of the temporarily approved transactions $\mathcal{A}$ in the near future. The function $f_{\mathcal{P}}$ generates the feature $\Delta\mathcal{P}$ (or `delta`, presented in Table 5.1), described in Equation 6.4, and depicted in Figure 6.1.

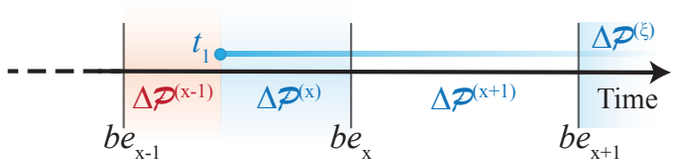


**Figure 6.1:** A transaction $t_1$ submitted at time $ep_{t_1}$ and yet-to-be included, such that $\mathcal{L}(t_1) = \mathcal{L}^{\xi}_{t_1}$, takes different $\Delta\mathcal{P}$ values over time. For instance, at height $x+1$ we have that $\Delta\mathcal{P}^{(x+1)} = be_{x+1} - ep_{t_1}$. Blue $\Delta\mathcal{P}$ represents a positive number, while the red $\Delta\mathcal{P}^{(x-1)}$ indicates a negative value.

**Definition 6.2.3: Pending transaction function**

$f_{\mathcal{P}}$ is the duration a transaction $t^{(x)}$ has been waiting inclusion into $\mathcal{A}$, starting from its inception until the closest block epoch $be_x$.

$$\begin{aligned} \Delta\mathcal{P}_t^{(x)} &= \beta_t{}^{(x)} - ep_t \\ (\beta, ep) \mapsto \Delta\mathcal{P} &= f_{\mathcal{P}}(\beta, ep) \end{aligned} \tag{6.4}$$

□

Note that if $t^{(x)}$ is not part of $\mathcal{P}^{(x)}$, then $\Delta\mathcal{P}^{(x)}$ assumes a negative value, as is evident from the case of $\Delta\mathcal{P}^{(x-1)}$ in Figure 6.1. The feature $\Delta\mathcal{P}$ enables us to consider the maximum amount of time a transaction can wait for approval if it has paid a fair fee. Moreover, since $\gamma$ represents the number of instances in $\boldsymbol{T}$, we can compute the time elapsed in relation to the number of blocks seen by $\boldsymbol{T}$ before being approved, and accordingly determine time with respect to both, an absolute view in seconds and a relative view in $\gamma$-occurrences. Consequently, a block-epoch-based transaction will have $\gamma$ different instances of the feature $\Delta\mathcal{P}$, as described in Section 5.1.2.

### Offset Function

The offset function $f_\delta$ is a revenue-oriented metric that orders pending transactions based on their feerate while considering the restrictions on block space. The output of this function is the engineered feature *offset* which is denoted by $\delta$.

**Definition 6.2.4: Offset function**

For each transaction **t** in a block-epoch, the offset value at height $x$ indicates the quantity of bytes that have already been taken up in the block space by unconfirmed transactions with a higher feerate. This value is represented as $\delta_t^{(x)}$.

$$\begin{aligned} \delta_i^{(x)} &= \sum_i^n q_i, \\ (S^{(x)}, q) &\mapsto \delta = f_\delta(S^{(x)}, q). \end{aligned} \tag{6.5}$$

□

The offset assigns a position to each transaction in the forthcoming block. A higher offset indicates a lower likelihood that $t$ is included in the set $\mathcal{A}^{(x)}$. Assuming that the set $S$ at height $x$ includes $n$ transactions ordered by feerate, the offset value for any index $0 \leq i \leq n$ can be defined as in Equation 6.5.

Like the scenario with $\Delta\mathcal{P}$, every block-epoch-based transaction possesses $\gamma$ distinct offset values, as the offset for each transaction is recalculated with every block creation. Algorithm 8 presents the procedure for calculating the offset for transactions in $S^{(x)}$. The algorithm is composed of two procedures: DEFINES and OFFSET. These procedures define the set $S$ and the offset $\delta$ for each transaction in $S$. Specifically, the DEFINES procedure takes as input $\mathcal{R}$ (with the $\Delta\mathcal{P}$ feature), a block height $x$, and it generates a set $S^{(x)}$. $S'$ contains all transactions that occurred between two block epochs. The set $S$ is then formed by adding any pending transactions from $\mathcal{P}$. The transactions in $S^{(x)}$ are ordered by feerate, after which the offset is calculated for each transaction.

The OFFSET procedure takes as input a transaction $t$ and the set $S$. It initializes $\delta$ and, for each transaction at a position $i$ after $t \in S$, it adds its size, $q_i$, to $\delta$.

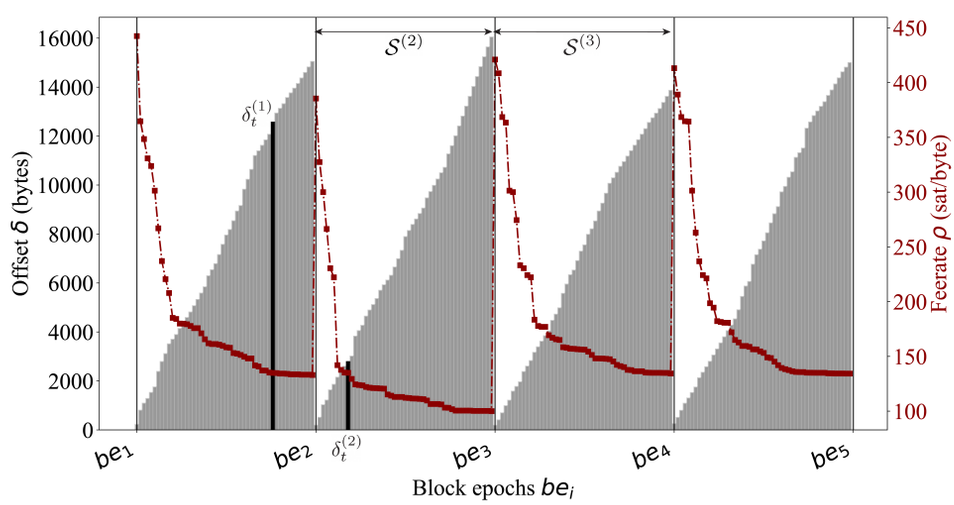


**Figure 6.2:** Data sampled for five consecutive blocks, and within each block-epoch time slot, transactions are arranged by feerate, followed by the calculation of their corresponding offset value. As observed in this example, the offset value for transaction $t^{(x)}$ fluctuates according to the block-epoch. Specifically, the offset value for $t^{(1)}$ at height $x = 1$ is larger than its offset value at height $x = 2$ for $t^{(2)}$. Thus, we can infer that $\delta_t^{(1)} \gg \delta_t^{(2)}$.

**Algorithm 8** Defining $S$ and $\delta$.

**procedure** DEFINES($\mathcal{R}_{\Delta\mathcal{P}}$, $x$) ▷ $\mathcal{R}$ including $\Delta\mathcal{P}$ feature
  $S' = \{t | t \in \mathcal{R}_{\Delta\mathcal{P}}, be_x \leq ep_t < be_{x+1}\}$ ▷ txs between $be_x$, and $be_{x+1}$
  $S \leftarrow \varnothing$
  **for all** $t \in S' \cup \mathcal{P}^{(x)}$ **do** ▷ waiting txs in $\mathcal{P}^{(x)}$
    $\rho_t \leftarrow f_\rho(\phi_t, q_t)$ ▷ calculate feerate of $t$
    $S \cup \{t\}$ ▷ add $t$ to the set $S^{(x)}$
  `sort`$(S, \rho)$ ▷ ascending order of txs in $S$ by feerate
  **for all** $t \in S$ **do**
    $\delta_t \leftarrow$ OFFSET$(t, S)$ ▷ set the offset for every transaction in $S$
  **return** $S$

**procedure** OFFSET($t$, $S$) ▷ index $i$ is the place of $t$ in the set $S$
  $\delta_t \leftarrow 0$
  $i \leftarrow 1$
  **for all** $t \in S$ after position $i$ **do** ▷ for txs in $S$ that come after $t$
    $\delta_t \leftarrow \delta_t + q_i$
    $i++$
  **return** $\delta_t$

Compared to other features, the offset requires a significantly higher computational overhead. The procedure DEFINES in Algorithm 8 has a time complexity of $O(n^2)$, where $n$ is the number of transactions in $S^{(x)}$. This is due to the fact that the execution time of OFFSET is upper-bounded by $O(n)$, and since the latter procedure is executed $n$ times, the total number of operations can be approximated by $\sum_{i=0,j=0}^{n} ij \sim O(n^2)$. Figure 6.2 depicts the trend of the calculated offset over time for five consecutive blocks. Within each block-epoch time frame ($be_1$–$be_5$), transactions waiting for confirmation are organized in the mempool according to their feerate and assessed for their relative offset value. For instance, transaction $t^{(x)}$ appears in the pool at height $x = 1$ and $x = 2$ with different offset values. As a result, the same transactions can provide distinct information based on their block-epoch snapshot, providing valuable insights into the network status at each block-epoch time slot.

### 6.2.3 Complete Set

After data collection and feature engineering, the runtime dataset $C$ is generated to include information about every transaction in a block-epoch-based manner. The creation of $C$ is described in Algorithm 9, where all the block

epochs present in the input dataset $\mathcal{R}$ are iterated over, and for each epoch, the algorithm adds the $\Delta\mathcal{P}$ feature, defines the set $\mathcal{P}$ and the set $S$ using the DEFINEP (Algorithm 10) and the DEFINES (Algorithm 8) functions, respectively. Subsequently, the algorithm appends the rows of $S$ for each block height $x$ to the complete set $\mathcal{C}$.

**Algorithm 9** Creation of $\mathcal{C}$.

```
1: procedure COMPLETE_SET(R)
2:     be_all ← list(R.bepoch)   ▷ list of all block epochs with no duplicates
3:     for all be ∈ be_all do
4:         x ← height(be)            ▷ gets height of a block from the epoch
5:         R_ΔP ← DELTA(R, x)                                  ▷ add ΔP feature
6:         P^(x) ← DEFINEP(R_ΔP, x, be)   ▷ make P set, used in DEFINES
7:         S^(x) ← DEFINES(R_ΔP, x)                            ▷ make S set
8:         C ← append rows in S^(x)
9:     return C
```

The $\mathcal{C}$ dataset is utilized to generate the training and test datasets $\mathcal{X}$, where the cardinality of $\mathcal{C}$ is greater than $\mathcal{X}$, which in turn is greater than the input dataset $\mathcal{R}$. Additionally, the features that are used in $\mathcal{X}$ is a subset of the features used in $\mathcal{C}$, which themselves are a subset of the features used in $\mathcal{R}$. To derive new features, as explained in Sections 6.1.2-6.2.2, several functions are applied to the datasets to generate new features with unique names. The pre-processing layer and ingestion engine exchange and update information, enabling the inclusion of these new features in the dataset $\mathcal{R}$. Subsequently, these new features can be incorporated into the training and test datasets, thereby enhancing model performance and improving prediction accuracy.

**Algorithm 10** Creation of $\mathcal{P}$.

```
1: procedure DEFINEP(R, x, be)
2:     be_{x−1} = epoch(x − 1)                          ▷ get epoch from height
3:     P^(x) ← {t|t ∈ R, φ_t ≥ E[f_t]}                      ▷ remove cheap txs
4:     P^(x) ← {t|t ∈ P^(x), ep_t ≤ be_{x−1}}               ▷ remove new txs
5:     return P^(x)
```

## 6.3 Machine Learning Model

We have chosen a supervised learning method for our model because the vast amount of available data on Bitcoin blockchain allows us to train and test our algorithm with precision. When there is an abundance of labeled data available, ResNet is considered the most appropriate models for generating accurate predictions [159, 160]. In line with this theory, we have employed the ResNet architecture, as presented in Section 2.3.3, to develop our prediction model for forecasting future trends in the Bitcoin blockchain market. The main purpose of the prediction model is to define whether or not a transaction $t$ at height $x$ is likely to be included in $\mathcal{A}^{(x)}$.

To optimize our ResNet model, we use the ReLU activation function. ReLU offers several advantages over other activation functions, such as being computationally efficient, easier to optimize, and able to prevent vanishing gradients, which can be a common issue in deep neural networks [121]. With ReLU, our model achieves better accuracy and faster training times, leading to more accurate predictions. Overall, our DNN prediction model using ReLU is a powerful tool for predicting future trends in the Bitcoin blockchain market, providing insights for both investors and researchers.

### 6.3.1 Training and Test Sets

Our ResNet model is trained and tested using two datasets: $\boldsymbol{X}$ for training and $\boldsymbol{Xte}$ for testing. These sets are constructed from the larger dataset $\mathcal{X}$ based on a percentage criterion. For example, if 5% of $\mathcal{X}$ is allocated for testing, the remaining 95% is used for training in $\boldsymbol{X}$. In accordance with the definitions of feature vector and complete transaction, represented by $\mathbf{t}$ and $\boldsymbol{T}$ respectively (as per definitions 6.2.1-6.2.2), the training and test datasets are characterized as an M-dimensional multivariate time series collection. Each pair $(\boldsymbol{T}_i, \boldsymbol{Y}_i)$ within this collection constitutes an instance of a block-epoch-based transaction $i$ with relative labeled information for the validation. In this notation, $\boldsymbol{Y}_i$ identifies information about the inclusion of a specific transaction, while $\boldsymbol{T}_i$ represents some of its corresponding features. More specifically, $\mathbf{Y}_i$ represents the corresponding one-hot label vector[4] of transaction $\boldsymbol{T}_i$. In particular, $\mathcal{X}$ is expressed as $(\boldsymbol{T}_1, \boldsymbol{Y}_1), (\boldsymbol{T}_2, \boldsymbol{Y}_2), \ldots, (\boldsymbol{T}_M, \boldsymbol{Y}_M)$. The one-hot label vector $\mathbf{Y}_i$ has a length of $\gamma_i$, and each of its elements, $j \in [1, \gamma_i]$, is equal to 1 if $j = \gamma_i$, which is the corresponding time slot of $\boldsymbol{T}$'s inclusion, and 0 otherwise. Table 6.3

4. A one-hot label vector is a representation of a categorical variable in ML, where each category is assigned a unique binary value.

| $\mathcal{X}$ | | $\boldsymbol{T}_i$ | | | | $\boldsymbol{Y}_i$ |
|---|---|---|---|---|---|---|
| $i$ | | **hash** | **bepoch** | **w time** | **offset** | **incl.** |
| $i=1$ | $\mathbf{t}_1$ | 49baa25... | ...22049 | -958 | 1,630,459 | 0 |
| | $\mathbf{t}_2$ | 49baa25... | ...23235 | 38 | 12,312,700 | 0 |
| | ... | | | | | |
| | $\mathbf{t}_{\gamma_1}$ | 49baa25... | ...27793 | 5399 | 897,480 | 1 |
| ... | | | | | | |
| $i=M$ | $\mathbf{t}_1$ | 860b21a... | ...21154 | -732 | 1,882,965 | 0 |
| | $\mathbf{t}_2$ | 860b21a... | ...21759 | 128 | 2,592,452 | 0 |
| | ... | | | | | |
| | $\mathbf{t}_{\gamma_M}$ | 860b21a... | ...23528 | 4892 | 978,382 | 1 |

**Table 6.3:** Representation of an M-dimension multivariate time series collection.

illustrates an instance of a multivariate time-series pair, $(\boldsymbol{T}_i, \boldsymbol{Y}_i)$. Specifically, the hash feature within the transaction remains constant throughout its lifespan, while the remaining features, identified as $be$ (or block epoch), $\Delta\mathcal{P}$, and $\delta_t$, are dependent on the contextual block-epoch.

**Algorithm 11** Creation of $\mathcal{X}$.

```
1:  procedure TRAINING_SET(C, k=[δ_t, ΔP, φ, ...])   ▷ k is vector of keys
2:      for all key in k do                          ▷ for each feature name in k
3:          X ← add_feature(C, key)                  ▷ add "key" column from C to X
4:      X ← INCLUSION(X)                             ▷ make Y
5:      X ← X.values                                 ▷ NumPy representation of Pandas dataframe
6:      X ← NORMALIZATION(X)                         ▷ z-score normalization
7:      return X
8:
9:  procedure INCLUSION(d)                           ▷ inputs a dataset
10:     d[incl] ← np.where(d[be] == d[β_t], 1, 0)    ▷ 1 if be =β_t, 0 otherwise
11:     return d                                     ▷ same dataset with new "inclusion" feature, or Y
```

Algorithm 11 outlines the procedure to generate the set $\mathcal{X}$. This involves utilizing the normalization techniques illustrated in Algorithm 12 in combination with the NumPy libraries to construct the set $\mathcal{X} = (\boldsymbol{T}, \boldsymbol{Y})$. Algorithm 11 computes the training set $\mathcal{X}$ for a given set of feature names $k$ and a the complete set $C$. The procedure begins by iterating through each feature in $k$ and adding the corresponding column from $C$ to $\mathcal{X}$. Then, the INCLUSION function is applied to $\mathcal{X}$ to create the binary $\mathbf{Y}$ feature, where 1 indicates the inclusion of a transaction and 0 otherwise. If the block-epoch value ($be$) for a block-epoch-based transaction matches the block epoch when the transaction is included

($\beta_t$), then the corresponding element in the new column is set to 1. Next, the NumPy representation of $\mathcal{X}$ is obtained and passed through the normalization process. Finally, the normalized NumPy array is returned as the final training set $\mathcal{X}$.

### Normalization

The selection of an appropriate normalization method is influenced by the properties of the data and the objectives of the specific task. Each normalization technique offers distinct advantages and disadvantages, and selecting an appropriate method can have a profound effect on the quality and effectiveness of the model or analysis. For example, the decimal scaling normalization method is advantageous for preserving the order of magnitude of the data, while min-max normalization is useful for comparing variables that have varying units and scales.

**Algorithm 12** Normalization of $\mathcal{X}$.

```
1: procedure NORMALIZATION(X)
2:     μ ← np.mean(X)          ▷ expected value (using NumPy as np)
3:     σ ← np.std(X)                          ▷ standard deviation
4:     X_norm ← (X−μ)/σ                ▷ set the normalize training set
5:     return X_norm
```

The normalization technique employed in Algorithm 12 is a commonly used method known as z-score normalization, or standardization. This method involves transforming a distribution of data points to have a mean of 0 and a standard deviation of 1 by subtracting the mean of each data point and dividing it by the standard deviation [161]. The z-score normalization technique is valuable for comparing variables with different units and scales and for identifying outliers. It is particularly advantageous when working with normally distributed data and it can help to ensure that input features have similar ranges, preventing the dominance of one feature over the others. Furthermore, it can aid in improving the convergence of training algorithms by preventing them from getting trapped in local optima.

## 6.3.2 Prediction Model

To ensure accuracy and maintain up-to-date knowledge of the network status, our model needs to be updated after some time, typically on a monthly basis

(weekly for a better outcome). For this study, we have considered to deploy two different models: a standard DNN and a ResNet model that utilizes skip connections.

Considering the superior performance demonstrated by the ResNet model compared to the DNN model [57], we adopt the former as the model of focus in this dissertation. The ResNet architecture consists of several densely connected layers, with each layer fully connected to the previous one. The activation function used for each hidden layer is ReLU, which facilitates the learning of non-linear relationships between the input and output variables. To initialize the weights in the neural network and improve the speed and stability of training, the He normalization technique[5] is used as the kernel initializer. Additionally, the ResNet model incorporates several skip connections, which enable information to bypass certain layers and be directly fed to subsequent layers, thus improving the flow of information throughout the network. The output layer of the ResNet model has a softmax activation function, which generates a probability distribution over the classes. The present study does not include the outcomes of the DNN model, as it has been surpassed in performance by the ResNet model. The results and discussions regarding the DNN model can be found in our previous work [57].

The trained ResNet model takes a transaction $t$ as an input and generates a vector $\boldsymbol{\theta}_t$, with the confidence level of inclusion or exclusion in the next mined block. Since we have a binary classification problem, the output vector $\boldsymbol{\theta}_t = [P_t(v_0), P_t(v_1)]$ assigns the class $v_1$ to inclusion and $v_0$ to exclusion. As such $\boldsymbol{\theta}_t$ represents the probability $P(v_i)$ of transaction $t$ falling within the class $v_i$, where $i \in \{0, 1\}$. We adopt a supervised classification approach whereby the known outcomes of transactions in the training set, denoted as $\boldsymbol{X}$, are used to assess the accuracy of the model during the training phase, which is accomplished through the use of the labels $\mathbf{Y}$. A subset $\boldsymbol{Xte} \subseteq \mathcal{X}$ of the data is reserved for testing.

During validation we employ a dynamic approach that alters the number of hidden layers in the neural network, with each node in the network being characterized by the ReLU, except for the output layer where the Normalized Exponential Function (softmax) is used. The weights are initialized using the He normalization technique, which accounts for ReLU, thereby facilitating convergence in deep models [162]. During training and testing phases, as

5. is a technique used to initialize the weights of artificial neural networks. By using He normalization, the weights are initialized in a way that prevents them from becoming too large or too small. This technique helps the network converge faster and improves its ability to learn complex patterns and representations from the data

outlined in the previous section, $X$ is normalized with the z-score method, which was useful as the features exhibit varying orders of magnitude.

The hyperparameters of the ResNet that cannot be estimated from data are determined manually through a trial-and-error. This include the number of hidden layers, the number of skip connections, the batch size, and the number of epochs. The batch size governs the granularity or precision of gradient descent, thereby optimizing the internal parameters of the model for every batch size of tuples. On the other hand, the number of epochs determines the number of times that the learning algorithm will iterate through the entire training dataset, ideally getting closer to the optimal solution with each iteration. The configuration of the model's hyperparameters is critical to achieve optimal model performance and accuracy.

## Summary

In this chapter, we provided an in-depth overview of the architecture of our ML model. We outlined the entire data processing and transformation pipeline, beginning with the ingestion engine. The ingestion engine was responsible for processing and transforming the data, selecting relevant features, and storing them locally.

We then delved into the pre-processing phase, which consisted of three key steps. First, we divided transactions into block-epoch-based tuples, enabling efficient analysis. Next, we performed feature extraction to derive meaningful characteristics from the data. Lastly, we created a complete dataset by integrating all relevant features.

Additionally, we introduced the ResNet model that we developed. We discussed the composition of the training set, the normalization of data, and the output of the model.

In the following section, we present experiments and evaluations of the ML model described thus far. A detailed account of the hyperparameters can be found in Appendix A.

# 7

# Evaluation

In this chapter, we present the evaluation of our ML model. In Section 7.1, we give a detailed description of the datasets used for both training and testing our model, including how we selected relevant features. In Section 7.2, we outline the evaluation metrics we use and elaborate on our definition of model accuracy, as our accuracy assessment transcends the mere measurement of the proportion of correctly classified instances out of the total instances. We also account for other metrics such as the completeness of the data used for training and testing the model, as well as the degree to which the dataset is updated. By incorporating these additional metrics in our assessments, we obtain a more comprehensive evaluation of our model's performance, while also accounting for potential sources of bias. In Section 7.3, we report the results of our analyses in terms of overall accuracy, feature importance, and model cyclicity. We investigate how the model's performance is affected by the selected features and how often the model's predictions are influenced by its current network status. Finally, in Section 7.4 we quantify how much our solution can benefit end-users.

## 7.1 Experimental Setup

In this section, we describe a comparative analysis of various datasets in relation to the disk space consumption associated with the Bitcoin blockchain. We introduce the distinct metrics used to evaluate the accuracy of the model and ultimately examine and enumerate the chosen features.

### 7.1.1 Datasets Analysis

We first investigate the data derived from the public Bitcoin blockchain. Our analysis includes over 30 million transactions across 15,000 blocks from January 2021 to May 2021. Table 7.1 demonstrates the requisite disk space for these three datasets when accommodating 100,000 to 5,000,000 transactions. As shown, the complete dataset $\mathcal{C}$ exhibits a superlinear growth pattern. This observation aligns well with our expectations, considering that $\mathcal{C}$ not only includes all transactions in $\mathcal{R}$, but also captures the block-epoch based dependent features delineated in Chapter 6, and possesses knowledge of $\mathcal{P}$ and $\mathcal{S}$ sets. The comparison in Table 7.1 highlights the disk space efficiency of the developed datasets in relation to the actual Bitcoin blockchain.

| Disk storage (bytes) | | | | |
|---|---|---|---|---|
| **N of txs** | **100k** | **500k** | **1M** | **5M** |
| **Dataset** | | | | |
| $\mathcal{R}$ | $2.9 \times 10^7$ | $1.45 \times 10^8$ | $2.9 \times 10^8$ | $1.2 \times 10^9$ |
| $\mathcal{C}$ | $4 \times 10^7$ | $7.3 \times 10^8$ | $1.6 \times 10^9$ | $1.37 \times 10^{10}$ |
| $\mathcal{X}$ | $7 \times 10^6$ | $1.3 \times 10^8$ | $2.88 \times 10^8$ | $2.4 \times 10^9$ |
| ₿ | $6 \times 10^7$ | $3 \times 10^8$ | $6 \times 10^8$ | $3 \times 10^9$ |

**Table 7.1:** This table displays the amount of disk space utilized by various sets of instances containing information on 100,000, 500,000, 1,000,000, and 5,000,000 transactions, respectively. The final row presents the corresponding space occupied by an equivalent number of transactions in the real Bitcoin blockchain.

### 7.1.2 Metrics

We obtain and store various instances of $\mathcal{R}$, one for each month of evaluation (see Table 7.2). For each evaluation period, 3,010 blocks[1] are fetched. A predictive model is constructed from each dataset $\mathcal{R}^i$, using the inclusion

1. Which is the equivalent of the number of blocks mined on 20 days on average

pattern delineated in Section 5. Also, a $C^i$ dataset is produced, from which novel information and features are derived. Afterwards, data is selected from the $C^i$ dataset to form the training and testing datasets ($X^i$). For each period $i$, a model is trained using the initial 50% of transactions in $\mathcal{R}^i$. For testing such model, the remaining 50% of transactions is used. Tests are performed and evaluated with parameters denoting the *completeness* and *freshness* of the testing set. These parameters are identified as $\alpha$ and $\psi$, respectively, as defined below.

### Completeness

**Definition 7.1.1: Completeness**

The completeness parameter $\alpha$ of a testing set identifies the proportion of transactions used for testing relative to the total number of points used for training.

$$\alpha = \frac{|\boldsymbol{Xte}|}{|\boldsymbol{X}|} \tag{7.1}$$

□

From Equation 7.1, we can see that when $\alpha = 0.5$, the testing volume of transactions is equal to half of the training volume. The completeness value is crucial for precise prediction in the absence of live (or real-time) information.[2]

| Raw dataset for each period | | | | |
|---|---|---|---|---|
| $i$ | Date | $\lvert\mathcal{R}^i\rvert$ | $\mathcal{R}^i$ size | ₿ price |
| 1 | Jan | 6.5M | 1.09 GB | 29k to 35k $ |
| 2 | Feb | 6.7M | 1.12 GB | 33k to 56k $ |
| 3 | Mar | 6.2M | 1.05 GB | 49k to 58k $ |
| 4 | Apr | 6.2M | 1.04 GB | 58k to 56k $ |
| 5 | May | 5.2M | 877 MB | 58k to 36k $ |

**Table 7.2:** Specification of the raw time-series datasets used for evaluation. For each month, 3,010 blocks are analyzed. $|\mathcal{R}^i|$ is the number of transactions analyzed in each set, while $\mathcal{R}^i$ size identifies the set's storage requirements. We also include the Bitcoin price at time of evaluation to discuss any correlation with model prediction and coin price at that time.

2. Since the offset value is determined by the number of transactions evaluated, having a complete set of transactions is crucial to compute the transaction space in the next mined

Due to the supervised nature of our testing methodology and the simultaneous analysis of millions of transactions, we were precluded from relying on unlabeled real-time data, and therefore we needed to distinguish a complete testing set from a non complete one. As $\alpha \longrightarrow 1$, the set becomes *complete*, and the constructed offset value for testing closely approximates the one employed for training, thus reducing false-positive points when $\alpha \ll 1$ or false negatives when $\alpha \gg 1$. A complete set offers an accurate representation of the mempool size over time.

### Freshness

Assuming `mo` represents the difference between the index $i$ in Table 7.2 of training and testing datasets, as:

$$\texttt{mo} = i^{X_{te}} - i^{X}$$

then the freshness is normalized through a sigmoid function to yield a bounded range of $[0, 1]$.

**Definition 7.1.2: Freshness**

The freshness parameter of a testing set, $\psi$, identifies the temporal distance between the test and training sets, normalized through a sigmoid function.

$$\psi = \text{sigmoid}(\texttt{mo}) \tag{7.2}$$

□

When training and test data are derived from the same month, where $\psi$ is equal to $\text{sigmoid}(0) = 0.5$, designating the model as new, or *fresh*. If testing is conducted with an older model, $\texttt{mo} > 0$ and $\psi \longrightarrow 1$. Conversely, if the model is trained a-posteriori and applied to prior data, $\texttt{mo} < 0$ and $\psi \longrightarrow 0$. The $\psi$ parameter reflects the degree of freshness of the tested transactions relative to the trained ones, thereby measuring the model's currency with respect to the existing network status. Additionally, information on $\psi$ proves valuable during subsequent analysis of model cyclicity.

---

block. Evaluating and testing live data results in having a complete set.

### 7.1.3 Features

The selection of features to be used for training our model, is a combination of parameters that are extracted from the blockchain, and data that are computed according to the guidelines presented in Section 6.1.1. The training set $\mathcal{X}$ is expected to contain relevant information about fairness and revenue, as detailed in Sections 5.3 and 5.2. Our model is trained using a set of features denoted by:

$$K_{\mathcal{X}} = [\phi, q, \rho, \Delta\mathcal{P}, \delta, \Delta\mathcal{P}_N, \delta_N]$$

where $\Delta\mathcal{P}_N$ and $\delta_N$ represent normalized values of $\Delta\mathcal{P}$ and $\delta$, respectively. The feature $\Delta\mathcal{P}_N$ is determined as the number of blocks a particular transaction $\mathbf{t}_\gamma$ has encountered since its inception (as indicated by Equation 7.3).

$$\begin{aligned} \Delta\mathcal{P}_N^{(\gamma)} &= \sum_{i=0}^{\gamma} \omega^{(i)} \quad \text{where} \\ \omega^{(i)} &= \begin{cases} 0, & \text{if } \mathbf{t}_i \notin \mathcal{P}^{(i)} \\ 1, & \text{if } \mathbf{t}_i \in \mathcal{P}^{(i)} \end{cases} \end{aligned} \tag{7.3}$$

The second feature, $\delta_N$, corresponds to the normalized offset in relation to the maximum block space of approximately 1.1 MB. This normalization results in $\delta_N$ being represented as a percentage, which provides information about what portion of the mempool is already occupied by richer transactions (as showed by Equation 7.4).

$$\delta_N^{(x)} = \frac{\delta^{(x)} \times 100}{Q} \tag{7.4}$$

## 7.2 Evaluation Metrics

While classification accuracy is our primary evaluation metric, it may not always be sufficient to fully assess performance. To address this, we also evaluate performance using the confusion matrix and the area under the curve metric. The confusion matrix provides information about the number of true and false positive and negative classifications made by our model, which help identify areas of strength and weakness. The area under the curve metric measures the performance of our model across a range of classification thresholds, providing a more nuanced assessment of its ability to correctly classify instances. The following sections provide a brief description of the evaluation metrics we have used, while Section 7.3 presents our evaluation results.

### 7.2.1 Classification Accuracy

To evaluate our model, we initially employ the *classification accuracy* metric, which measures the ratio of the number of correct predictions to the total number of input samples using the formula:

$$\text{Accuracy} = \frac{\text{Number of correct predictions}}{\text{Total number of predictions}}$$

Classification accuracy is a straightforward measure that we use as a general tool to compare accuracy between different models. However, it may not always provide an accurate evaluation of a model's performance, particularly when the class distribution is heterogeneous. In our study, we observed an unbalanced class distribution and chose not to reduce the number of sampled data. As a result, we incorporated additional metrics to evaluate our model.

### 7.2.2 Confusion Matrix

The confusion matrix is useful for analyzing the accuracy of our model. The confusion matrix **CM** is defined in Equation 7.5, and formalized in Table 7.3. The matrix **CM** is obtained by dividing the raw count of correctly and incorrectly classified instances by the total number of instances, and then scaling the resulting values by a factor $\mathbf{Fr}^{-1}$. The matrix $\mathbf{Fr}_{2,2}$ represents the total number of actual classifications for each class.

$$\begin{aligned} \mathbf{CM} &= \mathbf{Fr}^{-1} \cdot \begin{bmatrix} a_{00} & a_{01} \\ a_{10} & a_{11} \end{bmatrix} \\ \text{where} \quad \mathbf{Fr}_{2,2} &= [b_{ii}], \quad b_{ii} = \sum_j a_{ij} \end{aligned} \tag{7.5}$$

The values $a_{ij}$ in the confusion matrix **CM** represent the number of elements that truly belongs to class $i$ but were classified as belonging to class $j$. We use two metrics derived from **CM**, namely *recall* and *precision*. The recall $R_i$ for class $v_i$ represents the proportion of instances in $v_i$ that were correctly classified, while the precision $P_i$ for class $v_i$ represents the proportion of instances that were classified as belonging to $v_i$ that actually belong to $v_i$. These metrics are calculated using Equation 7.6.

$$R_i = \frac{a_{ii}}{\sum_{j=0}^{1} a_{ji}} \qquad P_i = \frac{a_{ii}}{\sum_{j=0}^{1} a_{ij}} \tag{7.6}$$

### 7.2.3 Area Under Curve

The Area Under Curve (AUC) measures the probability that a model will rank a randomly selected sample in class $v_1$ higher than another randomly selected sample in $v_0$. AUC is commonly used in binary classification problems. The range of values for the AUC is zero to one, with higher values indicating better classifier performance. An AUC value of one indicates that the classifier is able to perfectly distinguish between the two classes, while a value of 0.5 indicates that the model cannot differentiate between points in the $v_0$ and $v_1$ classes. A value of zero indicates that the classifier would predict all points in $v_0$ as $v_1$ and vice versa.

Evaluation of binary classification models benefits from careful consideration of several performance metrics, including the Area Under Curve of Receiver Operator Characteristic (AUC-ROC). To calculate the AUC-ROC, we follow the scheme presented in Table 7.3 and use the formulas:

$$\begin{aligned} TPR &= \frac{TP}{TP + FN} & FNR &= \frac{FN}{TP + FN} \\ TNR &= \frac{TN}{TN + FP} & FPR &= \frac{FP}{TN + FP} \end{aligned} \tag{7.7}$$

where *TP* represents true positives, *TN* represents true negatives, *FP* represents false positives, and *FN* represents false negatives. The True Positive Rate (TPR) identifies $R_1$, or *sensitivity*, while the True Negative Rate (TNR) represents the *specificity*, or the proportion of negative class $v_0$ samples that are correctly classified. The False Positive Rate (FPR) is equal to 1−specificity and represents the proportion of $v_0$ samples that are incorrectly classified. Finally, the False Negative Rate (FNR) indicates the proportion of positive class $v_1$ samples that are incorrectly classified.

The Receiver Operator Characteristic (ROC) curve is a graphical representation of the TPR against the FPR and is useful for evaluating the performance of binary classifiers. The AUC is equal to the area under the ROC curve.

## 7.3 Performance

In Section 7.3.1, we provide an overview of the classification accuracy of our classifier based on the evaluation metrics defined in Section 7.2. Specifically, we report the classification accuracy for each month of the evaluation period (January 2021 to May 2021) under optimal conditions of $\alpha = 1$ and $\psi = 0.5$. Additionally, a confusion matrix representing the entire evaluation period

| | | Actual values: 0 | Actual values: 1 |
|---|---|---|---|
| Predicted values | 0 | True Negative Rate | False Negative Rate |
| | 1 | False Positive Rate | True Positive Rate |

**Table 7.3:** The confusion matrix model is utilized as the foundation for computing the AUC-ROC.

is presented. Section 7.3.2 discusses the significance of selecting appropriate features, examines how the inclusion or exclusion of certain information affects accuracy, and highlights the potential impact of incorrect assumptions. In these experiments, we set hyperparameters to an optimal case scenario. Finally, in Section 7.3.3, we emphasize the importance of updating the model regularly. We evaluate different model parameters and report the AUC-ROC score for each of them, which are subsequently compared.

### 7.3.1 Overall Accuracy

Next, we report the overall classification accuracy of each month from January to May 2021 using the optimal parameters of $\alpha = 1$ and $\psi = 0.5$, summarized in Table 7.4. The average accuracy for the entire period of analysis is also included in the table. Table 7.5 displays the computed confusion matrix for all the points analyzed over the course of the evaluation, which includes more than 30 million transactions.

As indicated in Table 7.4, the overall accuracy of the model is above 90% for three out of five months during the entire training/test period, while it struggles between April and May due to the coin price plunge (discussed in Section 8). Nonetheless, even in our worst-case scenarios, the model remains relatively robust. The confusion matrix in Table 7.5 demonstrates that the model correctly classified 91% of the transactions in the $v_0$ class and 88% in the $v_1$ class.

| Classification accuracy 2021 (%) | | | | | | | |
|---|---|---|---|---|---|---|---|
| $\alpha$ | $\psi$ | Jan | Feb | Mar | Apr | May | **Overall** |
| 1 | 0.5 | 90.07 | 90.9 | 91.08 | 85.52 | 88.29 | 89.17 |

**Table 7.4:** The presented results include the classification accuracy for each month of the evaluation period, which spans from January to May 2021. The overall accuracy is calculated as the average classification accuracy across the entire evaluation period. The optimal parameters of $\alpha$ and $\psi$ are employed in order to ensure that the model is complete and up-to-date with respect to the tested data.

| Overall **CM** score | | |
|---|---|---|
| | $v_0$ | $v_1$ |
| $v_0$ | 0.91 | 0.09 |
| $v_1$ | 0.12 | 0.88 |

**Table 7.5:** The presented confusion matrix represents the overall score for a test conducted between January 2021 and May 2021, with parameters $\alpha = 1$ and $\psi = 0.5$. The matrix depicts how over 30 million transactions were classified using five distinct models, each of which corresponded to a different month, thereby providing a complete and up-to-date view. The false negative rate is determined to be 9% for the negative class, while the false positive rate is observed to be 12% for the positive class.

| Classification accuracy 2021 (%) | | | | | | |
|---|---|---|---|---|---|---|
| **Feature set** | Jan | Feb | Mar | Apr | May | **Overall** |
| 1 : **Primitive** | 75.13 | 78.54 | 77.77 | 62.52 | 69.97 | 72.78 |
| 2 : **Fairness** | 84.57 | 86.24 | 84.63 | 83.64 | 82.11 | 84.23 |
| 3 : **Revenue** | 88.24 | 87.73 | 89.4 | 80 | 86.21 | 86.31 |
| 4 : **Complete** | 89.51 | 90.36 | 90.04 | 85.35 | 88.23 | 88.69 |

**Table 7.6:** The accuracy of classification across various sets was assessed. Each set denotes a distinct feature property. The primitive set includes only transaction fee and size, while a revenue-based solution include features that are associated with miners' revenue, such as fee, offset, and feerate.

### 7.3.2 Features Performance

To validate our assumptions on the importance of certain features in predicting transaction inclusion, we conducted tests and verified the relevance of four specific feature subsets. The classification accuracy and confusion matrix for models trained using each of the four feature sets are presented in the following results.

The first set, denoted as *primitive information*, includes only fetched features such as transaction size and fee, commonly used by fee predictors but with poor results in terms of fee overpaying.

The second set, denoted as *fairness assumptions*, excludes features based on the revenue principle, assuming that a miner needs only to be fair to include transactions in the next block.

The third set, denoted as *revenue assumptions*, excludes features based on the fairness principle to monitor the impact of revenue on the transaction inclusion pattern.

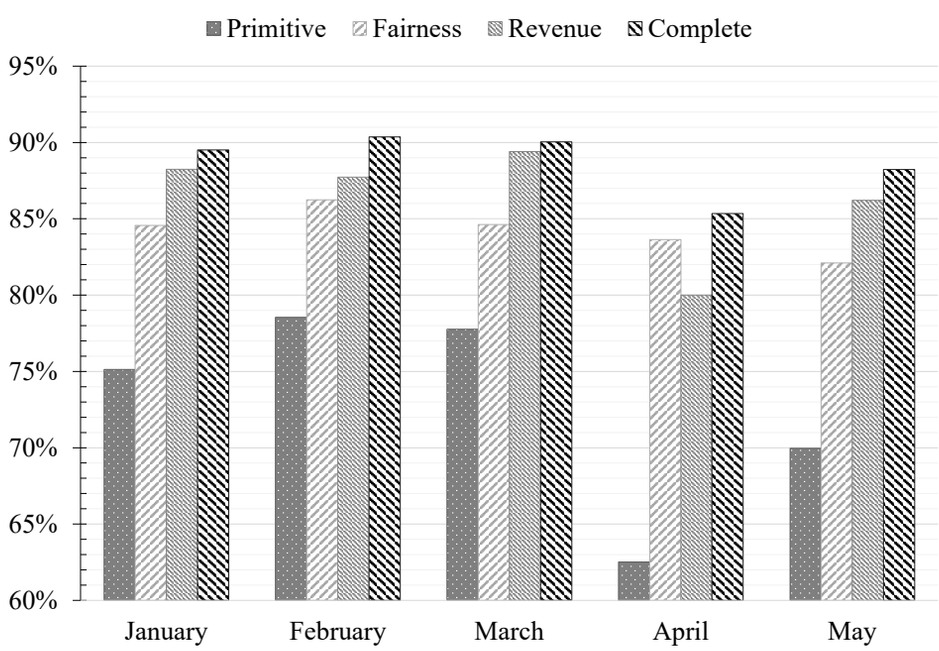


**Figure 7.1:** Classification accuracy outcomes for each set of features. The findings demonstrate a substantial enhancement in model accuracy when utilizing a complete feature set, as opposed to relying solely on transaction size and transaction fee as features.

Finally, the fourth set, denoted as *complete information*, includes fetched and extracted features, aiming to verify the reliability of our initial assumptions, including both fairness and revenue concepts. The specific feature sets for each evaluation are defined as follows:

1. Primitive: $[\phi, q]$
2. Fairness: $[\phi, q, \Delta\mathcal{P}, \Delta\mathcal{P}_N]$
3. Revenue: $[\phi, q, \rho, \delta, \delta_N]$
4. Complete: $[\rho, \Delta\mathcal{P}, \Delta\mathcal{P}_N, \delta, \delta_N]$

The experiments conducted in this study were designed with a completeness of $\alpha = 1$ and freshness of $\psi = 0.5$. Observed classification accuracy are reported in Table 7.6 and the corresponding plot is presented in Figure 7.1. We observed that the ResNet classifier struggles when Bitcoin prices experience a sudden and significant drop, such as in April 2021. Specifically, the accuracy dropped by 15% when the primitive set of features was used, while the accuracy drop was limited to 5% when complete information was used. This finding highlights the relevance of assumptions made in predicting transaction inclusion. Notably, when fairness and revenue principles were applied separately to the data, the model achieved an average improvement in accuracy ranging from 12% to 14%, and up to 23% when these principles were combined.

The variance of the fairness sub-feature set classification accuracy appeared to be smaller than that of revenue sub-feature set, underscoring the importance of the fairness concept in determining transaction inclusion. In April 2021, an inversion of the Bitcoin price uptrend was observed and miner revenue reached an all-time high. During this period, data indicates that miners appeared to be prioritizing revenue over fairness.

### 7.3.3 Model Cyclicity

To demonstrate the potential improvement in model classification accuracy when trained on well-formed data, this paragraph illustrates a deviation from the optimal parameter settings. This updated model is cyclically trained over time with complete ($\alpha = 1$) and fresh ($\psi = 0.5$) information. By varying the value of $\psi$, we can test the model's behavior with both older and newer transactions. Testing is conducted for each month with various combinations of values for $\alpha$ and $\psi$. Although some of these scenarios may be unrealistic, they

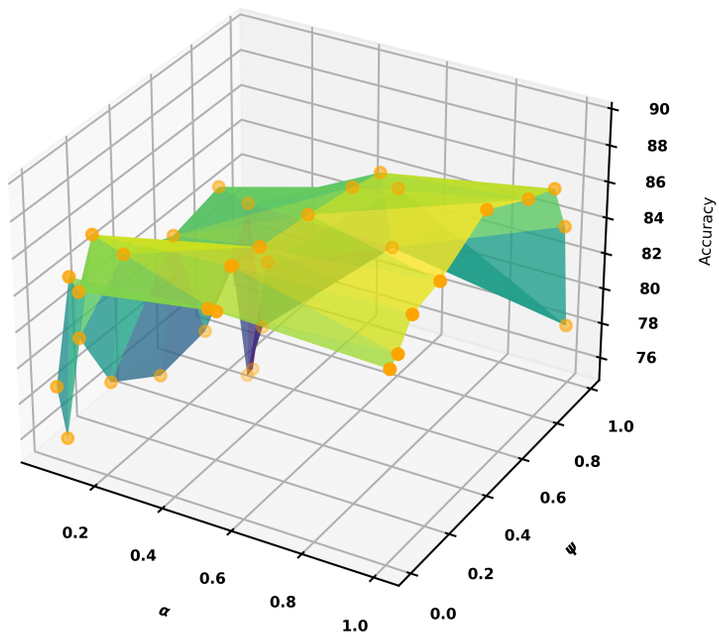


**Figure 7.2:** Classification accuracy values ($z$-axis) for multiple models, tested with diverse settings. The $y$-axis, represented by the $\psi$ parameter, indicates the extent to which a particular model is updated, while the $x$-axis identifies the model's completeness, as determined by the $\alpha$ parameter. To improve classification accuracy, it is important to highlight the importance of the model's cyclicity.

| Evaluations on model cyclicity | | | | |
|---|---|---|---|---|
| type | $\alpha$ | $\psi$ | Accuracy (%) | **AUC-ROC** |
| **Worst-** | 0.04 | 0.02 | 78.63 | 0.82 |
| **Average-** | 0.2 | 0.12 | 84.71 | 0.92 |
| **Optimal** | 1 | 0.5 | 91.08 | 0.97 |
| **Average+** | 0.2 | 0.88 | 81.25 | 0.89 |
| **Worst+** | 0.04 | 0.98 | 70.25 | 0.8 |

**Table 7.7:** AUC-ROC results obtained for different parameter values. The optimal evaluation is achieved when the model is complete and the testing is performed within the same month as the training. The average evaluation is obtained using a model that is 20% complete and with a two-month deviation between training and testing. The worst evaluation case corresponds to a model that is only 4% complete and tested four months after training.

are useful for monitoring the model's performance under different conditions. For each month, we perform tests on various combination of values for $\alpha$, which include 0.05, 0.1, 0.5, and 1, as well as $\psi$, which includes 0.01, 0.05, 0.12, 0.26, 0.5, 0.73, 0.88, 0.95, and 0.98.

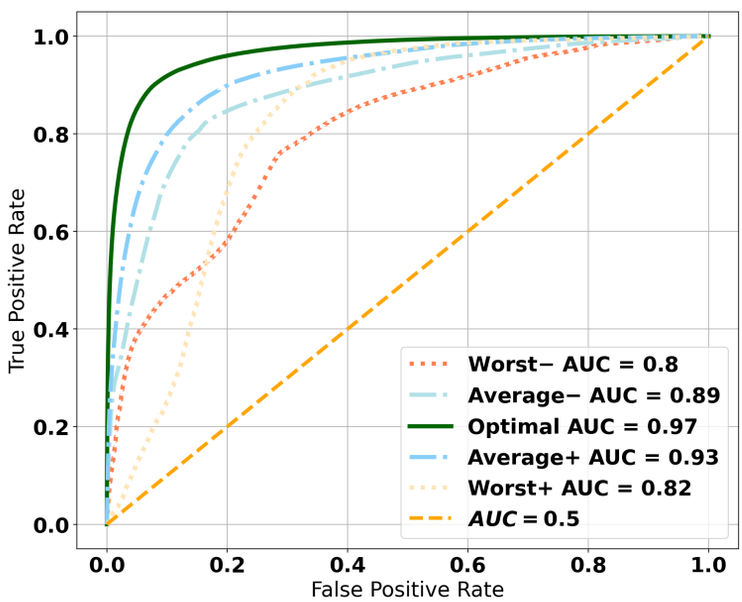


**Figure 7.3:** Five tests conducted to measure AUC-ROC in optimal, average, and worst-case scenarios. The optimal test was performed using $\alpha = 1$ and $\psi = 0.5$, and is indicated by the green continuous line. The two average tests were conducted with $\alpha = 0.2$ and $\psi = [0.12, 0.88]$, and are represented by the dot-dashed light blue lines. The two worst-case tests were conducted with $\alpha = 0.04$ and $\psi = [0.02, 0.98]$, and are represented by dotted yellow and red lines, respectively. When the AUC is equal to 0.5, the classifier can no longer distinguish between positive and negative class points.

The results are presented in Figure 7.2. Each data point corresponds to the average classification accuracy over five months, for a specific combination of parameter values ($\alpha$ on the x-axis and $\psi$ on the y-axis). The plot demonstrates that the accuracy is highest (indicated by yellow color) when $\psi$ is close to 0.5 and $\alpha$ is close to 1. When the precision of the offset decreases (smaller $\alpha$ values), the impact of model cyclicity ($\psi$) becomes less significant. These findings highlight the importance of selecting appropriate values for both parameters. Specifically, $\psi$ is relevant when it incorporates accurate information about the mempool size, which is provided by an appropriate choice of $\alpha$. By

contextualizing the model over time through the offset, accurate predictions can be made. Without an accurate calculation of the offset, the model would rely solely on the fairness concept, which appears to have less accuracy variance over time (as demonstrated in Figure 7.1, fairness bar).

Figure 7.3 displays the AUC-ROC curves obtained from five tests that were conducted using different parameter values. These values were carefully selected to represent optimal, average, and worst-case scenarios, as described in Table 7.7. We distinguish between two average cases and two worst cases, depending on whether testing was performed before (–), or after (+) training. In the optimal case, the model achieves a solid classification result, with an area under the curve of 0.97, indicating its ability to distinguish between classes. Even when allowing for a FPR of 10%, the FNR does not exceed 10%. Furthermore, if a FPR of 20% is accepted, the FNR remains below 5%.

## 7.4 Benefits for End-Users

Analyzing fee reduction for end-users is essential as it provides valuable insights into the extent to which our solution can benefit users. In this context, our study focused on testing the impact of fee reductions across all months of the evaluation period, covering all transactions in our local dataset $\mathcal{R}$. We specifically focused on transactions belonging to $v_1$, namely, those that were selected by miners in the next round of mining.

**Purpose** We aim to determine the extent to which users can potentially decrease their transaction fees while still maintaining a favorable probability of inclusion in the next mined block.

**Methodology** We analyze the effect of fee reductions, ranging from 0% to 80% of the original fee, on our ML model for each block-epoch-based transaction in our complete set $C$. We also take into account the overall adoption of our model, as this directly affects parameters like feerate and offset values at each block-epoch. To explore this effect, we test various levels of overall adoption, ranging from 1% to 100%. In the lowest adoption scenario, only a random 1% sample of transactions will have their fees reduced, while in the highest adoption scenario, fees of all transactions will be reduced.

**Experimental setup** The tests are conducted as simulations of reduced fees rather than real-world transactions executed on the Bitcoin network.

In these simulations, we utilize transactions stored in our local dataset, lower their transaction fees, and input them into our ML model to assess the variance in accuracy score. We have deliberately chosen to focus on labeled transactions in $v_1$, as they have already been selected for inclusion. Consequently, it is essential to examine the extent to which a fee reduction will affect their likelihood of being included.

**Analysis** In order to evaluate the significance of our results, we analyze the variance in the accuracy score of the identical ML model when applied with different fee and adoption parameters. This analysis helps us understand the impact of varying these parameters on the accuracy of our ML model.

**Results** Figure 7.4 indicates that on average, a hypothetical adoption rate of 80% can result in a reduction of transaction fees up to 30%, without compromising the 80% threshold of inclusion prediction score. Furthermore, tests showed that with complete adoption, transaction fees could be reduced by as much as 50%, without resulting in a predicted likelihood of transaction inclusion falling below 70% in any of the months evaluated. The remarkable finding was that our model demonstrated a predicted likelihood of transaction inclusion of over 80% in most months of the evaluation period, even when fees were reduced by as much as 10%. Hence, our model enables users to reduce their fee expenses with great confidence while still maintaining a high probability that their transactions will be included in the next mined block. Our analysis can help guide end-users in optimizing their transaction fees, resulting in significant cost savings. These findings contribute to our understanding of the practical applicability of our model and its ability to assist users in optimizing transaction costs.

**Limitations** By conducting these tests, we aim to determine the extent to which users can potentially decrease their transaction fees while still maintaining a favorable probability of inclusion in the next mined block. However, it is important to note that these findings are based on simulations. In practice, miners may decide to alter their policy regarding transaction inclusion if they observe changes in trends across the entire user base. Nonetheless, our model should possess the ability to accommodate such modifications if they are founded on comparable concepts as those expounded in our study. Analyzing fee reduction for end-users can provide valuable insights into the benefits that our solution can offer and help to guide decision-making processes related to transaction fees.

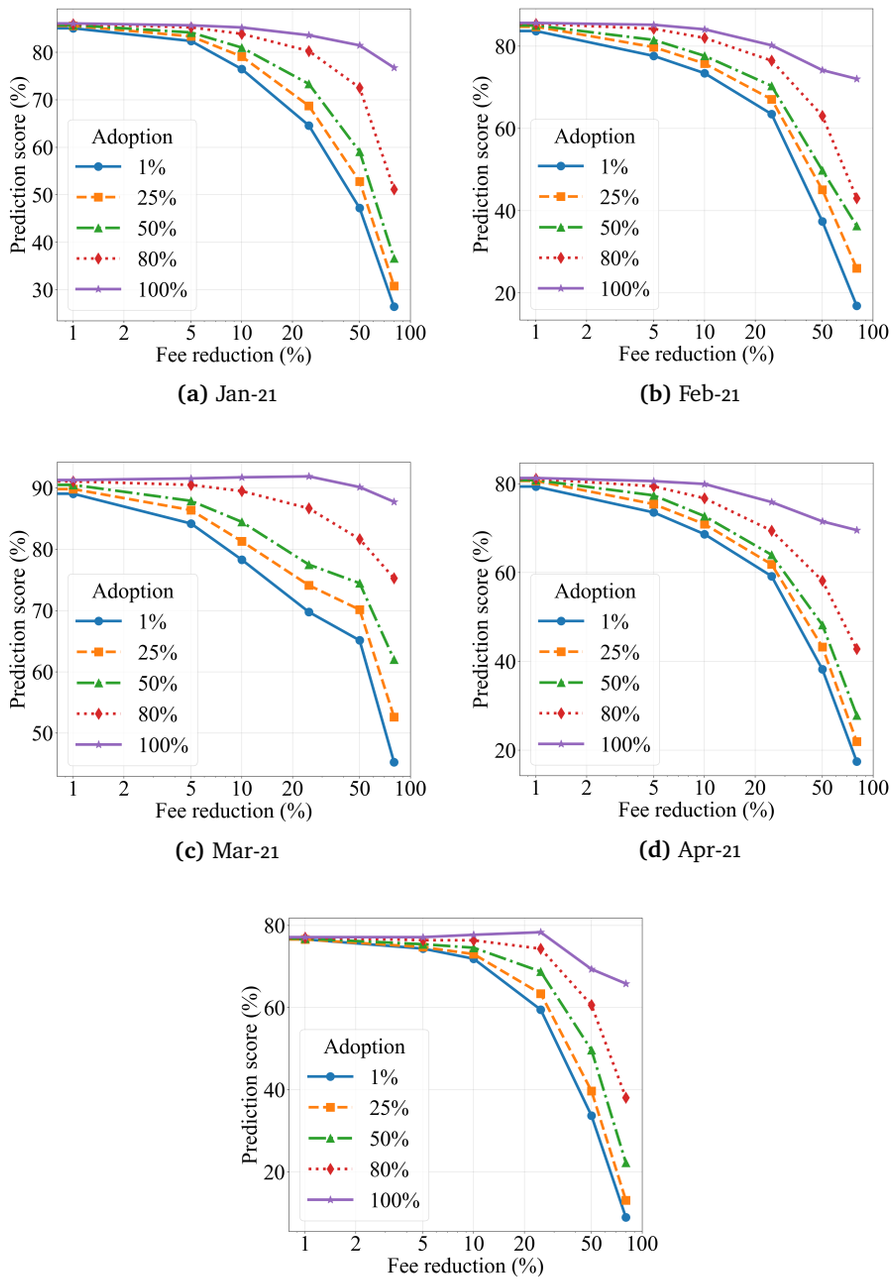


**(a)** Jan-21 **(b)** Feb-21

**(c)** Mar-21 **(d)** Apr-21

**(e)** May-21

**Figure 7.4:** Inclusion prediction score for transactions with reduced fees. In our simulated tests, the adoption rate refers to the proportion of users who have hypothetically adopted our model and subsequently decreased their fees to the percentage levels indicated on the x-axis. It is important to note that these tests do not involve real-life observed data, but rather simulated scenarios.

## 7.5 Miners' Profit After Fee Reduction

Our fee inclusion model enables users to achieve substantial savings in transaction fees within the Bitcoin network, while maintaining a high likelihood of inclusion. However, a pertinent question emerges regarding potential adverse implications of such fee reduction on miners. To address this question, we assess the extent to which miners are impacted by this fee reduction, using the methodology described in Section 3.1.2.

**Purpose** We aim to quantify the profit loss for miners resulting from a reduction in transaction fees, as predicted by our model.

**Methodology** In order to determine miners' profit, we employ the formulas described in Section 3.1.2. Specifically, we calculate the profit under two scenarios: without any fee reduction and with a 10% fee reduction. The latter calculates the profit assuming a 100% adoption rate of our model, which is expected to have a more pronounced negative impact on miners compared to lower adoption rates.

**Experimental setup** In this evaluation, we perform a profitability analysis specifically for a miner using the Antminer S19 Pro. Our assessment is based on several assumptions: each block comprises 2,500 transactions, and we consider the average transaction fee to be $ 7.5.[3] We analyze the daily profitability of miners in Qatar, where electricity prices are low, and in the US, where electricity prices are average. Our assessment includes various case scenarios, taking into account a range of Bitcoin prices from $ 10,000 to $ 100,000. Additionally, we take into account the block reward of ₿ 3.125, factoring in the imminent halving event that reduces the current block reward of ₿ 6.25. This emphasizes the importance of transaction fees in the overall profitability calculation.

**Analysis** We examine the daily profit of miners in Qatar and the US, taking into account the specified parameters mentioned earlier. Subsequently, we calculate the variance in profit resulting from a 10% reduction in fees.

**Results** The analysis conducted, as shown in Table 7.8, reveals that the reduction in fees generally leads to minimal losses for miners. However, in specific scenarios where the profitability approaches zero (such as when the Bitcoin price is at $10,000 and the miner operates in Qatar),

3. based on the yearly average fee in Bitcoin for 2023, sourced from blockchain.com at `https://www.blockchain.com/explorer/charts/fees-usd-per-transaction`

the losses exhibit a relatively higher percentage value (20%), yet remain insignificant in absolute terms. This relatively larger percentage of loss can be attributed to the marginal profit/loss nearing zero. It is crucial to note that despite the notable percentage, the actual impact on daily profit is minimal, amounting to few cents of difference. As the daily profit increases for miners, the impact of this fee reduction on their profit diminishes, with the loss remaining below 1.3%.

**Limitations** It is important to note that this analysis is conducted through simulation, which means that the expected profit and loss may slightly differ from real-world scenarios. In real-world situations, various factors such as fluctuations in electricity prices, Bitcoin price, transaction fees, and mining probabilities would be considered, potentially impacting the outcomes. Therefore, it is crucial to acknowledge that these simulated results provide an approximation and may vary when accounting for the complexities of actual operational environments.

## Summary

In this chapter, we presented the evaluation of our ML model. Firstly, we conducted a comparative analysis of various datasets used in the experiments. We defined metrics such as completeness and freshness to test the quality of these datasets.

| $e_p$ ($/kWh) | Daily profit with $ 7.5 fee | | | |
|---|---|---|---|---|
| Bitcoin price ($) | 10000 | 30000 | 60000 | 100000 |
| Qatar : 0.032 | 0.54 | 4.35 | 10.06 | 17.68 |
| US : 0.162 | -9.59 | -5.78 | -0.07 | 7.54 |
| | 10% fee deduction | | | |
| Qatar | 0.43 | 4.24 | 9.95 | 17.57 |
| US | -9.71 | -5.89 | -0.18 | 7.42 |

**Table 7.8:** The table presents the effects of a 10% fee reduction on miners operating in Qatar and the US across different Bitcoin price variations. The block reward is set at ₿ 3.125, with 2,500 transactions per block, $ 7.5 fee per transaction, and a single miner using Antminer S19 Pro.

Secondly, we defined evaluation metrics to assess the performance of the model. These metrics included classification accuracy, confusion matrix, and ROC analysis.

Thirdly, we evaluated the model's performance by considering different subsets of features and examining their individual contributions. We also conducted experiments to vary the model's freshness. The classification accuracy of the model reached peaks of 91%. Notably, using our complete set of features resulted in an average accuracy boost of 16% compared to the more common approach of using transaction size and fee alone.

Finally, we analyzed the potential benefits of our solution for end-users, as well as the corresponding potential loss that miners may incur. We demonstrated that a 10% reduction in fees would not negatively impact transaction inclusion. This finding highlights the positive impact our solution can have on transaction costs. Additionally, our analysis demonstrates that implementing a 10% fee reduction results in a minimal impact of less than 1.5% on miners' profits.

In the upcoming chapter, we discuss our results concerning several crucial aspects. These include the suitability of POW-based systems as a low payment scheme, the storage requirements for training the model, feature selection techniques, model cyclicity, transaction sampling approaches, and ethical considerations associated with POW.

# 8

# Discussion

This chapter focuses on the discussions drawn from the analysis performed on Bitcoin. The limitations of the low-payment scheme for users is discussed. The importance of selecting the appropriate set of features for building an accurate prediction model is highlighted, and the comparison between different feature sets is presented. The impact of exogenous events on the accuracy of the model is also discussed. The significance of model cyclicity and the appropriate choice of hyperparameters in boosting the accuracy score is analyzed. Overall, this chapter provides valuable insights into the importance of selecting appropriate parameters and features to build an accurate model that can be used in a PoW-based environment.

This dissertation is, to our knowledge, the first work that systematically use modern ML techniques to forecast transaction inclusion. Given this unique contribution, we acknowledge the challenges involved in conducting a comprehensive comparison with existing works. Therefore, interpreting our findings without a genuine real-world case comparison may appear less pertinent. Nevertheless, executing such assessments is a costly endeavor since it necessitates generating actual transactions with a relatively high fee based on the current average fee and subsequently adjusting it based on our model's prediction. Nonetheless, since our model accuracy exceeds 90%, the simulated outcomes demonstrate a high degree of solidity and dependability.

## 8.1 Bitcoin as Low-Payment Scheme

This dissertation provides insights on how suited POW-based systems, such as Bitcoin, are as low-payment schemes. We can list some reasons on why POW fails on this matter:

1. High Transaction Fees: the negative impact of interblock interval time and block size constraints on the system's throughput, fee markets have emerged. Fees provide a stable income for miners, which in turn leads to overpricing of transaction fees to guarantee immediate inclusion in the blockchain, causing users to pay fees that are two orders of magnitude higher than the recommended one.

2. Scalability Challenges: limitations on block size and frequency limits transaction throughput. As a consequence, it becomes challenging to handle a high volume of low-fee transactions in a timely manner.

3. Confirmation Time: POW systems have confirmation times that can vary depending on factors such as network congestion and mining difficulty. The time required for a transaction to be confirmed and included in a block can range from several minutes to hours. This delay is not suitable for low-payment schemes where quick and near-instantaneous transactions are desired.

4. Environmental Impact: POW algorithms require substantial energy consumption for mining activities. The process of solving computational puzzles in POW systems consumes a significant amount of electricity, leading to a substantial carbon footprint. This environmental impact and energy consumption make POW systems less desirable for low-fee transactions that do not justify the ecological cost.

To address issue number one, our study proposes a transaction inclusion model that extracts the necessary features for accurate classification. By training the model periodically, with a cadence of at least once a month, it is possible to classify incoming transactions into two classes with an accuracy score on average of 89%, which aims to optimize user expenditure.

## 8.2 Dataset Storage

Figure 8.1 illustrates the storage efficiency of the dataset we have generated. The complete set is somehow prohibitive to store and for that, our approach enables good results while saving a lot of space on disk. Compared to the actual size of the Bitcoin blockchain, our raw dataset $\mathcal{R}$ saves an average of 53.75% of disk space (see Figure 8.1).

Additionally, the training set $\mathcal{X}$, which contains block-epoch-based information, is 54.25% smaller on average than the original blockchain size, and saving up to 88.33% of disk space when smaller portions of the blockchain are analyzed.

We set a threshold of 3,000 blocks (approx. 20 days, or ca. 6 million transactions) for dataset evaluation, as the ResNet models we produce are designed for short-term predictions and are more accurate when generated cyclically. The dataset $\mathcal{C}$ has been found to be the heaviest among all the sets analyzed, with an average disk size of 158% greater than that of the Bitcoin blockchain when analyzing transactions greater than 100,000. For transactions below this threshold, $\mathcal{C}$ is 33% lighter than the Bitcoin blockchain. However, it is important to note that $\mathcal{C}$ is only stored during run-time and not permanently. In conclusion, the dataset $\mathcal{R}$ demonstrated to save 60% of space compared to the Bitcoin blockchain for

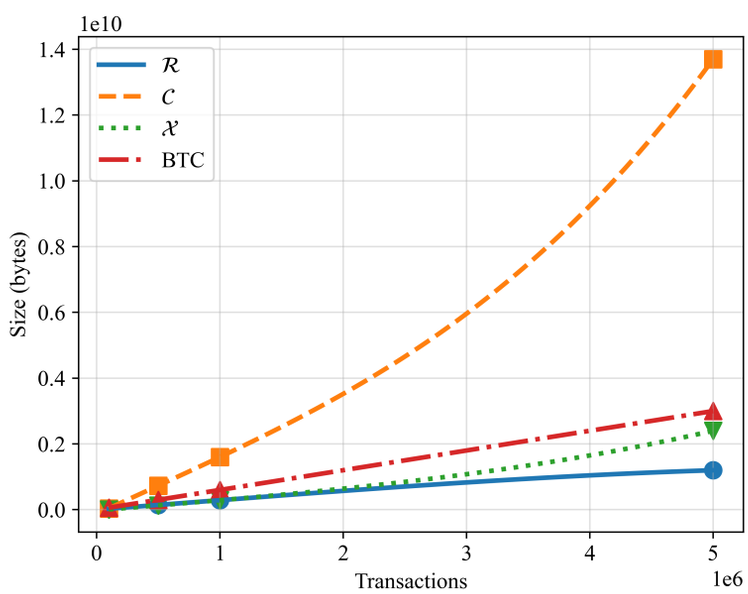


**Figure 8.1:** The following illustration demonstrates how various datasets we implemented scale in proportion to the size of the Bitcoin blockchain.

5 million transactions.

## 8.3 Selection of Features

During our experiments we outlined that careful selection of features is important Although more common and simpler fee estimators, which we refer to as primitive in this study, typically perform with an accuracy slightly above 70%. For example the command line call `Bitcoind estimatesmartfee` included in Bitcoin core, which relies solely on past blocks, transactions, and fee rates, our study employs a more comprehensive real-time based approach, with an accuracy score never below 85%.

We analyze the set of engineered features based on our intuition over a period of five months, which we refer to as the complete solution, and compare it with the primitive solution. We demonstrate that our proposed approach leads to a 16% improvement in accuracy score, on average. The accuracy score of the model experiences a downward trend during the months of April and May. This can be attributed to a series of events within the Bitcoin network, including a Bitcoin price drop of 46%, a surge in transaction fees to an all-time high, and an increase in miners' revenue. We argue that these exogenous events impacted the inclusion of transactions.

## 8.4 Model Cyclicity

The accuracy score of a classifier can be improved by maintaining the completeness and novelty of information in the model, particularly when unexpected events occur. This is demonstrated in Figure 7.2, which shows that classification accuracy drops when older models are used to classify recent data ($\psi \longrightarrow 1$), or when information in the test set is incomplete ($\alpha \longrightarrow 0$). Accuracy also drops considerably if models prior to the price inversion trend are used to classify more recent data. Two tests in April 2021 are compared in Table 8.1, one with complete data ($\alpha = 1$) and one with incomplete data ($\alpha = 0.5$), both classified with a model from January 2021. Despite data completeness, the mode incorrectly classifies 26% of transactions in $\upsilon_1$ as $\upsilon_0$ (false positive) due to the all-time-high fees in April. When data completeness is reduced to $\alpha = 0.5$, the false positives increase to 41%, while false negatives represent only 5%. In such cases, the model should be trained more frequently than once per month to reduce the number of misclassified transactions caused by deviations from

the previous inclusion pattern.

| Overall **CM** score, $\psi = 0.95$ | | | | |
|---|---|---|---|---|
| $\alpha$ | 0.5 | | 1 | |
| | $v_0$ | $v_1$ | $v_0$ | $v_1$ |
| $v_0$ | 0.95 | 0.05 | 0.89 | 0.11 |
| $v_1$ | 0.41 | 0.59 | 0.26 | 0.74 |

**Table 8.1:** This table displays the overall confusion matrix score for April 2021 data using the January 2021 model. The $\psi$ value is fixed at 0.95, while two different values of $\alpha$, 0.5 and 1, are evaluated. The importance of a complete dataset during training is highlighted, and the table demonstrates how classification accuracy can benefit from having complete information.

Figure 7.1 demonstrates that the selected features are crucial for accurate classification, and both parameters are fundamental for boosting the accuracy score. A complete set of information is needed to correctly calculate the offset value and have the right information on the current mempool size. An updated or new dataset helps to have knowledge of the current miner inclusion trend.

## 8.5 Transactions Sampling

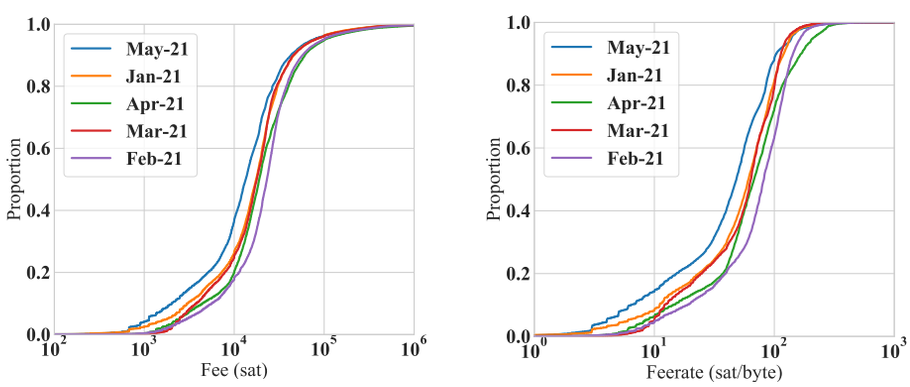


**Figure 8.2:** Cumulative distribution functions for transaction fees and feerate in our dataset.

Despite obtaining a good classification accuracy score, we observe that the model could be biased towards a specific range of transaction fees. In fact, bias

gets into the model through the data that is used for building our classification model [163]. We carry out a supervised approach, thus our model only knows the outcome for transactions occurred in the blockchain. If most users pay a fee greater than the optimal value, the model lacks samples for small transaction fee values.

Figure 8.2 shows the fee and feerate Cumulative Distribution Function during the period of analysis. We observe that after the price drop occurred in late April 2021, fees were considerably lower (May 2021), and that transaction fees between $10^4$ and $10^5$ sat represent nearly the 75% of the total. Although the recommended transaction feerate should be 1 sat/byte, we observed an extremely low number of accepted transactions that utilize such a low fee rate. Consequently, one might conclude that our model is biased and it is not accurate when predicting transactions with feerate of 1 sat/byte. However, the overall fee trend of approved transactions delineates a pattern itself, meaning that a too low fee will rarely end up in an inclusion, which is in line with our model's outcome. In fact, lower fee transactions are evicted from the network and never included. Our model optimizes expenditure within the range of the already approved transactions, and its scope is not to detect possible evicted transactions, but to determine an inclusion in the next block. Information about eviction is not of particular relevance. Finally, any transaction issuer could consult the model's output in order to trade-off its probability of inclusion with more, or less fee to pay.

## 8.6 Ethical Concerns of Proof-of-Work

The computational power and energy required to mine results in a high energy consumption as the network scales and gets more secure. The carbon footprint can have negative impact to the environment, contributing to climate change and other environmental problems. Moreover, the cost of energy is a major barrier to entry for smaller miners, and despite the availability of renewable energy sources such as hydroelectric, solar, or wind power, many miners still depend on non-renewable sources like coal or natural gas. This reliance on non-renewable sources negatively impact the environment and it does contribute to greenhouse gas emissions. However, if most miners adopt renewable energy sources, a POW-based blockchain system has the potential to replace the worldwide banking system. Compared to the operational costs of the banking system, the operational costs of POW are relatively low. However, the transaction throughput may become a bottleneck to its adoption.

Another ethical concern related to POW is the unequal distribution of mining power. Mining requires specialized hardware and software, that is expensive to purchase and maintain. Consequently, mining is often more accessible to those with greater financial resources, leading to a concentration of mining power among a small group of individuals or organizations. This can give rich entities undue influence over the network, raising concerns about the overall decentralization and democratic governance of the network.

Mining generates a significant amount of e-waste. The specialized hardware used for mining quickly becomes obsolete as new, more powerful hardware is developed, contributing to the global issue of e-waste and further emphasizing the sustainability issues of POW mining at scale.

Acknowledging these ethical concerns, POW it is still considered the most secure and widely-used consensus mechanism in the blockchain industry. Our dissertation does not aim to question the applicability or sustainability of POW, although we are aware of its limitations. Instead, our study focuses on a widespread phenomenon related to blockchain technology, recognizing that alternative consensus mechanisms may exist that offer solutions to the ethical concerns associated with POW. Nevertheless, we propose an approach to reduce the cost for users in the Bitcoin network by employing transaction inclusion prediction. This reduces the negative burdens associated with the network.

## Summary

This chapter examined the limitations of Bitcoin as a low-payment scheme, emphasizing high transaction fees, scalability challenges, confirmation time, and environmental impact. A transaction inclusion model was proposed with periodic training to optimize user expenditure.

The chapter also discussed the efficiency of dataset storage, with the generated dataset saving significant disk space. It highlighted the importance of selecting the right features for accurate prediction models, showing a 16% improvement compared to more simple estimators.

The impact of external events on model accuracy was considered, suggesting that factors like price drops and fee surges affected transaction inclusion. Model cyclicity was emphasized, recommending frequent training to maintain accuracy when faced with deviations.

The chapter also addressed the potential bias in the model towards a specific range of transaction fees. It acknowledged that the model's performance may be affected when predicting transactions with extremely low feerate, however, the model optimizes expenditure within the range of already approved transactions.

In summary, the discussion chapter provided insights into the limitations of Bitcoin as a low-payment scheme, the importance of feature selection, efficient dataset storage, model cyclicity, and ethical concerns associated with POW systems.

# 9

# Concluding Remarks

The high fees reates that haunts POW-based systems at scale, makes groundbreaking system such as Bitcoin less appealing for end-users. This dissertation aims to improve our understanding modeling of the transaction fee mechanism and provide a method for users to optimize their fee expenditure. In this chapter, we provide a comprehensive listing of our contributions, we aim to provide a conclusive affirmation of the key arguments, and provide insights that we have developed throughout the course of this work.

To summarize the focus of this dissertation, our starting point is the thesis that:

***Our thesis is that Bitcoin transaction fees can accurately be modeled and predicted using ML methods, improving utility and efficiency for clients using such cryptocurrencies, while maintaining a fair compensation for miners.***

We conclude that our research has provided valuable insights into the challenges posed by the scalability bottleneck and high fees in POW-based systems such as Bitcoin. By thoroughly examining the transaction fee mechanism and integrating POW-based blockchains with ML models, we have made significant contributions to improving the utility and efficiency of cryptocurrencies for clients. Our findings demonstrate the efficacy of a formal transaction inclusion

model in predicting transaction acceptance, shedding light on the underlying mechanisms and patterns governing miners' decisions. Moreover, our work has the potential to enhance the overall user experience, trust, and reliability of cryptocurrencies, empowering Bitcoin users with precise transaction inclusion predictions and enabling them to make more informed decisions regarding suitable fees. Through the strategic integration of POW-based systems and ResNet, we have paved the way for a more robust and user-centric cryptocurrency ecosystem.

## 9.1 Summary of Research Methodology and Findings

In Chapter 3, we discuss the principles and rules governing the Bitcoin ecosystem at scale, with a focus on the interdependence between users and miners. We explain how miners make profits, with related cost of mining, and miners' importance in transaction inclusion. The emergence of a fee market in POW-based blockchains is also explored, including the auction schemes that miners could adopt, and how this can lead to fee dynamism in Bitcoin. The chapter also relates these issues to the high fees and overpaying in Bitcoin, which are dictated by the mass adoption of Bitcoin and its inner throughput limitations. Understanding such fee market is important for formalizing a transaction inclusion pattern.

Chapter 4 presents the design and implementation of the Blockchain Analytics System (BAS), which we developed for acquiring and storing a local dataset of the Bitcoin blockchain. The chapter presents the methods and techniques used for data acquisition, including web scraping, APIs, and direct access to the blockchain using Bitcoin Core software. The acquired data is then structured and pre-processed to be suitable for analysis in subsequent chapters.

Chapter 5 discusses the use of time-series data analysis as a tool for predicting future trends. The methodology is based on the collection of time-series data, where transactions are sampled on a monthly basis with a fixed interval, and a notion of relative time is incorporated, represented by block creation epochs. The chapter presents a comprehensive model for the inclusion of transactions in a POW-based blockchain system, with a focus on the factors of revenue and fairness. Revenue serves as an incentive for miners to participate in the network and validate transactions, while fairness ensures equal opportunity for all users to have their transactions included in the blockchain upon paying

an adequate fee value. The model takes into account both revenue and fairness as complementary factors for an accurate study and prediction of transaction inclusion.

Chapter 6 presents ML architecture. The chapter covers three critical stages: the ingestion engine, the pre-processing stage, and the ML model. The ingestion engine is responsible for processing and transforming raw data obtained from the blockchain. The pre-processing phase transforms raw data into a suitable form for the analysis, including feature extraction and additional data processing to generate a complete dataset. Finally, the chapter describes the ML model used for the prediction.

Chapter 7 evaluates ML model used in the study. It describes the datasets used for training and testing the model, the evaluation metrics employed, and the results of the analyses. The section reports on the overall accuracy of the model, feature importance, and model cyclicity. The findings of this study offer valuable insights into the effectiveness of the model as well as the appropriateness of the selected features for the intended purpose. Specifically, the study demonstrates the efficiency of the ML model in predicting transaction inclusion, which can potentially serve as a powerful tool for end-users. By utilizing our model, transaction issuers can maintain a high degree of confidence, with a likelihood of inclusion higher than 80%, in the next mined block while saving up to 10% in transaction fees.

## 9.2 Contributions

After examining the research presented in this dissertation and analyzing our thesis statement, we have drawn the following list of contributions:

1. Our research sheds light on the complexities of the transaction fee mechanism in Bitcoin, and the results of our study provide valuable insights into the underlying mechanisms and patterns governing miners' decisions to include individual transactions.

2. By integrating POW-based blockchains and ML models, we have shown that it is possible to improve the utility and efficiency of cryptocurrencies for clients, and we demonstrate the efficacy of a formal transaction inclusion model in predicting transaction acceptance in the blockchain.

3. Our work has significant implications for improving the overall user

experience and enhancing the trust and reliability of cryptocurrencies, providing Bitcoin users with a notable precision in predicting transaction inclusion and enabling them to better select suitable fees.

In summary, answering our thesis statement we can say that, *yes*, our thorough examination of POW-based blockchains and the application of ML models has indeed demonstrated that the strategic integration of these technologies can improve utility and efficiency for clients using cryptocurrencies, while still ensuring miners to get their revenue. Our research has demonstrated the efficacy of a formal model and ML prototype in predicting transaction inclusion, providing valuable insights into the underlying mechanisms governing miners' decisions and paving the way for improved utility and efficiency of cryptocurrencies for clients. Our work has significant implications for enhancing the trust and reliability of cryptocurrencies and improving the overall user experience by enabling Bitcoin users to better select suitable fees and predict transaction inclusion with notable precision.

## 9.3 Future Work

To enhance our confidence in the effectiveness of our model, it is crucial to conduct real-world tests of transaction fee reduction. In these tests, transactions would be submitted based on the predictions generated by our model, allowing to calculate the potential cost savings for end-users. This practical validation would provide valuable insights into the actual benefits and performance of our model in a live environment. The primary goal is to determine the extent to which transaction issuers can reduce their fees while still maintaining a high degree of confidence in the inclusion model's output. By conducting such research, it will be possible to quantify the amount of overspending that occurs in the Bitcoin network and contribute to improving the overall user experience.

It is crucial to continue observing blockchain data as the inclusion model may change over time, especially for developers who wish to utilize POW-based systems without overpaying for transaction space in blocks. Therefore, we are currently working on a modified version of the inclusion model that aims to improve the accuracy score. Our approach takes a holistic view of new block alternatives and penalizes transaction offset levels falling in the $> 1\,\text{MB}$ space of the mempool, thereby orienting the model towards a stronger second-price auction approach.

Furthermore, it would be beneficial to categorize transactions at each block epoch into ranks and incorporate transaction rank as a feature in the prediction model. Additionally, to mitigate training data bias arising from high-fee transactions, it would be valuable to introduce a significant number of low-fee transactions into the actual blockchain and record their latency in the model. By adopting these approaches, we can gain more precise insights into the dynamics of transaction inclusion, leading to the development of a more resilient and effective model that better serves end-users.

# References


[1] Alex Tapscott and Don Tapscott. How blockchain is changing finance. *Harvard Business Review*, 1(9):2–5, 2017.

[2] Philip Treleaven, Richard Gendal Brown, and Danny Yang. Blockchain technology in finance. *Computer*, 50(9):14–17, 2017. doi: 10.1109/MC.2017.3571047.

[3] Primavera De Filippi. *Blockchain and the Law: The Rule of Code*. Harvard University Press, 2018. ISBN 9780674985933. doi: 10.4159/9780674985933.

[4] Marko Hölbl, Marko Kompara, Aida Kamišalić, and Lili Nemec Zlatolas. A systematic review of the use of blockchain in healthcare. *Symmetry*, 10(10):470, 2018.

[5] Sabine Kolvenbach, Rudolf Ruland, Wolfgang Gräther, and Wolfgang Prinz. Blockchain 4 education. In *Proceedings of 16th European Conference on Computer-Supported Cooperative Work-Panels, Posters and Demos*. European Society for Socially Embedded Technologies (EUSSET), 2018.

[6] Rodrigo Q. Saramago, Leander Jehl, Hein Meling, and Vero Estrada-Galiñanes. A tree-based construction for verifiable diplomas with issuer transparency. In *2021 IEEE International Conference on Decentralized Applications and Infrastructures (DAPPS)*, pages 101–110, 2021. doi: 10.1109/DAPPS52256.2021.00017.

[7] Roi Bar Zur, Ittay Eyal, and Aviv Tamar. Efficient mdp analysis for selfish-mining in blockchains. In *Proceedings of the 2nd ACM Conference on Advances in Financial Technologies*, pages 113–131, 2020.

[8] Satoshi Nakamoto. Bitcoin: A peer-to-peer electronic cash system. *Decentralized business review*, page 21260, 2008.

[9] Peter R Rizun. A transaction fee market exists without a block size limit. *Block Size Limit Debate Working Paper*, pages 2327–4697, 2015.

[10] C. Decker and R. Wattenhofer. Information propagation in the bitcoin network. In *IEEE P2P 2013 Proceedings*, pages 1–10, Sept 2013. doi: 10.1109/P2P.2013.6688704.

[11] David Chaum. Achieving electronic privacy. *Scientific American*, 267(2): 96–101, 1992. ISSN 00368733, 19467087. URL http://www.jstor.org/stable/24939181.

[12] Adam Back. Hashcash - a denial of service counter-measure. Published at http://www.hashcash.org, 2002.

[13] Hal Finney. Reusable proofs of work. https://nakamotoinstitute.org/finney/rpow/index.html, 2004. Accessed: 2022-06-20.

[14] Shaurya Malwa. The first bitcoin transaction was sent to hal finney 12 years ago. https://decrypt.co/53727/the-first-bitcoin-transaction-was-sent-to-hal-finney-12-years-ago, 2021. Decrypt, Accessed: 2022-06-23.

[15] Aggelos Kiayias, Alexander Russell, Bernardo David, and Roman Oliynykov. Ouroboros: A provably secure proof-of-stake blockchain protocol. In *Annual international cryptology conference*, pages 357–388. Springer, 2017.

[16] Vitalik Buterin and Virgil Griffith. Casper the friendly finality gadget. *CoRR and arXiv*, abs/1710.09437, 2017. URL http://arxiv.org/abs/1710.09437.

[17] Jae Kwon. Tendermint: Consensus without mining. *Draft v. 0.6, fall, Cornell.edu*, 1(11), 2014.

[18] Ethan Buchman. *Tendermint: Byzantine fault tolerance in the age of blockchains*. PhD thesis, University of Guelph, 2016.

[19] Sunny King and Scott Nadal. Ppcoin: Peer-to-peer crypto-currency with proof-of-stake. *self-published paper, August*, 19(1), 2012.

[20] Yossi Gilad, Rotem Hemo, Silvio Micali, Georgios Vlachos, and Nickolai Zeldovich. Algorand: Scaling byzantine agreements for cryptocurrencies.

In *Proceedings of the 26th Symposium on Operating Systems Principles*, SOSP '17, page 51–68, New York, NY, USA, 2017. Association for Computing Machinery. ISBN 9781450350853. doi: 10.1145/3132747.3132757.

[21] David Schwartz, Noah Youngs, Arthur Britto, et al. The ripple protocol consensus algorithm. *Ripple Labs Inc White Paper*, 5(8):151, 2014.

[22] Brad Chase and Ethan MacBrough. Analysis of the XRP ledger consensus protocol. *CoRR*, abs/1802.07242, 2018. URL `http://arxiv.org/abs/1802.07242`.

[23] Marta Lokhava, Giuliano Losa, David Mazières, Graydon Hoare, Nicolas Barry, Eli Gafni, Jonathan Jove, Rafał Malinowsky, and Jed McCaleb. Fast and secure global payments with stellar. In *Proceedings of the 27th ACM Symposium on Operating Systems Principles*, SOSP '19, page 80–96, New York, NY, USA, 2019. Association for Computing Machinery. ISBN 9781450368735. doi: 10.1145/3341301.3359636.

[24] Team Rocket, Maofan Yin, Kevin Sekniqi, Robbert van Renesse, and Emin Gün Sirer. Scalable and probabilistic leaderless BFT consensus through metastability. *CoRR*, abs/1906.08936, 2019. URL `http://arxiv.org/abs/1906.08936`.

[25] Ben Fisch, Joseph Bonneau, Nicola Greco, and Juan Benet. Scaling proof-of-replication for filecoin mining. *Protocol Labs: San Francisco, CA, USA*, 2018.

[26] Juan Benet and Nicola Greco. Filecoin: A decentralized storage network. *Protoc. Labs*, pages 1–36, 2018.

[27] Lin Chen, Lei Xu, Nolan Shah, Zhimin Gao, Yang Lu, and Weidong Shi. On security analysis of proof-of-elapsed-time (poet). In Paul Spirakis and Philippas Tsigas, editors, *Stabilization, Safety, and Security of Distributed Systems*, pages 282–297, Cham, 2017. Springer International Publishing. ISBN 978-3-319-69084-1.

[28] I Stewart. Proof of burn. bitcoin.it `https://en.bitcoin.it/wiki/Proof_of_burn`, 2012.

[29] Kostis Karantias, Aggelos Kiayias, and Dionysis Zindros. Proof-of-burn. In Joseph Bonneau and Nadia Heninger, editors, *Financial Cryptography and Data Security*, pages 523–540, Cham, 2020. Springer International

Publishing. ISBN 978-3-030-51280-4.

[30] Iddo Bentov, Charles Lee, Alex Mizrahi, and Meni Rosenfeld. Proof of activity: Extending bitcoin's proof of work via proof of stake [extended abstract]y. *SIGMETRICS Perform. Eval. Rev.*, 42(3):34–37, dec 2014. ISSN 0163-5999. doi: 10.1145/2695533.2695545.

[31] Bram Cohen and Krzysztof Pietrzak. The chia network blockchain. *chivescoin.org*, 1:1–44, 2019.

[32] Dan Boneh, Joseph Bonneau, Benedikt Bünz, and Ben Fisch. Verifiable delay functions. In *Annual international cryptology conference*, pages 757–788. Springer, 2018.

[33] Benjamin Wesolowski. Efficient verifiable delay functions. In *Annual International Conference on the Theory and Applications of Cryptographic Techniques*, pages 379–407. Springer, 2019.

[34] Stefano De Angelis, Leonardo Aniello, Roberto Baldoni, Federico Lombardi, Andrea Margheri, and Vladimiro Sassone. Pbft vs proof-of-authority: applying the cap theorem to permissioned blockchain. In *Italian Conference on Cyber Security (06/02/18)*, January 2018. URL `https://eprints.soton.ac.uk/415083/`.

[35] Parinya Ekparinya, Vincent Gramoli, and Guillaume Jourjon. The attack of the clones against proof-of-authority. *CoRR*, abs/1902.10244, 2019. URL `http://arxiv.org/abs/1902.10244`.

[36] Giuseppe Ateniese, Long Chen, Mohammad Etemad, and Qiang Tang. Proof of storage-time: Efficiently checking continuous data availability. Cryptology ePrint Archive, Paper 2020/840, 2020. URL `https://eprint.iacr.org/2020/840`. `https://eprint.iacr.org/2020/840`.

[37] Juan Benet, David Dalrymple, and Nicola Greco. Proof of replication. *Protocol Labs, July*, 27:20, 2017.

[38] Alex Smola and SVN Vishwanathan. Introduction to machine learning. *Cambridge University, UK*, 32(34):2008, 2008.

[39] Sergios Theodoridis and Konstantinos Koutroumbas. *Pattern Recognition, Fourth Edition*. Academic Press, 2009. ISBN 9781597492720.

[40] Hoon Sohn, Charles R Farrar, Norman F Hunter, and Keith Worden. Structural health monitoring using statistical pattern recognition techniques. *J. Dyn. Sys., Meas., Control*, 123(4):706–711, 2001.

[41] A.K. Jain, R.P.W. Duin, and Jianchang Mao. Statistical pattern recognition: a review. *IEEE Transactions on Pattern Analysis and Machine Intelligence*, 22(1):4–37, 2000. doi: 10.1109/34.824819.

[42] CD McGillem, JI Aunon, and DG Childers. Signal processing in evoked potential research: applications of filtering and pattern recognition. *Critical reviews in bioengineering*, 6(3):225—265, 1981. ISSN 0731-6984. URL `http://europepmc.org/abstract/MED/7023835`.

[43] Frank Y Shih. *Image processing and pattern recognition: fundamentals and techniques*. John Wiley & Sons, 2010.

[44] King-Sun Fu and Rosenfeld. Pattern recognition and image processing. *IEEE Transactions on Computers*, C-25(12):1336–1346, 1976. doi: 10.1109/TC.1976.1674602.

[45] Michael S. Lew, Nicu Sebe, Chabane Djeraba, and Ramesh Jain. Content-based multimedia information retrieval: State of the art and challenges. *ACM Trans. Multimedia Comput. Commun. Appl.*, 2(1):1–19, feb 2006. ISSN 1551-6857. doi: 10.1145/1126004.1126005.

[46] Lina Zhou, Shimei Pan, Jianwu Wang, and Athanasios V. Vasilakos. Machine learning on big data: Opportunities and challenges. *Neurocomputing*, 237:350–361, 2017. ISSN 0925-2312. doi: https://doi.org/10.1016/j.neucom.2017.01.026.

[47] Junfei Qiu, Qihui Wu, Guoru Ding, Yuhua Xu, and Shuo Feng. A survey of machine learning for big data processing. *EURASIP Journal on Advances in Signal Processing*, 2016(1):67, 2016. doi: 10.1186/s13634-016-0355-x.

[48] Alexandra L'Heureux, Katarina Grolinger, Hany F. Elyamany, and Miriam A. M. Capretz. Machine learning with big data: Challenges and approaches. *IEEE Access*, 5:7776–7797, 2017. doi: 10.1109/ACCESS.2017.2696365.

[49] Ziad Obermeyer and Ezekiel J Emanuel. Predicting the future—big data, machine learning, and clinical medicine. *The New England journal of medicine*, 375(13):1216, 2016.

[50] Luigi Tommaso Luppino, Mads Adrian Hansen, Michael Kampffmeyer, Filippo Maria Bianchi, Gabriele Moser, Robert Jenssen, and Stian Normann Anfinsen. Code-aligned autoencoders for unsupervised change detection in multimodal remote sensing images. *IEEE Transactions on Neural Networks and Learning Systems*, pages 1–13, 2022. doi: 10.1109/TNNLS.2022.3172183.

[51] Kee Yuan Ngiam and Ing Wei Khor. Big data and machine learning algorithms for health-care delivery. *The Lancet Oncology*, 20(5):e262–e273, 2019. ISSN 1470-2045. doi: https://doi.org/10.1016/S1470-2045(19)30149-4.

[52] Ahcéne Boubekki, Jonas Nordhaug Myhre, Luigi Tommaso Luppino, Karl Øyvind Mikalsen, Arthur Revhaug, and Robert Jenssen. Clinically relevant features for predicting the severity of surgical site infections. *IEEE Journal of Biomedical and Health Informatics*, 26(4):1794–1801, 2022. doi: 10.1109/JBHI.2021.3121038.

[53] Bilal Babar, Luigi Tommaso Luppino, Tobias Boström, and Stian Normann Anfinsen. Random forest regression for improved mapping of solar irradiance at high latitudes. *Solar Energy*, 198:81–92, 2020. ISSN 0038-092X. doi: https://doi.org/10.1016/j.solener.2020.01.034.

[54] Bruno Miranda Henrique, Vinicius Amorim Sobreiro, and Herbert Kimura. Literature review: Machine learning techniques applied to financial market prediction. *Expert Systems with Applications*, 124:226–251, 2019.

[55] Wei-Yang Lin, Ya-Han Hu, and Chih-Fong Tsai. Machine learning in financial crisis prediction: a survey. *IEEE Transactions on Systems, Man, and Cybernetics, Part C (Applications and Reviews)*, 42(4):421–436, 2011.

[56] Sead Fadilpašić. Stop overpaying bitcoin transaction fees. 2019. Accessed: 2020-07-23. `https://bit.ly/2Cy5VtH`.

[57] Enrico Tedeschi, Tor-Arne S Nordmo, Dag Johansen, and Håvard D Johansen. Predicting transaction latency with deep learning in proof-of-work blockchains. In *2019 IEEE International Conference on Big Data (Big Data)*, pages 4223–4231. IEEE, 2019.

[58] Enrico Tedeschi, Tor-Arne S. Nordmo, Dag Johansen, and Håvard D. Johansen. On optimizing transaction fees in bitcoin using ai: Investigation

on miners inclusion pattern. *ACM Trans. Internet Technol.*, 22(3), jul 2022. ISSN 1533-5399. doi: 10.1145/3528669.

[59] John Nash. Non-cooperative games. *Annals of mathematics*, pages 286–295, 1951.

[60] Peter Godfrey Smith. Theory and reality: an introduction to the philosophy of science, 2003.

[61] Peter J. Denning. Is computer science science? *Commun. ACM*, 48(4): 27–31, apr 2005. ISSN 0001-0782. doi: 10.1145/1053291.1053309.

[62] Peter J Denning. Computing is a natural science. *Communications of the ACM*, 50(7):13–18, 2007.

[63] D. E. Comer, David Gries, Michael C. Mulder, Allen Tucker, A. Joe Turner, Paul R. Young, and Peter J. Denning. Computing as a discipline. *Commun. ACM*, 32(1):9–23, jan 1989. ISSN 0001-0782. doi: 10.1145/63238.63239.

[64] David Lorge Parnas and Paul C. Clements. A rational design process: How and why to fake it. *IEEE Transactions on Software Engineering*, SE-12(2):251–257, 1986. doi: 10.1109/TSE.1986.6312940.

[65] Enrico Tedeschi. Trading network performance for cash in the bitcoin blockchain. Master's thesis, UiT Norges arktiske universitet, 2017.

[66] Enrico Tedeschi, Håvard D. Johansen, and Dag Johansen. Trading network performance for cash in the bitcoin blockchain. In *Proceedings of the 8th International Conference on Cloud Computing and Services Science, CLOSER 2018, Funchal, Madeira, Portugal, March 19-21, 2018.*, pages 643–650, 2018. doi: 10.5220/0006805906430650.

[67] Dag Johansen, Pål Halvorsen, Håvard Johansen, Håkon Riiser, Cathal Gurrin, Bjørn Olstad, Carsten Griwodz, Åge Kvalnes, Joseph Hurley, and Tomas Kupka. Search-based composition, streaming and playback of video archive content. *Multimedia Tools and Applications*, 61(2):419–445, 2012. doi: 10.1007/s11042-011-0847-5.

[68] D. Johansen, K. Marzullo, and K. Lauvset. An approach towards an agent computing environment. In *Proceedings. 19th IEEE International Conference on Distributed Computing Systems. Workshops on Electronic Commerce and Web-based Applications. Middleware*, pages 78–83, 1999.

doi: 10.1109/ECMDD.1999.776418.

[69] Haakon Riiser, Pål Halvorsen, Carsten Griwodz, and Dag Johansen. Low overhead container format for adaptive streaming. In *Proceedings of the First Annual ACM SIGMM Conference on Multimedia Systems*, MMSys '10, page 193–198, New York, NY, USA, 2010. Association for Computing Machinery. ISBN 9781605589145. doi: 10.1145/1730836.1730859.

[70] Håvard D. Johansen, Eleanor Birrell, Robbert van Renesse, Fred B. Schneider, Magnus Stenhaug, and Dag Johansen. Enforcing privacy policies with meta-code. In *Proceedings of the 6th Asia-Pacific Workshop on Systems*, APSys '15, New York, NY, USA, 2015. Association for Computing Machinery. ISBN 9781450335546. doi: 10.1145/2797022.2797040.

[71] Håvard Johansen, André Allavena, and Robbert van Renesse. Fireflies: Scalable support for intrusion-tolerant network overlays. In *Proceedings of the 1st ACM SIGOPS/EuroSys European Conference on Computer Systems 2006*, EuroSys '06, page 3–13, New York, NY, USA, 2006. Association for Computing Machinery. ISBN 1595933220. doi: 10.1145/1217935.1217937.

[72] Joakim Aalstad Alslie, Aril Bernhard Ovesen, Tor-Arne Schmidt Nordmo, Håvard Dagenborg Johansen, Pål Halvorsen, Michael Alexander Riegler, and Dag Johansen. Áika: A distributed edge system for ai inference. *Big Data and Cognitive Computing*, 6(2), 2022. ISSN 2504-2289. doi: 10.3390/bdcc6020068.

[73] Tor-Arne S. Nordmo, Aril B. Ovesen, Hårvard D. Johansen, Michael A. Riegler, Pål Halvorsen, and Dag Johansen. Dutkat: A multimedia system for catching illegal catchers in a privacy-preserving manner. In *Proceedings of the 2021 Workshop on Intelligent Cross-Data Analysis and Retrieval*, ICDAR '21, page 57–61, New York, NY, USA, 2021. Association for Computing Machinery. ISBN 9781450385299.

[74] Aril Bernhard Ovesen, Tor-Arne Schmidt Nordmo, Håvard Dagenborg Johansen, Michael Alexander Riegler, Pål Halvorsen, and Dag Johansen. File system support for privacy-preserving analysis and forensics in low-bandwidth edge environments. *Information*, 12(10), 2021. ISSN 2078-2489. doi: 10.3390/info12100430.

[75] Rodrigo Q Saramago, Leander Jehl, Hein Meling, and Vero Estrada-Galiñanes. A tree-based construction for verifiable diplomas with issuer transparency. In *2021 IEEE International Conference on Decentralized*

*Applications and Infrastructures (DAPPS)*, pages 101–110. IEEE, 2021.

[76] Racin Nygaard, Hein Meling, and Leander Jehl. Distributed storage system based on permissioned blockchain. In *Proceedings of the 34th ACM/SIGAPP Symposium on Applied Computing*, pages 338–340, 2019.

[77] Petter Olsen, Melania Borit, and Shaheen Syed. Applications, limitations, costs, and benefits related to the use of blockchain technology in the food industry. *Nofima rapportserie*, 2019.

[78] Petter Olsen and Melania Borit. The components of a food traceability system. *Trends in Food Science & Technology*, 77:143–149, 2018.

[79] Petter Olsen and Melania Borit. How to define traceability. *Trends in food science & technology*, 29(2):142–150, 2013.

[80] Ignacio Amores-Sesar, Christian Cachin, and Enrico Tedeschi. When Is Spring Coming? A Security Analysis of Avalanche Consensus. In Eshcar Hillel, Roberto Palmieri, and Etienne Rivière, editors, *26th International Conference on Principles of Distributed Systems (OPODIS 2022)*, volume 253 of *Leibniz International Proceedings in Informatics (LIPIcs)*, pages 10:1–10:22, Dagstuhl, Germany, 2023. Schloss Dagstuhl – Leibniz-Zentrum für Informatik. ISBN 978-3-95977-265-5. doi: 10.4230/LIPIcs.OPODIS.2022.10.

[81] Alex Pellegrini and Luca Zanolini. An algebraic model for quorum systems. *CoRR*, abs/2005.08536, 2020. URL `https://arxiv.org/abs/2005.08536`.

[82] Christian Cachin, Jovana Micic, and Nathalie Steinhauer. Quick order fairness. *CoRR*, abs/2112.06615, 2021. URL `https://arxiv.org/abs/2112.06615`.

[83] Christian Cachin and Luca Zanolini. Asymmetric byzantine consensus. *CoRR*, abs/2005.08795, 2020. URL `https://arxiv.org/abs/2005.08795`.

[84] Orestis Alpos and Christian Cachin. Consensus beyond thresholds: Generalized byzantine quorums made live. *CoRR*, abs/2006.04616, 2020. URL `https://arxiv.org/abs/2006.04616`.

[85] Marcus Brandenburger, Christian Cachin, and Nikola Knežević. Don't

trust the cloud, verify: Integrity and consistency for cloud object stores. *ACM Trans. Priv. Secur.*, 20(3), jul 2017. ISSN 2471-2566. doi: 10.1145/3079762. URL https://doi.org/10.1145/3079762.

[86] Christian Cachin, Angelo De Caro, Pedro Moreno-Sanchez, Björn Tackmann, and Marko Vukolic. The Transaction Graph for Modeling Blockchain Semantics. *Cryptoeconomic Systems*, 0(1), apr 5 2021. https://cryptoeconomicsystems.pubpub.org/pub/cachin-blockchain-semantics.

[87] Ignacio Amores-Sesar, Christian Cachin, and Anna Parker. Generalizing weighted trees: A bridge from bitcoin to ghost. In *Proceedings of the 3rd ACM Conference on Advances in Financial Technologies*, AFT '21, page 156–169, New York, NY, USA, 2021. Association for Computing Machinery. ISBN 9781450390828. doi: 10.1145/3479722.3480995.

[88] Ignacio Amores-Sesar, Christian Cachin, and Jovana Mićić. Security Analysis of Ripple Consensus. In Quentin Bramas, Rotem Oshman, and Paolo Romano, editors, *24th International Conference on Principles of Distributed Systems (OPODIS 2020)*, volume 184 of *Leibniz International Proceedings in Informatics (LIPIcs)*, pages 10:1–10:16, Dagstuhl, Germany, 2021. Schloss Dagstuhl–Leibniz-Zentrum für Informatik. ISBN 978-3-95977-176-4. doi: 10.4230/LIPIcs.OPODIS.2020.10.

[89] Enrico Tedeschi. Bitcoin blockchain optimized for machine learning prediction model, 2022. URL https://doi.org/10.18710/8IKVEU.

[90] Roger Maull, Phil Godsiff, Catherine Mulligan, Alan Brown, and Beth Kewell. Distributed ledger technology: Applications and implications. *Strategic Change*, 26(5):481–489, 2017.

[91] Gavin Wood et al. Ethereum: A secure decentralised generalised transaction ledger. *Ethereum project yellow paper*, 151(2014):1–32, 2014.

[92] Serguei Popov. The tangle. *White paper*, 1(3), 2018.

[93] Leemon Baird. The swirlds hashgraph consensus algorithm: Fair, fast, byzantine fault tolerance. *Swirlds Tech Reports SWIRLDS-TR-2016-01, Tech. Rep*, 34, 2016.

[94] Leemon Baird, Mance Harmon, and Paul Madsen. Hedera: A public hashgraph network & governing council. *White Paper*, 1, 2019.

[95] Jeff Kauflin. Hedera hashgraph thinks it can one-up bitcoin and ethereum with faster transactions. https://bit.ly/3QjR8Df, 2018.

[96] Ralph Charles Merkle. *Secrecy, authentication, and public key systems*. Stanford university, 1979.

[97] Giuseppe DeCandia, Deniz Hastorun, Madan Jampani, Gunavardhan Kakulapati, Avinash Lakshman, Alex Pilchin, Swaminathan Sivasubramanian, Peter Vosshall, and Werner Vogels. Dynamo: Amazon's highly available key-value store. In *Proceedings of Twenty-First ACM SIGOPS Symposium on Operating Systems Principles*, SOSP '07, page 205–220, New York, NY, USA, 2007. Association for Computing Machinery. ISBN 9781595935915. doi: 10.1145/1294261.1294281. URL https://doi.org/10.1145/1294261.1294281.

[98] Christian Cachin and Marko Vukolic. Blockchain consensus protocols in the wild. *CoRR*, abs/1707.01873, 2017. URL http://arxiv.org/abs/1707.01873.

[99] Ha Nguyen and Linh Do. The adoption of blockchain in food retail supply chain: Case: Ibm food trust blockchain and the food retail supply chain in malta. 2018.

[100] Elli Androulaki, Artem Barger, Vita Bortnikov, Christian Cachin, Konstantinos Christidis, Angelo De Caro, David Enyeart, Christopher Ferris, Gennady Laventman, Yacov Manevich, et al. Hyperledger fabric: a distributed operating system for permissioned blockchains. In *Proceedings of the thirteenth EuroSys conference*, pages 1–15, 2018.

[101] DL Chaum. Computer systems established, maintained and trusted by mutually suspicious groups (doctoral dissertation). *University of California Berkeley, Berkeley, CA*, 1982.

[102] Alan T Sherman, Farid Javani, Haibin Zhang, and Enis Golaszewski. On the origins and variations of blockchain technologies. *IEEE Security & Privacy*, 17(1):72–77, 2019.

[103] Leslie Lamport, Robert Shostak, and Marshall Pease. The byzantine generals problem. *ACM Transactions on Programming Languages and Systems*, 4(3):382–401, 1982.

[104] Fred B Schneider. Byzantine generals in action: Implementing fail-stop

processors. *ACM Transactions on Computer Systems (TOCS)*, 2(2):145–154, 1984.

[105] Miguel Castro and Barbara Liskov. Practical byzantine fault tolerance and proactive recovery. *ACM Transactions on Computer Systems (TOCS)*, 20(4):398–461, 2002.

[106] Leslie Lamport. *The Part-Time Parliament*, page 277–317. Association for Computing Machinery, New York, NY, USA, 2019. ISBN 9781450372701. URL https://doi.org/10.1145/3335772.3335939.

[107] Cynthia Dwork and Moni Naor. Pricing via processing or combatting junk mail. In Ernest F. Brickell, editor, *Advances in Cryptology — CRYPTO' 92*, pages 139–147, Berlin, Heidelberg, 1993. Springer Berlin Heidelberg. ISBN 978-3-540-48071-6.

[108] John R Douceur. The sybil attack. In *Peer-to-Peer Systems: First InternationalWorkshop, IPTPS 2002 Cambridge, MA, USA, March 7–8, 2002 Revised Papers 1*, pages 251–260. Springer, 2002.

[109] Reserve Bank of Australia. Digital currencies. https://www.rba.gov.au/education/resources/explainers/pdf/cryptocurrencies.pdf?v=2022-08-26-13-22-14, 2022. The Reserve Bank of Australia (RBA) is Australia's central bank and derives its functions and powers from the Reserve Bank Act 1959.

[110] Rick Miller. Bitcoin is a cryptocurrency, but is it money? *Forbes*, 2021. Accessed: 2022-08-26.

[111] Nicholas Weaver. Risks of cryptocurrencies. *Commun. ACM*, 61(6): 20–24, may 2018. ISSN 0001-0782. doi: 10.1145/3208095. URL https://doi.org/10.1145/3208095.

[112] Tom M Mitchell and Tom M Mitchell. *Machine learning*, volume 1. McGraw-hill New York, 1997.

[113] Soumya Raychaudhuri, Patrick D. Sutphin, Jeffrey T. Chang, and Russ B. Altman. Basic microarray analysis: grouping and feature reduction. *Trends in Biotechnology*, 19(5):189–193, 2001. ISSN 0167-7799. doi: https://doi.org/10.1016/S0167-7799(01)01599-2.

[114] Anthony McGregor, Mark Hall, Perry Lorier, and James Brunskill. Flow

clustering using machine learning techniques. In *International workshop on passive and active network measurement*, pages 205–214. Springer, 2004.

[115] Sinno Jialin Pan and Qiang Yang. A survey on transfer learning. *IEEE Transactions on Knowledge and Data Engineering*, 22(10):1345–1359, 2010. doi: 10.1109/TKDE.2009.191.

[116] Leo Breiman. Random forests. *Machine Learning*, 45(1):5–32, 2001. doi: 10.1023/A:1010933404324.

[117] James A Anderson. *An introduction to neural networks*. MIT press, 1995.

[118] Stuart J Russell. *Artificial intelligence a modern approach*. Pearson Education, Inc., 2010.

[119] Geoffrey Hinton and Terrence J Sejnowski. *Unsupervised learning: foundations of neural computation*. MIT press, 1999.

[120] John J Hopfield. Neural networks and physical systems with emergent collective computational abilities. *Proceedings of the national academy of sciences*, 79(8):2554–2558, 1982.

[121] Xavier Glorot, Antoine Bordes, and Yoshua Bengio. Deep sparse rectifier neural networks. In *Proceedings of the fourteenth international conference on artificial intelligence and statistics*, pages 315–323. JMLR Workshop and Conference Proceedings, 2011.

[122] Anne Håkansson and Ronald Hartung. *Artificial Inteeligence. Concepts, Areas, Techniques and Applications*. Studentlitteratur, 2020. ISBN 9789144125992.

[123] Kaiming He, Xiangyu Zhang, Shaoqing Ren, and Jian Sun. Deep residual learning for image recognition. In *Proceedings of the IEEE conference on computer vision and pattern recognition*, pages 770–778, 2016.

[124] Yahya Shahsavari, Kaiwen Zhang, and Chamseddine Talhi. A theoretical model for fork analysis in the bitcoin network. In *2019 IEEE International Conference on Blockchain (Blockchain)*, pages 237–244. IEEE, 2019.

[125] David Easley, Maureen O'Hara, and Soumya Basu. From mining to markets: The evolution of bitcoin transaction fees. *Journal of Financial*

*Economics*, 134(1):91 – 109, 2019. ISSN 0304-405X. doi: https://doi.org/10.1016/j.jfineco.2019.03.004.

[126] Kerem Kaskaloglu. Near zero bitcoin transaction fees cannot last forever. *The International Conference on Digital Security and Forensics (DigitalSec2014)*, pages 91–99, 2014.

[127] Malte Möser and Rainer Böhme. Trends, tips, tolls: A longitudinal study of Bitcoin transaction fees. In *Financial Cryptography and Data Security: FC 2015.*, number 8976 in LNCS, pages 19–33, Berlin, Heidelberg, 2015. Springer Berlin Heidelberg. ISBN 978-3-662-48051-9. doi: 10.1007/978-3-662-48051-9_2.

[128] Soumya Basu, David A. Easley, Maureen O'Hara, and Emin Gün Sirer. Towards a functional fee market for cryptocurrencies. *CoRR*, abs/1901.06830, 2019. URL `http://arxiv.org/abs/1901.06830`.

[129] Vitalik Buterin. First and second-price auctions and improved transaction-fee markets. `https://ethresear.ch/t/first-and-second-price-auctions-and-improved-transaction-fee-markets/2410`, 2018.

[130] Johnnatan Messias, Mohamed Alzayat, Balakrishnan Chandrasekaran, and Krishna P Gummadi. On blockchain commit times: An analysis of how miners choose bitcoin transactions. In *The Second International Workshop on Smart Data for Blockchain and Distributed Ledger (SDBD2020)*, 2020.

[131] Juanjuan Li, Xiaochun Ni, Yong Yuan, and Feiyue Wang. A novel gsp auction mechanism for dynamic confirmation games on bitcoin transactions. *IEEE Transactions on Services Computing*, pages 1–1, 2020. doi: 10.1109/TSC.2020.2994582.

[132] Juanjuan Li, Yong Yuan, and Fei-Yue Wang. A novel gsp auction mechanism for ranking bitcoin transactions in blockchain mining. *Decision Support Systems*, 124:113094, 2019.

[133] Javier Diez-Sierra and Manuel del Jesus. Long-term rainfall prediction using atmospheric synoptic patterns in semi-arid climates with statistical and machine learning methods. *Journal of Hydrology*, 586:124789, 2020. ISSN 0022-1694. doi: https://doi.org/10.1016/j.jhydrol.2020.124789.

[134] Saurav Nanda, Faheem Zafari, Casimer DeCusatis, Eric Wedaa, and Bai-

jian Yang. Predicting network attack patterns in sdn using machine learning approach. In *2016 IEEE Conference on Network Function Virtualization and Software Defined Networks (NFV-SDN)*, pages 167–172, 2016. doi: 10.1109/NFV-SDN.2016.7919493.

[135] Abbas Yazdinejad, Hamed HaddadPajouh, Ali Dehghantanha, Reza M. Parizi, Gautam Srivastava, and Mu-Yen Chen. Cryptocurrency malware hunting: A deep recurrent neural network approach. *Applied Soft Computing*, 96:106630, 2020. ISSN 1568-4946. doi: https://doi.org/10.1016/j.asoc.2020.106630.

[136] RSJD Baker et al. Data mining for education. *International encyclopedia of education*, 7(3):112–118, 2010.

[137] Ioanna Lykourentzou, Ioannis Giannoukos, Vassilis Nikolopoulos, George Mpardis, and Vassili Loumos. Dropout prediction in e-learning courses through the combination of machine learning techniques. *Computers & Education*, 53(3):950 – 965, 2009. ISSN 0360-1315. doi: https://doi.org/10.1016/j.compedu.2009.05.010.

[138] Indranil Bose and Radha K Mahapatra. Business data mining—a machine learning perspective. *Information & management*, 39(3):211–225, 2001.

[139] Jared Dean. *Big data, data mining, and machine learning: value creation for business leaders and practitioners*. John Wiley & Sons, 2014.

[140] Min Chen, Yixue Hao, Kai Hwang, Lu Wang, and Lin Wang. Disease prediction by machine learning over big data from healthcare communities. *IEEE Access*, 5:8869–8879, 2017. doi: 10.1109/ACCESS.2017.2694446.

[141] Sumeet Dua, U Rajendra Acharya, and Prerna Dua. *Machine learning in healthcare informatics*, volume 56. Springer, 2014.

[142] Salvatore Stolfo, David W Fan, Wenke Lee, Andreas Prodromidis, and P Chan. Credit card fraud detection using meta-learning: Issues and initial results. In *AAAI-97 Workshop on Fraud Detection and Risk Management*, 1997.

[143] Theodore B Trafalis and Huseyin Ince. Support vector machine for regression and applications to financial forecasting. In *Proceedings of the IEEE-INNS-ENNS International Joint Conference on Neural Networks. IJCNN 2000. Neural Computing: New Challenges and Perspectives for the*

*New Millennium*, volume 6, pages 348–353. IEEE, 2000.

[144] Yu Zheng, Like Liu, Longhao Wang, and Xing Xie. Learning transportation mode from raw gps data for geographic applications on the web. In *Proceedings of the 17th international conference on World Wide Web*, pages 247–256. ACM, 2008.

[145] Xiaolei Ma, Haiyang Yu, Yunpeng Wang, and Yinhai Wang. Large-scale transportation network congestion evolution prediction using deep learning theory. *PloS one*, 10(3):e0119044, 2015.

[146] Tom Augspurger, Chris Bartak, Phillip Cloud, Andy Hayden, Stephan Hoyer, Wes McKinney, Jeff Reback, Chang She, Masaaki Horikoshi, Joris Van den Bossche, et al. Pandas: Python Data Analysis Library. software v0.21.0, Pandas community, 2012. URL `http://pandas.pydata.org/`.

[147] Pauli Virtanen, Ralf Gommers, Travis E. Oliphant, Matt Haberland, Tyler Reddy, David Cournapeau, Evgeni Burovski, Pearu Peterson, Warren Weckesser, Jonathan Bright, Stéfan J. van der Walt, Matthew Brett, Joshua Wilson, K. Jarrod Millman, Nikolay Mayorov, Andrew R. J. Nelson, Eric Jones, Robert Kern, Eric Larson, C J Carey, İlhan Polat, Yu Feng, Eric W. Moore, Jake VanderPlas, Denis Laxalde, Josef Perktold, Robert Cimrman, Ian Henriksen, E. A. Quintero, Charles R. Harris, Anne M. Archibald, Antônio H. Ribeiro, Fabian Pedregosa, Paul van Mulbregt, and SciPy 1.0 Contributors. SciPy 1.0: Fundamental Algorithms for Scientific Computing in Python. *Nature Methods*, 17:261–272, 2020. doi: 10.1038/s41592-019-0686-2.

[148] Martín Abadi, Ashish Agarwal, Paul Barham, Eugene Brevdo, Zhifeng Chen, Craig Citro, Greg S. Corrado, Andy Davis, Jeffrey Dean, Matthieu Devin, Sanjay Ghemawat, Ian Goodfellow, Andrew Harp, Geoffrey Irving, Michael Isard, Yangqing Jia, Rafal Jozefowicz, Lukasz Kaiser, Manjunath Kudlur, Josh Levenberg, Dandelion Mané, Rajat Monga, Sherry Moore, Derek Murray, Chris Olah, Mike Schuster, Jonathon Shlens, Benoit Steiner, Ilya Sutskever, Kunal Talwar, Paul Tucker, Vincent Vanhoucke, Vijay Vasudevan, Fernanda Viégas, Oriol Vinyals, Pete Warden, Martin Wattenberg, Martin Wicke, Yuan Yu, and Xiaoqiang Zheng. TensorFlow: Large-scale machine learning on heterogeneous systems, 2015. URL `https://www.tensorflow.org/`. Software available from tensorflow.org.

[149] François Chollet et al. Keras. https://github.com/fchollet/keras, 2015.

[150] Mahmoudreza Tahmassebpour. A new method for time-series big data effective storage. *IEEE Access*, PP:1–1, 05 2017. doi: 10.1109/ACCESS.2017.2708080.

[151] J. Doyne Farmer and John J. Sidorowich. Predicting chaotic time series. *Phys. Rev. Lett.*, 59:845–848, Aug 1987. doi: 10.1103/PhysRevLett.59.845. URL https://link.aps.org/doi/10.1103/PhysRevLett.59.845.

[152] George Foster. Quarterly accounting data: Time-series properties and predictive-ability results. *The Accounting Review*, 52(1):1–21, 1977. ISSN 00014826. URL http://www.jstor.org/stable/246028.

[153] William WS Wei. Time series analysis. In *The Oxford Handbook of Quantitative Methods in Psychology: Vol. 2*. 2006.

[154] James Douglas Hamilton. *Time series analysis*. Princeton university press, 2020.

[155] Wayne A Fuller. *Introduction to statistical time series*, volume 428. John Wiley & Sons, 2009.

[156] Kyle Croman, Christian Decker, Ittay Eyal, Adem Efe Gencer, Ari Juels, Ahmed Kosba, Andrew Miller, Prateek Saxena, Elaine Shi, Emin Gün Sirer, Dawn Song, and Roger Wattenhofer. On scaling decentralized Blockchains. In *Financial Cryptography and Data Security. FC 2016.*, volume 9604 of *LNCS*, pages 106–125, Berlin, Heidelberg, 2016. Springer Berlin Heidelberg. ISBN 978-3-662-53357-4. doi: 10.1007/978-3-662-53357-4_8.

[157] Amitanand S. Aiyer, Lorenzo Alvisi, Allen Clement, Mike Dahlin, Jean-Philippe Martin, and Carl Porth. Bar fault tolerance for cooperative services. In *Proceedings of the Twentieth ACM Symposium on Operating Systems Principles*, SOSP '05, pages 45–58, New York, NY, USA, 2005. ACM. ISBN 1-59593-079-5. doi: 10.1145/1095810.1095816.

[158] Nicolas Houy. The bitcoin mining game. *Available at SSRN 2407834*, 2014.

[159] Ian Goodfellow, Yoshua Bengio, and Aaron Courville. *Deep learning*. MIT

press, 2016.

[160] Yann LeCun, Yoshua Bengio, and Geoffrey Hinton. Deep learning. *nature*, 521(7553):436–444, 2015.

[161] Sotiris B Kotsiantis, Dimitris Kanellopoulos, and Panagiotis E Pintelas. Data preprocessing for supervised leaning. *International journal of computer science*, 1(2):111–117, 2006.

[162] Kaiming He, Xiangyu Zhang, Shaoqing Ren, and Jian Sun. Delving deep into rectifiers: Surpassing human-level performance on imagenet classification. In *Proceedings of the IEEE international conference on computer vision*, pages 1026–1034, 2015.

[163] Jindong Gu and Daniela Oelke. Understanding bias in machine learning. *CoRR*, abs/1909.01866, 2019. URL http://arxiv.org/abs/1909.01866.

[164] James Lovejoy and Anne Ouyang. 51% attacks. MIT media lab, 2020. URL https://dci.mit.edu/51-attacks. MIT digital currency initiative.

[165] David Siegel, Mark Ly, Greg Fraser, Scott Miller, Caleb Silver, et al. Definition of 51 attack. Investopedia, https://www.investopedia.com/terms/1/51-attack.asp, 2017.

[166] Atsushi Kajii and Stephen Morris. The robustness of equilibria to incomplete information. *Econometrica*, 65(6):1283–1309, 1997. ISSN 00129682, 14680262. URL http://www.jstor.org/stable/2171737.

# List of Symbols

| Sign | Description | Unit |
|---|---|---|
| $B_{\text{day}}$ | Blocks mined in a day | |
| $H$ | Total hash rate of Bitcoin network | hash/s |
| $M$ | Revenue of a block. Sum of all $\phi$ in a block | ₿ or $ |
| $Q$ | Block size, $\sim 1.1\,\text{MB}$ | bytes |
| $R$ | Block reward, currently at ₿ 6.25, halved every 210, 000 blocks | ₿ |
| $S$ | Set of ordered pending transactions | |
| $\Delta\mathcal{P}$ | It represents the waiting time for a transaction $t$, before it is included in a block | s |
| $\beta_t$ | Block epoch ($be$) of the block before $t$'s inclusion | |
| $\delta_t$ | Feature that represents the offset, in bytes, of a certain transaction $t$ | bytes |
| $\eta_{\text{day}}$ | Consumption per day | kWh |
| $\eta$ | Cost per hash | kWh/hash |
| $\langle C \rangle$ | Expectation value of a miner's hashing cost per block | ₿ |
| $\langle V \rangle$ | Expectation value of a miner's revenue per block | ₿ |
| $\langle \Pi \rangle$ | Expectation value of a miner's profit per block | ₿ |
| $\mathbb{E}[f]$ | Expected transaction fee value. What is considered to be "a fair amount" | ₿ |
| $\mathbb{P}_{orphan}$ | Probability that, mined a new block, it gets orphaned | $[0, 1]$ |
| $\mathbb{T}$ | Set containing occurrences of block creation times, in epochs | |

| Sign | Description | Unit |
|---|---|---|
| $\mathcal{A}$ | Set of temporary approved transactions | |
| $\mathcal{D}_B$ | Locally stored dsataset containing raw fetched blocks | |
| $\mathcal{D}_T$ | Locally stored dsataset containing raw fetched transactions | |
| $\mathcal{L}_t^x$ | Lifespan of a transaction $t$ | |
| $\mathcal{M}$ | Set containing all active miners in Bitcoin | |
| $\mathcal{P}$ | Set of relapsed pending transactions, RPT | |
| $\mathcal{R}$ | Raw dataset, containing the stored portion of the blockchain | |
| $\mathcal{T}'$ | Calculated block interval time | s |
| $\mathcal{T}$ | Interblock time interval, equals to 600 $s$ | s |
| $\phi$ | Transaction fee | ₿ |
| $\boldsymbol{T}$ | Complete block-epoch-based representation of a transaction | |
| $\boldsymbol{Xte}$ | Testing set | |
| $\boldsymbol{X}$ | Training set | |
| $\boldsymbol{\theta}_t$ | Model output array, $\boldsymbol{\theta}_t = [P_t(\upsilon_0),\ P_t(\upsilon_1)]$ | |
| $\rho$ | Price per byte for block space, or feerate | sat/bytes |
| BTCP | Bitcoin price in U.S. dollars. | $/₿ |
| $\upsilon_0$ | Class of not approved transactions | |
| $\upsilon_1$ | Class of approved transactions | |
| $\xi$ | Latest block created | height |
| $be_\xi$ | Latest block creation time (epoch), $x = -1$ | s |
| $be_x$ | Block creation time (epoch). It represents the epoch of a certain block at height $x$ | s |
| $d_t$ | Difficulty to solve Proof-of-Work at time $t$ | |
| $e_p$ | Electricity price | $/kWh |

| Sign | Description | Unit |
|---|---|---|
| $ep_t$ | Timestamp of a transaction $t$. Epoch which represents first appearance of $t$ in the network | s |
| $g_B$ | Gain in USD for mining a block $B$ | $ |
| $ha_t$ | Transaction hash | |
| $ha_x$ | Block hash at height $x$ | |
| $h$ | Miner's individual hash rate | hash/s |
| $inp$ | Transaction input of the UTXO model. Money received in a specific transaction | ₿ |
| $l_t$ | Latency of a transaction $t$ | s |
| $out$ | Transaction output of the UTXO model. Money sent in a specific transaction | ₿ |
| $q$ | Transaction size | bytes |
| $t_B$ | Number of transaction approved in a block $B$. | |
| $t_a$ | Transaction that belongs to the set $\mathcal{A}$ of the Temporarily Approved Transaction | |
| $t_p$ | Transaction that belongs to the set $\mathcal{P}$ of the Relapsed Pending Transaction | |

# A

# Other Definitions

## A.1 Bitcoin

### Orphaning

The likelihood of a miner, denoted as $m$, successfully publishing a block decreases if the chosen block is slow to propagate to other miners. In such a scenario, even if $m$ successfully solves a block $b$, this block may be discarded if a newer block $b'$ mined by another miner $m'$ propagates faster. This phenomenon is referred to as *orphaning*, and the probability of orphaning is determined by the block propagation time $\tau$. As the block creation time follows a Poisson distribution, it can be formalized as:

$$\mathbb{P}_{orphan} = 1 - e^{-\frac{\tau}{T}} \tag{A.1}$$

### 51% Attack

51% refers to an attack on a POW-based blockchain by an attacker that amasses a majority of the hash rate in the targeted cryptocurrency [164]. Proof-of-Work is intended to make such attack prohibitively expensive, but if accomplished, the attacker could rewrite the blockchain and reverse transactions that are considered settled. For instance, if an attacker tries to double spend its tokens, it will first purchase goods with them. Once the transaction is approved, the

attacker forks the blockchain and it uses its 51% hash rate to re-build and overtake the honest chain, and new blocks, including the malicious transactions that spends again the same token, is included and approved by the network. Such attack would not destroy Bitcoin or any other cryptocurrency, but it could provide severe damage to its users, and to the fame of the currency itself [165].

### Full Node

Node that stores and processes the entirety of every block, saving locally the entire blockchain.

### Light Node

Node that only stores the part of the blockchain it needs.

### Bitcoin-cli

Bitcoin-cli is a command-line interface for interacting with a local or remote Bitcoin Core instance, which is a full node implementation of the Bitcoin protocol. It allows users to send commands to the Bitcoin Core daemon (bitcoind) and receive the results. This enables developers to easily query the Bitcoin blockchain, retrieve transaction details, and perform other actions such as sending transactions, or managing wallets.

## A.2 Machine Learning

### Model Hyperparameters

Our implementation of ResNet consists of three sets of residual blocks, each set consisting of two fully connected (Dense) layers followed by a skip connection (Add) that bypasses the two Dense layers. The first layer in the ResNet is a Dense layer with 256 hidden units and a ReLU activation function. The output of the first Dense layer is passed through three more Dense layers with 256 hidden units each and ReLU activation functions. Then, the output of the first Dense layer is added to the output of the last Dense layer in this set using a skip connection. The output of the first residual block is then passed through

two more residual blocks, each consisting of two Dense layers with 64 hidden units and ReLU activation functions. The output of the second residual block is added to the output of the first residual block using another skip connection. The output of the second set of residual blocks is passed through one more residual block with 64 hidden units, and its output is added to the output of the second residual block using another skip connection. The final layers of the network are two Dense layers with 32 and 16 hidden units, respectively, both with ReLU activation functions. The output layer is a Dense layer with two number of units and a softmax activation function, which gives the probability distribution over the possible classes.

The weight initialization of all the Dense layers is done using the He normal initializer, which helps in initializing weights that are well-suited for deep neural networks. Finally, the ResNet is compiled using the categorical cross-entropy loss function, an Adam optimizer, and accuracy as the evaluation metric.

## A.3 Statistics

### Bayesian Nash equilibrium

In game theory, Bayesian Nash equilibrium (BNE) is a strategy profile that maximizes the expected payoff for each player given a prior beliefs and strategies played by other players. A strategy profile $\sigma$ is a BNE if and only if for every player $i$, each one with their prior beliefs and strategies of other players fixed, $\sigma_i$ maximizes the expected payoff [166].

$$\sigma \text{ is BNE} \iff \forall i, \sum_i \text{payoff}(\sigma_i) \geq \sum_i \text{payoff}(\sigma\prime_i) \tag{A.2}$$

for any possible strategy $\sigma\prime$.

# B

# Publications

This dissertation is based on the work presented in the following five publications:

## Publication I

Tedeschi, E., Johansen, H.D. and Johansen, D., 2018. “Trading Network Performance for Cash in the Bitcoin Blockchain”, in CLOSER 2018, *the 8th International Conference on Cloud Computing and Services Science*, pp. 643-650.

### Scope

In this paper we perform an initial longitudinal study on the Bitcoin network, where we observe a consistent correlation between fee paid and transactions latency. Using linear regression methods we design a model for fee-cost estimation, and we outline that paying above a certain threshold it will not result in better acceptance performances.

### Abstract

Public blockchains have emerged as a plausible cloud-like substrate for applications that require resilient communication. However, sending messages over existing public blockchains can be cumbersome and costly as miners require payment to establish consensus on the sequence of messages. In this paper we analyze the network performance of the Bitcoin public ledger when used as a massaging substrate. We present several real-world observations on its characteristics, transaction visibility, and fees paid to miners; and we propose two models for fee-cost estimation. We find that applications to some extent can improve messaging latency by paying transaction fees. We also suggest that spendings should be kept below 300 Satoshi per byte.

## Publication II

E. Tedeschi, T. S. Nordmo, D. Johansen and H. D. Johansen, "Predicting Transaction Latency with Deep Learning in Proof-of-Work Blockchains", 2019 IEEE International Conference on Big Data (Big Data), 2019, pp. 4223-4231, https://doi.org/10.1109/BigData47090.2019.9006228.

### Scope

In this paper we illustrate our first model idea using DNN to predict transaction latency in POW-based blockchains. This solution is based on our previous longitudinal study and on a careful feature selection. This paper defines what we consider the foundations for defining transaction inclusion pattern.

### Abstract

Proof-of-work based cryptocurrencies, like Bitcoin, have a fee market where transactions are included in the blockchain according to a first-price auction for block space. Many attempts have been made to adjust and predict the fee volatility, but even well-formed transactions sometimes experience delays and evictions unless an enormous fee is paid. In this paper, we present a novel machine-learning model, solving a binary classification problem, that can predict transaction fee volatility in the Bitcoin network so that users can optimize their fees expenses and the approval time for their transactions. The model's output will give a confidence score whether a new incoming transaction

will be included in the next mined block. The model is trained on data from a longitudinal study of the Bitcoin blockchain, containing more than 10 million transactions. New features that we generate include information on how many bytes were already occupied by other transactions in the mempool, assuming they are ordered by fee density in each mining pool. The collected dataset allows to generate a model for transaction inclusion pattern prediction in the Bitcoin network, hence telling whether a transaction is well formed or not, according to the previous transactions analyzed. With this, we obtain a prediction score for up to 86%.

## Publication III

Enrico Tedeschi, Tor-Arne S. Nordmo, Dag Johansen, and Håvard D. Johansen. 2022. “On Optimizing Transaction Fees in Bitcoin using AI: Investigation on Miners Inclusion Pattern”. Association for Computing Machinery (ACM) Trans. Internet Technol. 22, 3, Article 77 (August 2022), 28 pages. https://doi.org/10.1145/3528669

### Scope

In this paper we refine ML methods to obtain a better inclusion prediction for transactions in the Bitcoin network, and we describe new methods for data gathering and manipulation. Data are stored on a time-series like approach and the study is characterized by a formal definition of the model for transaction inclusion pattern. A new series of evaluations and experiments are conducted. The results obtained here represent the main contribution of our dissertation.

### Abstract

The transaction-rate bottleneck built into popular proof-of-work-based cryptocurrencies, like Bitcoin and Ethereum, leads to fee markets where transactions are included according to a first-price auction for block space. Many attempts have been made to adjust and predict the fee volatility, but even well-formed transactions sometimes experience unexpected delays and evictions unless a substantial fee is offered. In this paper, we propose a novel transaction inclusion model that describes the mechanisms and patterns governing miners decisions to include individual transactions in the Bitcoin system. Using this

model we devise a ML approach to predict transaction inclusion. We evaluate our predictions method using historical observations of the Bitcoin network from a five month period that includes more than 30 million transactions and 120 million entries. We find that our ML model can predict fee volatility with an accuracy of up to 91%. Our findings enable Bitcoin users to improve their fee expenses and the approval time for their transactions.

## Publication IV

Amores-Sesar, I., Cachin, C. and Tedeschi, E., 2022. "When is Spring coming? A Security Analysis of Avalanche Consensus". `https://doi.org/10.48550/arXiv.2210.03423`.

### Scope

In this paper we study the security of a DAG-based blockchain, Avalanche. We provide a detailed formulation of the Avalanche blockchain consensus protocol using pseudo-code, addressing features that were omitted from the original white-paper. Additionally, the paper provides an analysis of the formal properties of Avalanche as a generic broadcast protocol that orders related transactions. The analysis highlights a vulnerability that affects the liveness of the protocol and proposes a potential solution to address the issue. Despite the success of Avalanche, the consensus protocol lacks a complete abstract specification and formal analysis, making this work a valuable contribution to the field.

### Abstract

Avalanche is a blockchain consensus protocol with exceptionally low latency and high throughput. This has swiftly established the corresponding token as a top-tier cryptocurrency. Avalanche achieves such remarkable metrics by substituting proof of work with a random sampling mechanism. The protocol also differs from Bitcoin, Ethereum, and many others by forming a Directed Acyclic Graph (DAG) instead of a chain. It does not totally order all transactions, establishes a partial order among them, and accepts transactions in the DAG that satisfy specific properties. Such parallelism is widely regarded as a technique that increases the efficiency of consensus. Despite its success, Avalanche consensus lacks a complete abstract specification and a matching

formal analysis. To address this drawback, this work provides first a detailed formulation of Avalanche through pseudo-code. This includes features that are omitted from the original white-paper or are only vaguely explained in the documentation. Second, the paper gives an analysis of the formal properties fulfilled by Avalanche in the sense of a generic broadcast protocol that only orders related transactions. Last but not least, the analysis reveals a vulnerability that affects the liveness of the protocol. A possible solution that addresses the problem is also proposed.

## Publication V - Dataset

Tedeschi, Enrico, 2022, "Bitcoin blockchain optimized for machine learning prediction model", `https://doi.org/10.18710/8IKVEU`, DataverseNO, V1

### Scope

This dataset stores part of the Bitcoin blockchain. Blocks are sampled every month and information about transactions and blocks are separated to save disk space and avoid redundancies. This dataset is used in the work presented by Tedeschi et al. [58] which is submitted for review, in order to generate a machine learning model that predicts transaction inclusion. In each month of analysis, there is a block folder and a transaction folder. Information can be merged runtime through 'bhash' attribute (block hash). (2022-02-12)

# C

# Source Code

## C.1 Blockchain APIs

**Listing C.1:** RAW BLOCK JSON response of `blockchain.com` APIs at height 600000

```
{
  "hash": "000000...",
  "ver": 536870912,
  "prev_block": "000000...",
  "mrkl_root": "66...",
  "time": 1571443461,
  "bits": 387294044,
  "next_block": ["000000..."],
  "fee": 3764047,
  "nonce": 1066642855,
  "n_tx": 1925,
  "size": 870371,
    ...
  "height": 600000,
  "weight": 2848472,
  "tx": [
    {
      "hash": "93955...",
      "ver": 1,
      "size": 200,
```

```
      "fee": 0,
      "relayed_by": "0.0.0.0",
        ...
      "time": 1571443461,
      "block_index": 600000,
      "block_height": 600000,
      "inputs": [ ... ],
      "out": [ ... ]
    },
    { ... },    //More txs in the blocks.
  ]
}
```

## C.2 Data Storage

**Listing C.2:** Transaction info.txt file

```
{"__fileinfo__":
  [
    {"filename": "data/dataset/Feb-21/transactions/Dt0.csv",
      "start": 668405,
      "end": 668514,
      "start_ha": "0000000000000...",
      "end_ha": "0000000000000...",
      "start_time": 1612054039,
      "end_time": 1612116675},
    {"filename": ... }
  ]
}
```

## C.3 Data Manipulation

**Listing C.3:** Calculate transaction fee

```
def transaction_fee(jsontx):
  """ calculates transaction fee based on UTXO model.
  :param jsontx: transaction in json format
  :return: int, transaction fee in satoshi """
  if 'fee' in jsontx:
```

```
    fee = jsontx['fee']
  else:
    inputs = 0
    outputs = 0
    for inp in jsontx['inputs']:
      if 'prev_out' in inp:
        inputs += inp['prev_out']['value']
    for out in jsontx['out']:
      outputs += out['value']
    fee = inputs - outputs
  if fee < 0:
    fee = scraper.TransactionPage(jsontx['hash']).
       get_transaction_fee()
  return fee
```